

**The design and synthesis of selective  
adsorbents for nuclear fission product removal  
using continuous chromatography: A new  
concept in  
nuclear reprocessing and waste management**

by

**Daniel Rowbotham**

A thesis submitted in partial fulfilment for the requirements for the degree of PhD via  
MPhil at the University of Central Lancashire

18/01/2023

## **Student Declaration**

**Type of Award**                      PhD via MPhil

**School**                                      Forensic and Applied Sciences

### **Concurrent registration for two or more academic awards**

I declare that while registered as a candidate for the research degree, I have not been a registered candidate or enrolled student for another award of the University or other academic or professional institution

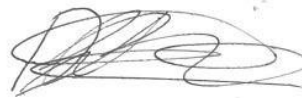
### **Material submitted for another award**

I declare that no material contained in the thesis has been used in any other submission for an academic award and is solely my own work

### **Use of a Proof-reader**

No proof-reading service was used in the compilation of this thesis.

Signature of Candidate



Print name:

DANIEL ROWBOTHAM

## Abstract

The current nuclear fuel reprocessing technique - PUREX - has remained in operation, unchallenged for over 50 years. The underlying reason for this is that development of alternative processes have not achieved the required criteria.

The PUREX process has however, some inherent challenges that hinder its efficiency for separating uranium and plutonium from other radionuclides in spent nuclear fuel liquors which are discussed within this thesis. In addition, the PUREX process produces High Level Waste (HLW) which contains both relatively short lived beta/gamma emitters (cesium and strontium) and longer lived minor actinides (neptunium and americium) which ultimately present waste disposal challenges.

An Alternative Reprocessing Technique (ART) is described for efficient separation of radionuclides from spent fuel dissolver liquors which could potentially eliminate High Level Waste and enhance the efficiency – or even replace - the PUREX process. A highly selective phosphate (ammonium molybdophosphate, AMP) has been shown to remove cesium from nitric acid liquors but not containing greater concentrations of uranium and/or plutonium.

This research is split into 3 main parts; [1] optimisation of the synthesis of AMP/PAN (polyacrylonitrile) to maximise ion exchange performance; [2] focus on synthesis and development of mixed metal phosphates/polyacrylonitrile composites for strontium adsorption and [3] scoping the capabilities of a Simulated Moving Bed Chromatography technique to be applied to ART for the downstream extraction of fission products from spent fuel dissolver liquors following the removal of cesium.

Previously studies of cesium and strontium adsorbents for their extraction from HLW were reviewed. These adsorbents are evaluated for their ion exchange performance as a function of selectivity, stability, kinetics and capacity.

The outstanding material for cesium extraction from spent fuel dissolver liquors is currently AMP as it displays a high affinity for cesium with high capacities and rapid ion exchange kinetics whilst exhibiting high thermal and radiolytic stability. It can also be encapsulated into a polyacrylonitrile support for synthesis of spherical beads that are more applicable to an industrial process. The preparative routes were varied in order to produce optimised composite spherical beads that had superior selectivity, uptake and kinetics compared with previously prepared material.

There is a wide library of selective strontium adsorbent materials but do not possess all the characteristics required for applications in nuclear reprocessing.

This study was therefore designed to address the preparation and development of novel highly selective materials that could be used in ART and to evaluate Simulated Moving Bed Chromatography for radionuclide extraction.

A selection of mixed metal phosphate powders was provided, untested for their strontium uptake capabilities. The powders were encapsulated in PAN to mimic the AMP/PAN composite in the hope they would display comparatively uptake capacities and kinetics for strontium.

Initial results of AMP/PAN synthesis optimisation revealed that beads of 1-2mm in diameter exhibited limited uptake in 1 M and 3 M HNO<sub>3</sub> with a cesium concentration of 5 mM. Smaller beads <1 mm in diameter produced using a new bead preparative technique displayed an increase in cesium uptake by almost 10 fold from a similar concentration cesium solution. In addition, the selectivity of cesium was also high in the presence of a large excess of cerium

ions. The uptake of cesium when the oxidation state of cerium was increased to 4+, was noticeably lower but reasons for this are inconclusive as of yet. The results were compared to previously produced AMP/PAN composites. The modified AMP/PAN beads showed evidence of more internal voids, but less ordered channels and greater surface area. These characteristics resulted in a significant, greater cesium uptake.

A series of untested mixed metal phosphate powders synthesised via a fast flow synthesis were selected for their uptake capabilities for strontium. Most of the adsorbents exhibited rapid uptake kinetics with near complete adsorption of strontium in pH values of ~5. They were subsequently encapsulated into a polyacrylonitrile matrix to produce spherical beads ~0.5 – 1mm in diameter and re-tested for their ion exchange performance. Kinetics results were constant with the starting powders but capacities and  $K_d$  values decreased. Their stability in acidic media was also limited.

Various commercial Purolite resins were investigated using an isocratic SMBC technique using a multi-ion feed solution (Zr, Mo, Ce). Initial results were compared to previous single column work performed with the same resins. The elution of the different ions displayed some very distinctive differences to single column results due to the different underlying fundamentals of SMB. Ce was used in high excess as a uranium simulant and presented competitive adsorption behaviours. These preliminary studies were used to gain an initial insight to its potential use in spent fuel nuclear reprocessing.

# Table of Contents

<b>Student Declaration</b> .....	<b>ii</b>
<b>Abstract</b> .....	<b>iii</b>
<b>Table of Contents</b> .....	<b>vi</b>
<b>List of Figures</b> .....	<b>x</b>
<b>List of Tables</b> .....	<b>xii</b>
<b>List of Equations</b> .....	<b>xiv</b>
<b>Acknowledgements</b> .....	<b>xv</b>
<b>Abbreviations</b> .....	<b>xvii</b>
<b>Aims and Objectives</b> .....	<b>1</b>
<b>Chapter 1 Introduction</b> .....	<b>3</b>
1.1 Background .....	3
1.2 The Nuclear Fuel Cycle .....	5
1.2.1 Uranium Ore Mining and Milling .....	6
1.2.2. Uranium Ore Conversion .....	7
1.2.3 Enrichment .....	8
1.2.4. Fabrication of fuel.....	9
1.2.5. Nuclear Fission Process .....	10
1.2.5.1. Types of Nuclear Reactors .....	11
1.2.5.1.1. Light Water Reactors (LWR).....	11
1.2.5.1.2. Advanced Gas cooled Reactor (AGR) .....	13
1.2.5.1.3. Very High Temperature Reactor (VHTR) .....	14
1.2.6. Nuclear fission waste .....	15
1.2.6.1 High Level Waste (HLW).....	15
1.2.6.2 Intermediate Level Waste (ILW) .....	16
1.2.6.3 Low Level Waste LLW.....	16
1.2.7 Waste management and Reprocessing .....	17
1.2.7.1 Vitrification.....	17
1.2.7.2 Plutonium Uranium Redox Extraction PUREX.....	18
1.2.7.2.1 Challenges of the PUREX process .....	21
1.2.8 UCLan’s Concept (ART).....	22
1.3 Continuous Ion Exchange Chromatography .....	25

1.3.1 Principles of Ion Exchange .....	26
1.3.1.1. Batch ion exchange .....	28
1.3.1.2. Ion Exchange equilibrium and selectivity.....	29
1.3.2. Kinetics of ion exchange chromatography.....	30
1.3.3. Capacity .....	31
1.3.4. Moving Bed Ion Exchange .....	32
1.3.5. Simulated moving bed chromatography (SMB or SMBC).....	34
1.3.6. Continuous Annular chromatography .....	35
1.3.7. Ion Exchange and chromatography in the Nuclear Industry.....	35
1.4. References.....	36
<b>Chapter 2 Experimental methodology and Materials .....</b>	<b>42</b>
2.1. Analytical equipment.....	44
2.1.1. Surface area and pore size analysis.....	44
2.1.1.1 Types of isotherm .....	45
2.1.1.2 Brunauer-Emmett-Teller (BET).....	46
2.1.1.3 Sample preparation and experimental procedure.....	48
2.1.2 Thermo Gravimetric Analysis (TGA).....	48
2.1.2.1 Sample preparation and experimental procedure.....	50
2.1.3 Inductively Coupled Plasma –Mass Spectroscopy (ICP-MS) .....	50
2.1.4 Scanning Electron Microscopy (SEM).....	53
2.1.4.1 Sample Preparation and experimental procedure.....	53
2.1.5 Fourier Transform – Infrared Spectroscopy (FT – IR) .....	54
2.1.5.1 Sample Preparation and experimental procedure.....	55
2.2 Cation uptake experiments.....	55
2.3 Composite adsorbent bead formation .....	56
2.3.2 Synthesis of strontium adsorbent composites .....	57
2.3.3 Bulb Pipette Nozzle .....	59
2.3.4 Confined Jet .....	60
2.3.5 Dual Glass nozzle .....	61
2.4 Simulated Moving Bed Chromatography .....	64
2.4.1 Materials and procedure.....	64
<b>Chapter 3 Selective cesium separation from spent fuel dissolver liquors. ....</b>	<b>69</b>
3.1 Review of selective cesium adsorbents. ....	69
3.1.1 Crown ethers. ....	69
3.1.2 Phosphotungstic acid. ....	70
3.1.3 Ammonium Molybdophosphate. ....	71
3.1.4 Titanosilicates. ....	73
3.1.5 Polyacrylonitrile as a support. ....	73
3.1.6 AMP/PAN composite. ....	74

3.2 Characterisation of materials. ....	76
3.3 Results and Discussion. ....	77
3.3.1 Cesium uptake with AMP PAN composite - high and low concentration of cesium. ....	80
3.3.2 Modifications to the synthesis of AMP/PAN ....	82
3.3.2.1 Uptake of Cs – altering the ratio of AMP:PAN ....	82
3.3.2.2 Effect of Gelling Temperature. ....	85
3.3.2.3 Reducing molecular weight of PAN ....	87
3.3.2.4 Reducing solvent volume. ....	91
3.3.2.6 Reducing bead size. ....	93
3.3.2.6.2 Glass Nozzle. ....	94
3.3.3 Selectivity of AMP/PAN. ....	96
3.3.4 Effect of Ce oxidation state on cesium uptake. ....	100
3.3.5 Kinetics of cesium uptake. ....	102
3.3.6 Irradiation studies with varying cesium concentration. ....	104
3.3.6.1 Kinetics. ....	105
3.3.6.2 Isothermal analysis. ....	109
3.3.7 Morphology. ....	113
3.3.8 Thermal Stability. ....	116
3.3.9 Surface area. ....	120
3.3.10 Pore size/volume distribution. ....	121
3.4 Conclusions. ....	123
3.5 References. ....	126
<b>Chapter 4 Strontium removal from spent fuel dissolver liquors .....</b>	<b>133</b>
4.1 Review of selective strontium adsorbents ....	133
4.1.1 Mixed oxides – Zirconium and Manganese. ....	133
4.1.2 Crown ethers ....	134
4.1.3 Layered Metal Sulfides ....	135
4.1.4 Ion-imprinted polymers ....	136
4.1.5 Lead Hexacyanoferrates. ....	137
4.1.6 Antimony oxides. ....	138
4.1.7 Molybdophosphates ....	139
4.2 Results and Discussion ....	140
4.2.1 Strontium batch uptake measurements ....	143
4.2.1.1 Powder adsorbents ....	143
4.2.1.2 Composite MMP/PAN adsorbents. ....	145
4.2.2 Kinetics ....	147
4.2.2.1 Powder adsorbent Kinetics. ....	147
4.2.2.2 Composite MMP/PAN adsorbent kinetics ....	149



4.2.3 Acid Stability .....	150
4.2.3.1 1M HNO <sub>3</sub> Experiments .....	150
4.2.4 Selectivity .....	152
4.2.5 Morphology.....	154
4.2.6 Thermal Stability .....	157
4.2.7 Porosity and Surface area.....	158
4.3 Conclusions.....	160
4.4 References.....	162
<b>Chapter 5 Separation of Fission products via Simulated Moving Bed Chromatography .....</b>	<b>165</b>
5.1 Principles of SMB.....	165
5.1.1 Step mode .....	166
5.1.2 Isocratic mode.....	167
5.1.3 Parameters.....	170
5.2 Results and Discussion .....	172
5.2.1 SMBC experiment 1: 1M HNO <sub>3</sub> C100x10MBH .....	173
5.2.2 SMBC experiment 2: 3M HNO <sub>3</sub> C100x10MBH .....	175
5.2.3 SMBC experiment 3: 3M HNO <sub>3</sub> C100H .....	177
5.2.4 SMBC experiment 4: 1M HNO <sub>3</sub> S910.....	180
5.2.5 SMBC experiment 5: 3M HNO <sub>3</sub> S910.....	182
5.3. Conclusions.....	184
<b>Chapter 6 Summary and Future work.....</b>	<b>187</b>
<b>Publications from this project.....</b>	<b>192</b>

## List of Figures

Figure 1.1 The Nuclear Fuel Cycle [4].....	5
Figure 1.2 Uranium Milling process [5] .....	6
Figure 1.3 Yellow cake conversion process <sup>[7]</sup> .....	7
Figure 1.1.4 Centrifuges used in the enrichment process <sup>[10]</sup> .....	8
Figure 1.5 Fuel Fabrication process <sup>[8]</sup> .....	9
Figure.1.6 The splitting of a uranium nucleus via bombardment of neutrons. Taken from source <sup>[11]</sup> .....	10
Figure 1.7 Diagram of water flow in an LWR. Taken from source [14].....	12
Figure 1.8 Schematic of an AGR. Taken from source <sup>[16]</sup> .....	13
Figure 1.9 Conceptual schematic of a VHTR. Taken from source <sup>[17]</sup> .....	14
Figure 1.10 Illustration of the one-stage vitrification process <sup>[13]</sup> .....	18
Figure 1.11 The PUREX process taken from source <sup>[16]</sup> .....	19
Figure 1.12 ART: UCLan’s new reprocessing concept .....	23
Figure 1.13 Typical breakthrough curve <sup>[24]</sup> .....	32
Figure 1.14 Higgins Loop, a packed moving bed technique <sup>[32]</sup> .....	33
Figure 2.1 Gas adsorption stages. Take from source [1] .....	44
Figure 2.2 Typical curves of each of the five isotherm models. [2] .....	45
Figure 2.3 Figure 2.3 Types of hysteresis loop. H1 defines uniform spherical particles and subsequent pore size uniformity. H2 is characteristic of “ink-bottle” shaped pores with a pore network. H3 is attributed to slit shaped pores. H4 also defines slit shaped po .....	46
Figure 2.4 TGA plot of silver-filled thermosetting ink. [7] .....	49
Figure 2.5 Synthesis of AMP/PAN beads by gravity dropping. Taken from P. Kavi. [10] .	59
Figure 2.6 Confined jet design.....	60
Figure 2.7 Glass Nozzle setup .....	62
Figure 2.8 2-Layer sealed coaxial needle with threaded luer lock fastenings for gas and mixture feed inlets .....	63
Figure 3.2.1 Keggin structure of the phosphomolybdate anion (PMo12O40 <sup>3-</sup> ). .....	79
Figure 3.2 Internal Morphology of an AMP/PAN 70 bead displaying encapsulated AMP particulate .....	80
Figure 3.3 Cross section of AMP/PAN bead of 1-2mm in diameter synthesised with a reaction temperature of 80°C .....	86
Figure 3.4 SEM images of electrospinning products from PAN (Mw = 87,000)/DMF solution at different concentrations: (a) 2 wt.%, (b) 3 wt.%, and (c) 4 wt.%. Taken from source [36] .....	90
Figure 3.5 SEM images of the electrospinning products from PAN (Mw = 30,000)/DMF solutions at different concentrations: (a) 2 wt.%, (b) 3 wt.%, and (c) 4 wt.%. Taken from source [36] .....	90
Figure 3.6 Cross section of a single bead of AMP/PAN 70 produced using the glass nozzle method. ....	96
Figure 3.7 Cs ions rate of uptake at different temperature in 1 M HNO <sub>3</sub> .....	103
Figure 3.8 Cs ions rate of uptake at 25 °C in different acidity .....	104
Figure 3.9 Optical images of virgin and irradiated AMP powder and AMP-PAN composite beads. ....	105

Figure 3.10A to D: Measured Cs <sup>+</sup> capacities (mg/g) over time (min) and with Cs <sup>+</sup> concentration (mM) for virgin AMP (3.10A), irradiated AMP (3.10B), virgin AMP-PAN (3.10C) and irradiated AMP-PAN (3.10D) from 3 M HNO <sub>3</sub> solution. ....	107
Figure 3.11 Variation of Cs <sup>+</sup> K <sub>d</sub> values and capacity after 24 h exposure to AMP and AMP-PAN. ....	108
Figure 3.12A to D: Pseudo-second order Langmuir isothermal plots for virgin and irradiated AMP (3.12A and 3.12B), and virgin and irradiated AMP-PAN (3.12C and 3.12D), calculated from the data in Figure 3.12A to 3.12D.....	111
Figure 3.13 Cross section of AMP/PAN 70 taken from Kavi, P .....	114
Figure 3.14 Cross section of AMP/PAN 70 1-2mm bead diameter .....	114
Figure 3.15 External surface of AMP/PAN 70 1-2mm bead.....	115
Figure 3.16 Internal section of AMP/PAN 70 1-2mm bead diameter .....	115
Figure 3.17 Internal section of AMP/PAN 70 ~400µm beads. The polyhedral particulate is suggested to be AMP particles. ....	116
Figure 3.18 TGA spectrum of virgin and irradiated AMP.....	117
Figure 3.19 TGA spectra of virgin and irradiated AMP/PAN 70.....	118
Figure 3.20 TGA spectra of AMP/PAN 70 with 85,000Mw PAN and 150,000Mw PAN. ....	119
Figure 4.1 FT-IR of Sr adsorbent powders .....	141
Figure 4.2 FT-IR of Sr adsorbent PAN composites.....	142
Figure 4.3 Maximum Capacity observed for MMP and MMP/PAN adsorbent materials .	146
Figure 4.4 Rate of uptake of strontium using powder adsorbents in a 31 lppm Sr solution (pH stock solution 4.8).....	148
Figure 4.5 Rate of uptake of strontium using MMP/PAN materials in de-ionised water (pH stock solution 4.8).....	149
Figure 4.6 Cross section of HT50/PAN bead .....	154
Figure 4.7 Internal section of HT50/PAN bead.....	155
Figure 4.8 Cross section of HT52/PAN bead .....	155
Figure 4.9 Figure 4.9 External image of HT52/PAN bead Magx100.....	156
Figure 4.10 External section of HT52/PAN bead.....	156
Figure 4.11 TGA spectrum of MMP/PAN .....	157
Figure 5.1 Schematic of four zone SMBC <sup>[1]</sup> .....	166
Figure 5.2 Raffinate from SMBC elution using C100x10MBH, 1M HNO <sub>3</sub> .....	173
Figure 5.3 Extract from SMBC elution using C100x10MBH, 1M HNO <sub>3</sub> .....	174
Figure 5.4 Raffinate from SMBC elution using C100x10MBH, 3M HNO <sub>3</sub> .....	175
Figure 5.5 Extract from SMBC elution using C100x10MBH, 3M HNO <sub>3</sub> .....	176
Figure 5.6 Raffinate from SMBC elution using C100H, 3M HNO <sub>3</sub> .....	178
Figure 5.7 Extract from SMBC elution using C100H, 3M HNO <sub>3</sub> .....	179
Figure 5.8 Raffinate from SMBC elution using S910, 1M HNO <sub>3</sub> .....	180
Figure 5.9 Extract from SMBC elution using S910, 1M HNO <sub>3</sub> .....	181
Figure 5.10 Extract from SMBC elution using S910, 3M HNO <sub>3</sub> . ....	182
Figure 5.11 Extract from SMBC elution using S910, 3M HNO <sub>3</sub> .....	183

## List of Tables

Table 1.1. Above values for 45GWd/t U burn up and 8 year cooling post reactor, data provided by NNL .....	24
Table 1.2 Types of ion exchangers.....	27
Table 1.3 Selectivity of different media for cesium/sodium <sup>[24]</sup> .....	30
Table 2.1 Analytical Equipment.....	42
Table 2.2 Experimental and other equipment .....	43
Table 2.3 Materials used for analysis by ICP-MS.....	52
Table 2.4 Materials used in the make-up of stock solutions .....	55
Table 2.5 Materials used in the synthesis of AMP/PAN.....	56
Table 2.6 Strontium adsorbent powders.....	58
Table 2.7 Commercial ion exchange materials used for SMB taken from source [13] .....	65
Table 2.8 Stock solution composition for SMBC experiments.....	65
Table 3.1 Material Characterisation techniques.....	76
Table 3.2 Effect of differing cesium concentrations in 1M HNO <sub>3</sub> on capacity and K <sub>d</sub> values 3ppm initial $\sigma$ 0.019, 514ppm initial $\sigma$ 0.043.....	81
Table 3.3 Effect of AMP concentration on cesium uptake from 1M HNO <sub>3</sub> . AMP/PAN 70 $\sigma$ 0.046, AMP/PAN 50 $\sigma$ 0.044.....	82
Table 3.4 Effect of gel temperature of cesium uptake in 1M HNO <sub>3</sub> . 80°C $\sigma$ 0.042, 50°C $\sigma$ 0.027 .....	87
Table 3.5 Effect of PAN molecular weight on cesium uptake from 1M HNO <sub>3</sub> . 150kPAN $\sigma$ 0.035, 85k PAN $\sigma$ 0.004 .....	89
Table 3.6 Effect of reducing solvent volume on uptake of cesium in 1M HNO <sub>3</sub> . 50ml of solvent was used as opposed to 100ml. reduced solvent $\sigma$ 0.006, original $\sigma$ 0.035 .....	91
Table 3.7 Effect of increasing surfactant concentration on cesium uptake x1 tween $\sigma$ 0.012, x5 tween $\sigma$ 0.003.....	92
Table 3.8 Comparison of cesium uptake as a function of bead size. $\sigma$ <1mm0.028, 1-2mm $\sigma$ 0.042 .....	94
Table 3.9 Cesium uptake of composite produced using the glass nozzle technique. 1M $\sigma$ 0.047, 3M $\sigma$ 0.010.....	95
Table 3.10 Selectivity of AMP/PAN in the presence of high concentrations of cerium in 3M HNO <sub>3</sub> . Cs:Ce(iv) ratio of 1:50.....	98
Table 3.11 Selectivity of AMP/PAN in the presence of high concentrations of cerium in 3M HNO <sub>3</sub> . Cs:Ce(iv) ratio of 1:450.....	99
Table 3.12 Selectivity of AMP/PAN in the presence of high concentrations of cerium in 3M HNO <sub>3</sub> . Cs:Ce(III) ratio of 1:225.....	100
Table 3.13 Cesium selectivities.....	101
Table 3.14 Kinetics of cesium uptake using AMP/PAN 70 produced using glass nozzle .....	102
Table 3.15 Comparison of calculated Langmuir and Freundlich isothermal parameters.....	112
Table 3.16 Surface area of various AMP/PAN materials and AMP alone. Bead size measurements refer to the diameter.....	120
Table 3.17 Average pore diameter of various materials. Measurements of bead sizes refer to the diameter.....	121
Table 3.18 Accumulative pore volume of AMP/PAN 70 .....	122
Table 4.1 IR peaks present in the MMP and MMP/PAN materials .....	142
Table 4.2 Strontium uptake of powder adsorbents in de-ionised water (pH of stock solution was 4.86).....	144
Table 4.3 Equilibrated Strontium uptake measurements of MMP/PAN.....	145
Table 4.4 Strontium uptake of MMP's in 1M HNO <sub>3</sub> (pH 2.8).....	151
Table 4.5 Strontium uptake of MMP/PAN composites in 1M HNO <sub>3</sub> .....	151

Table 4.6 Selectivity of MMP/PAN composites in natural pH of stock solution (4.4)	153
Table 4.7 Surface area of MMP/PAN composite beads	158
Table 4.8 Average pore diameter of MMP/PAN composite beads	159
Table 4.9 Accumulative pore volume of MMP/PAN composite beads	159
Table 5.1 Retention times for Zr,Ce,Mo in 1M HNO <sub>3</sub> at flow rate 5ml/min	171
Table 5.2 Retention times for Zr,Ce,Mo in 3M HNO <sub>3</sub> at flow rate 5ml/min	171

## List of Equations

Equation 1.1 Reaction of TBP with uranium and plutonium.....	19
Equation 1.2 Exchange of hydrogen with cesium [24].....	26
Equation 1.3 Ion exchange of sodium in a mixed bed system [24] .....	27
Equation 2.1 BET method of gas sorption.....	47
Equation 2.2 Calculation of distribution coefficient.....	51
Equation 2.3 Calculation of capacity .....	51
Equation 2.1 Ion exchange of cesium with ammonium in AMP.....	79
Equation 2.2 Theoretical dissociation of AMP.....	83
Equation 2.3 Dissociation of Phosphoric Acid .....	84
Equation 2.4 Langmuir Isotherm .....	109
Equation 2.5 Pseudo first order Langmuir .....	109
Equation 2.6 Second Order Langmuir .....	109
Equation 2.7 Freundlich Isotherm.....	109
Equation 2.8 Second Order Freundlich.....	109
Equation 5.1 Calculation of Henry coefficient .....	168
Equation 5.2 Calculation of flow rate ratio.....	168
Equation 5.3 Mass balancing equation .....	168

## **Acknowledgements**

Firstly, a big thanks to Professor Gary Bond, who gave me the opportunity to undertake this research and provided valuable knowledge and guidance in completing it.

A special thanks must be given to Professor Harry Eccles, whose patience, guidance, wisdom and full support enabled me to complete this thesis. The amount of his valuable time he has given to me cannot be given back and has been crucial in the completion of this work. He has imparted a great deal of knowledge to me through some of his many stories. He is also the most generous Yorkshireman I have ever met.

I am also extremely grateful for the training and guidance received from Dr Runjie Mao, who always made time for me when he was busy.

I would like to thank the University of Central Lancashire and the EPSRC for providing the funds for this research.

I am truly grateful for the analytical suite technicians; Tamar Garcia Sorribes, Peter Bentley and Sameera Mahroof who have continually fixed the ICP-MS despite its resistance to maintenance and have always provided assistance when needed.

More personally, I would like to thank my Mum, who has had no clue what this work was about but continued to support me regardless.

Finally, I am indebted to my partner Trina, who has given me her full support during this project and has made several fair attempts at pretending to be interested in my work. Nice one.



## Abbreviations

Cs	Cesium
Sr	Strontium
Ba	Yttrium
TBP	Tri-Butyl Phosphate
PUREX	Plutonium Uranium Redox Extraction
AMP	Ammonium phosphomolybdate
U	Uranium
Pu	Plutonium
Ce	Cerium
Zr	Zirconium
Mo	Molybdenum
CO <sub>2</sub>	Carbon dioxide
β	Beta
α	Alpha
γ	Gamma
Gy	Gray
LWR	Light Water Reactor
BWR	Boiling Water Reactor

PWR	Pressurised Water Reactor
ppb	Parts Per Billion
ppm	Parts Per Million
nm	Nanometre
mM	Millimole
$\mu\text{m}$	Micrometre
$K_d$	Distribution coefficient
HLW	High Level Waste
ILW	Intermediate Level waste
LLW	Low Level Waste
NNL	National Nuclear Laboratory
AGR	Advanced Gas cooled Reactor
VHTR	Very High Temperature Reactor
Np	Neptunium
Am	Americium
THOREX	Thorium Redox Extraction
$\text{NO}_3$	Nitrate
$\text{HNO}_3$	Nitric acid

ART	Alternative Reprocessing Technology
GEN III	Generation 3 reactors
GEN IV	Generation 4 reactors
MA	Minor Actinide
HALES	Highly Active Liquor Evaporation and Storage
g/l	Grams per Litre
SMB	Simulated Moving Bed
SMBC	Simulated Moving Bed Chromatography
SO <sub>3</sub> H	Sulfonic acid
N <sub>+</sub> (CH) <sub>3</sub>	Trimethylamine
COO <sup>-</sup>	Carboxylate
NR <sub>2</sub>	Imide
Na	Sodium
H <sub>2</sub> O	Water
H	Hydrogen
Li	Lithium
K	Potassium
Mg	Magnesium
Co	Cobalt
Ca	Calcium
La	Lanthanum
CH <sub>3</sub> COO <sup>-</sup>	Acetate
C <sub>2</sub> O <sub>4</sub> <sup>-</sup>	Oxalate
SO <sub>4</sub> <sup>2-</sup>	Sulfate

mol/L	Moles per Litre
CAC	Continuous Annular Chromatography
SIXEP	Sellafield Ion Exchange Effluent Plant
UCLan	University of Central Lancashire
SEM	Scanning Electron Microscopy
ICP-MS	Inductively Coupled Plasma –Mass Spectroscopy
TGA	Thermo Gravimetric Analysis
BET	Brunauer-Emmett-Teller
FT – IR	Fourier Transform – Infrared Spectroscopy
OK	Odourless Kerosene
AMP/PAN	Ammonium phosphomolybdate/polyacrylonitrile
PAN	Polyacrylonitrile
MMP	Mixed Metal Phosphate
MMP/PAN	Mixed Metal Phosphate/Polyacrylonitrile
Mw	Molecular Weight
Bq	Becquerel
cm <sup>3</sup>	Centimetres cubed
m <sup>3</sup>	Metres cubed
μm <sup>3</sup>	Micrometres cubed.
CsMP	Cesium phosphomolybdate
te	Tonne

H	Henry coefficient
$\varepsilon$	Overall void fraction
$t^R$	Retention time
$t_0$	retention time of inert tracer (acetone)
$m_j$	ratio of net fluid flow rate to phase flow rate
$Q_j$	fluid flow rate in zone j
$V_{jD}$	extra column volume in zone j
HWR	Heavy Water Reactor

## Aims and Objectives

The aims of this project and thesis were to:

- Demonstrate that UCLan's alternative reprocessing technology (ART) concept is credible
- Modify the synthesis of cesium selective AMP/PAN and refine the production of AMP/PAN composite beads in order to optimise ion exchange performance and indicate how production costs could be reduced;
- Investigate the selectivity of AMP/PAN for cesium in the presence of a high excess of cerium a simulant for uranium and plutonium to assess its suitability for application in nuclear reprocessing;
- Synthesise and develop highly selective strontium adsorbents for potential use in spent nuclear fuel reprocessing;
- Undertake initial scoping studies with Simulated Moving Bed technology, to assess its potential use in an Alternative Reprocessing Technique (ART)

These would be achieved by the following objectives:

- Varying the reaction conditions such as temperature, viscosity, solvent volume and molecular weight of polyacrylonitrile to effect the cesium uptake capabilities of AMP/PAN and employ the use of various injection nozzles for bead formation;
- Batch ion exchange studies contacting AMP/PAN with solutions containing a high excess of cerium - a simulated substitute for uranium and plutonium;
- Perform strontium uptake experiments using mixed metal phosphate powders to evaluate selectivity, kinetics, stability and capacities;

- Encapsulate mixed metal phosphates into a polyacrylonitrile support to mimic AMP/PAN composite bead structure and observe ion exchange performance of the subsequent composites.
- Perform isocratic SMB studies using commercial resins previously tested in batch and single column studies for their performance capabilities with various other fission products to produce indicative baseline chromatograms for future comparisons.

# Chapter 1 Introduction

## 1.1 Background

The synthesis of selective adsorbents for fission product removal in separation science dates back over 50 years and there is now a comprehensive list of materials to choose from to remove ionic species such as  $^{137}\text{Cs}$  and  $^{90}\text{Sr}$  from different aqueous media. These two isotopes are of particular interest due to their high decay heat and radioactivity of their decay products –  $^{137}\text{Ba}$  and  $^{90}\text{Y}$  respectively. Although the library of materials for selective isotopic separation is substantial, there is yet to be a set of materials produced that are capable of functioning efficiently in the conditions found in spent fuel dissolver liquor and is thus one of the reasons the PUREX process is still unchallenged. A large amount of the current known selective adsorbents for various fission products have seen application in seawater decontamination due to fairly neutral pH value. The majority of the high radioactivity and heat decay in spent nuclear fuel comes from  $^{137}\text{Cs}$  and  $^{90}\text{Sr}$  [1] which causes some degradation of the tri-butyl phosphate (TBP) in the PUREX process [2]. A substantial challenge that scientists faces, is producing a material that is selective for various fission products whilst also overcoming the risk of radiolytic damage. It would therefore be of great advantage to synthesis multiple materials that remove cesium and strontium from the spent fuel dissolver liquor first, thus reducing radioactivity of downstream liquors. With the bulk of the radiation removed, the materials for the removal of other fission products don't have to be as resistant to radiation and heat, which means there is a wider pool of materials to choose from (some of these are discussed later).



Over the past 4-5 decades, ammonium phosphomolybdate (AMP) has been investigated for its selective removal of cesium ions from different media. As AMP powder is highly microcrystalline, the theoretical capacity is very high but roughly only 40% can be utilised in practice. A challenge presented in respect to AMP, is the understanding of its uptake mechanism. There have only been assumptions and theoretical conclusions regarding how the exchange between a target ion and the AMP takes place and which atoms are involved (discussed later in Chapter 3). Irrespective AMP still stands out as one of the best Cs adsorbents in strong acidic conditions and can be incorporated into different composites, these are discussed later along with a range of other cesium extractants.

Selective Sr adsorbents are more abundant than Cs adsorbents but tend not to perform well in strongly acidic media i.e. when pH values are lower than 2. This is a challenge as the aqueous solution used in the current reprocessing process is strong nitric acid (3-7M)<sup>[3]</sup>. It is therefore seen as necessary to design and synthesise a suitable strontium adsorber that has the same properties as AMP/PAN but selectively uptakes strontium. It would be advantageous if an adsorbent material could be produced that selectively uptakes both cesium and strontium in the presence of uranium – this could be the basis for future work.

Although conventional ion exchange processes have found favour at the front end of the nuclear fuel cycle and for purification of cooling water for power reactors, elsewhere they have struggled to make an impact. Conventional batch ion exchange processes are labour intensive, have limited efficiency and their cost effectiveness is questionable. The use of continuous chromatography could potentially overcome challenges presented by batch processes through efficient use of the ion exchange adsorbents accompanied with a cost effective and continuous process that requires less labour. The vision conceptualised throughout this thesis justifies the possible use of AMP/PAN to selectively remove cesium from spent fuel dissolver liquors and begins to explore the possibilities of a Simulated Moving Bed chromatographic technique for use in reprocessing spent nuclear fuel,

reducing and potentially eliminating High Level Waste for future nuclear fuel systems. The use of SMBC in the nuclear industry is almost non-existent, especially in the context of aiming to potentially eliminate HLW by extracting strontium and cesium prior to other fission by-products. The SMBC work presented herein is therefore preliminary and future endeavours to further this work would benefit from a highly developed SMBC methodology.

## 1.2 The Nuclear Fuel Cycle

There are two types of Nuclear Fuel Cycle; Closed and Open. These cycles outline the processes needed to obtain useable fuel for nuclear reactors. The Closed Nuclear Fuel Cycle is more relevant to this work as spent fuel is reprocessed (the current reprocessing technique is explained in section 1.2.6), as opposed to an Open Nuclear Fuel Cycle where the spent fuel is treated for disposal.

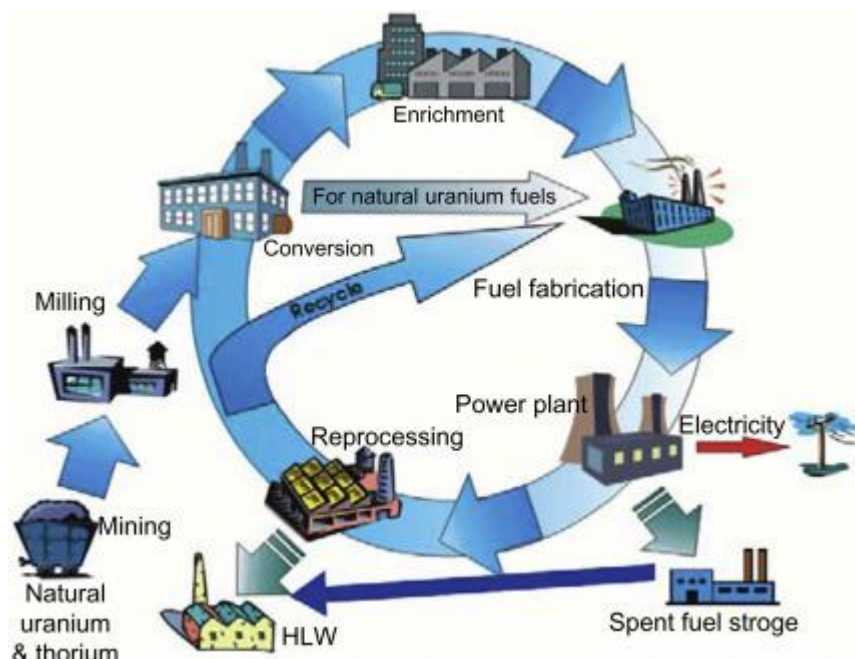


Figure 1.1 The Nuclear Fuel Cycle [4]

The nuclear fuel cycle can be seen in Fig 1.1 where both closed and open cycles are described. The closed nuclear fuel cycle will follow the continuous loop in the image whereas an open fuel cycle will deviate from the loop and go into spent fuel storage. The fundamental processes of obtaining useable nuclear fuel remain the same between the two cycles and are detailed in the following sub-sections.

### 1.2.1 Uranium Ore Mining and Milling

The nuclear fuel cycle begins with mining uranium ore. Naturally occurring uranium has an enrichment of about 0.7%, meaning the amount of fissile  $U^{235}$  in naturally occurring uranium ore is very low, hence the need for enrichment (see 1.3.3).

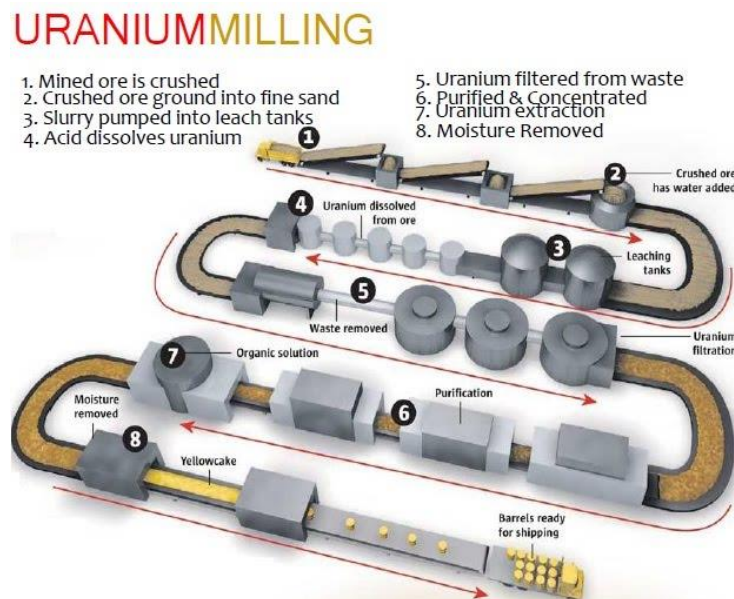


Figure 1.2 Uranium Milling process [5]

The ore exists typically as uranite ( $\text{UO}_2$ ) which can be found in various types of rock including granite. The rocks are milled after mining from natural deposits to turn it into a more practical form to extract the natural uranium. This milled material is commonly known as “yellow cake”.<sup>[6]</sup> The yellow cake requires conversion before it can be enriched (see following sections).

### 1.2.2. Uranium Ore Conversion

The now milled uranium ore must be converted to  $\text{UF}_6$  prior to enrichment, this involves reacting the milled material firstly with nitric acid. The resulting uranyl nitrate solution is subject to a solvent extraction process using TBP with odourless kerosene and the uranium is collected from the organic phase. The extractant is washed and calcined to produce  $\text{UO}_3$  which is then reduced to  $\text{UO}_2$  by hydrogen.

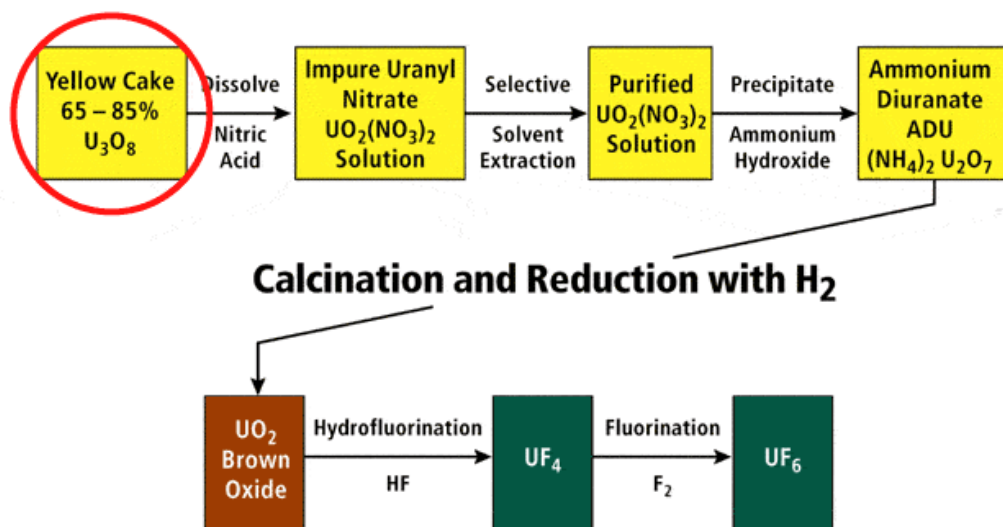


Figure 1.3 Yellow cake conversion process<sup>[7]</sup>

The  $\text{UO}_2$  is reacted with hydrofluoric acid (or hydrogen fluoride gas) to produce  $\text{UF}_4$  and then further fluorinated using fluorine gas to produce the desired  $\text{UF}_6$ .<sup>[8]</sup> This process is

labour intensive and extremely dangerous due to the use of chemicals such as hydrofluoric acid. As the yellow cake had not been enriched prior to conversion, the radiological impact is very low compared to the chemical hazards.

### 1.2.3 Enrichment

As the percentage of fissile  $U^{235}$  is still around 0.7%, this needs to be increased to a maximum of 5% (used in most current reactors using uranium as fuel) prior to fuel fabrication for nuclear fission to be more efficient and produce more energy per gram of material. The current enrichment process uses gas centrifuges. <sup>[9]</sup>



*Figure 1.1.4 Centrifuges used in the enrichment process <sup>[10]</sup>*

Molecules of  $UF_6$  containing  $U^{235}$  are around 1% lighter than the molecules containing other isotopes and thus can be separated when spun at speeds in excess of 50,000 rpm. The desired  $UF_6$  containing  $U^{235}$  collects near the centre and is collected.

#### 1.2.4. Fabrication of fuel

The last stage of the fuel cycle prior to nuclear fission is the fabrication of useable fuel. The enriched  $\text{UF}_6$  is collected and converted to  $\text{UO}_2$  using either a wet or dry process. The dry process involves producing uranyl fluoride by mixing  $\text{UF}_6$  with steam and then reduced by dilute hydrogen. The product is pure  $\text{UO}_2$  powder.

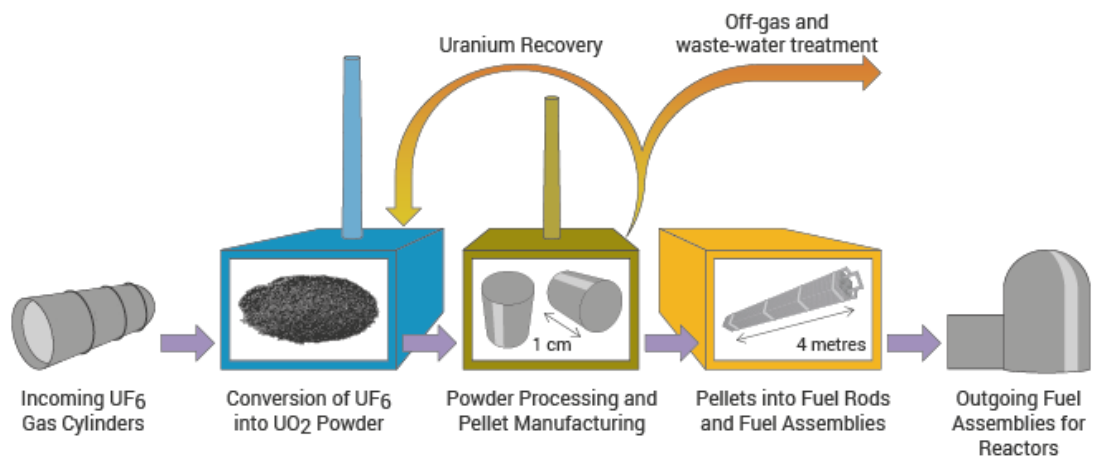


Figure 1.5 Fuel Fabrication process <sup>[8]</sup>

In the wet process, water is used to produce uranyl fluoride to which ammonia is added. The resulting mixture is filtered and reduced to produce pure  $\text{UO}_2$ . The powder produced can be pelletised and assembled into fuel rods for transport. [E]

### 1.2.5. Nuclear Fission Process

The initial process of nuclear fission involves the bombardment of the nucleus of a heavy atom – such as U-235. The speed of neutrons in thermal reactors is moderated to increase the likelihood of hitting a uranium atom.

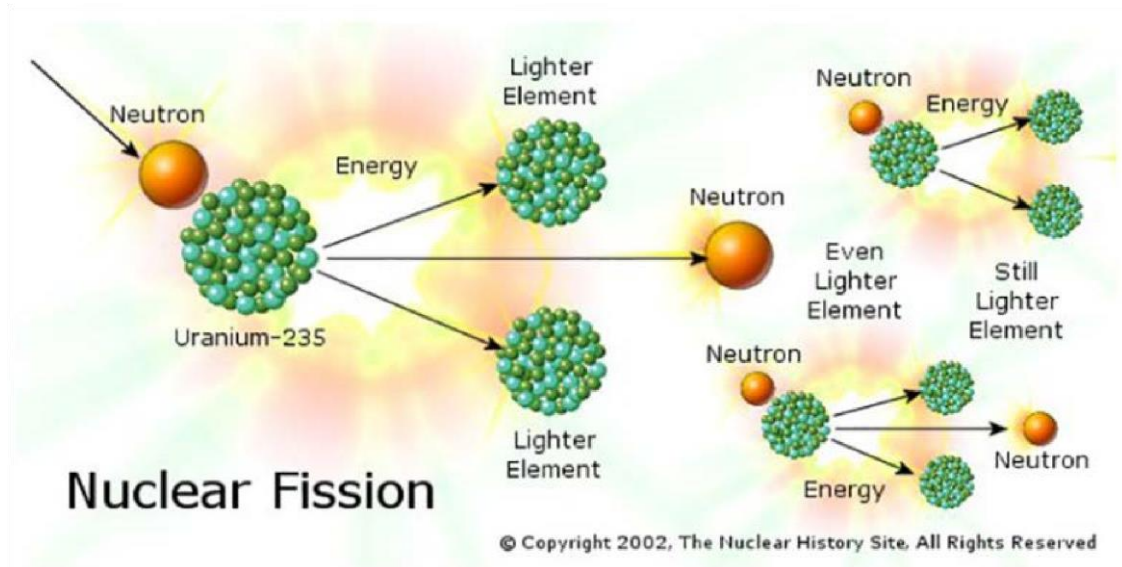


Figure.1.6 The splitting of a uranium nucleus via bombardment of neutrons. Taken from source <sup>[11]</sup>

The U-235 nuclei split into lighter nuclei, with the simultaneous release of more neutrons, which causes a chain reaction with further fissionable elements and creation of smaller fissionable atoms as is displayed in figure 1.1. The kinetic energy created from fission is then converted into thermal energy (1g of uranium-235 can produce ~250,000kWh if complete fission takes place). <sup>[12]</sup>

Roughly 6% of the heat generated inside the reactor is due to the decay of fission products<sup>[12]</sup>. Sufficient cooling methods (water, gaseous CO<sub>2</sub> or molten metal) are present to maintain a safe operating temperature. The most notable example of the importance of cooling is demonstrable through the cooling failure at Fukushima. Despite the cooling

failure around an hour after the reactor had shutdown, decay heat continued to be generated from the fuel. Spent fuel can still generate decay heat (around 10kW/tonne a year after removal from the reactor).<sup>[12]</sup> After around one to three years the fuel is removed from a reactor such as an AGR ( see section 1.3.5.2), largely as a result of diminishing U-235 content but also because of the growth of fission products, some of which are neutron poisons e.g. Gd.<sup>[12][13]</sup> The removed fuel can then either be reprocessed (see section 1.3.7) or interim stored as spent fuel.

#### 1.2.5.1. Types of Nuclear Reactors

There have been, currently are, and will be many new types of nuclear fission reactors. The common trait they all share is the generation of energy with production of waste consisting of a wide range of radionuclides .Some may be useful as future fuel e.g. Am once they have been separated whilst others have little or no use now. The new reprocessing concept detailed in the following sections, would potentially be applicable to both GEN III and GEN IV reactor systems (some briefly described below) due to the production of cesium and strontium as fission by-products. There are about 400 nuclear reactors in operation globally, with more than 100 planned before 2050.

##### 1.2.5.1.1. Light Water Reactors (LWR)

There are two currently operation types of LWR's; Pressurised Water Reactor (PWR) and Boiling Water Reactor (BWR). The fuel used in these reactors is conventional UO<sub>2</sub> fuel pins with the moderator being water, as opposed to deuterated water used in Heavy Water reactors (HWR).<sup>[14]</sup> In addition to being a moderator for the neutrons, the water flow cools the fuel rods as is displayed in figure 1.2.



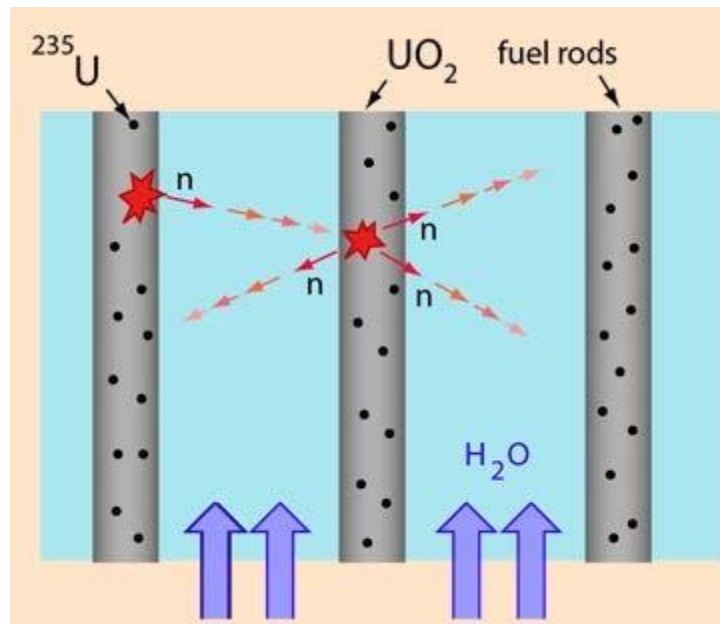


Figure 1.7 Diagram of water flow in an LWR. Taken from source [14]

Once the fissile uranium has been depleted, the fuel rods will be removed under radiologically secure conditions. There will be an abundance of highly radioactive and heat decaying isotopes in the spent fuel – particularly cesium and strontium. Their decay products –  $\text{Ba}^{137}$  and  $\text{Y}^{90}$  respectively - produce huge amounts of radioactivity and heat which results in the classification of High Level Waste detailed in section 1.2.6. This type of waste is produced by most currently operational reactors using uranium as nuclear fuel.

### 1.2.5.1.2. Advanced Gas cooled Reactor (AGR)

Currently operational in the UK, the AGR at Heysham Power Station uses the hot CO<sub>2</sub> gas to generate steam via heat exchangers for delivery to turbines, which in turn powers the electricity generators. The fuel employed is a collection of pins containing U-235 enriched uranium dioxide pellets held within a graphite core.<sup>[15]</sup> Figure 1.3 shows the key components of an AGR.

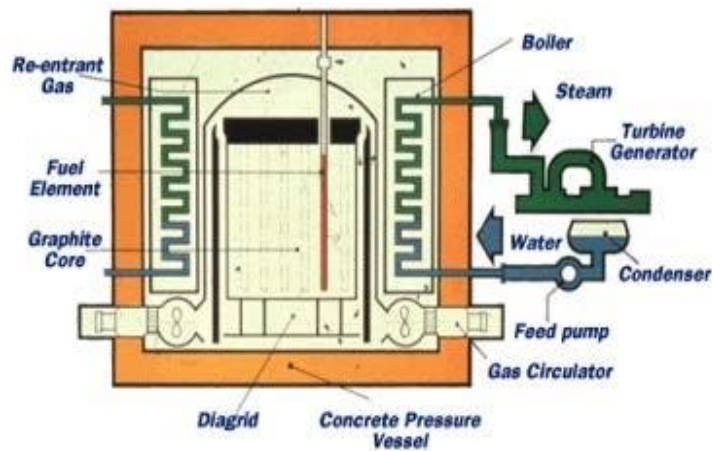


Figure 1.8 Schematic of an AGR. Taken from source <sup>[16]</sup>

The fuel that resides in the reactors lasts for 1 to 3 years depending on the enrichment value before it is removed. It has been a customary process for many years that the spent fuel is transported to Sellafield for reprocessing.

### 1.2.5.1.3. Very High Temperature Reactor (VHTR)

One of the conceptualised Gen IV nuclear systems is the Very High Temperature Reactor (VHTR). This type of reactor is designed to generate not only electricity, but also hydrogen as a product of the fission process of water in the hydrogen production plant. A schematic can be seen in figure 1.4

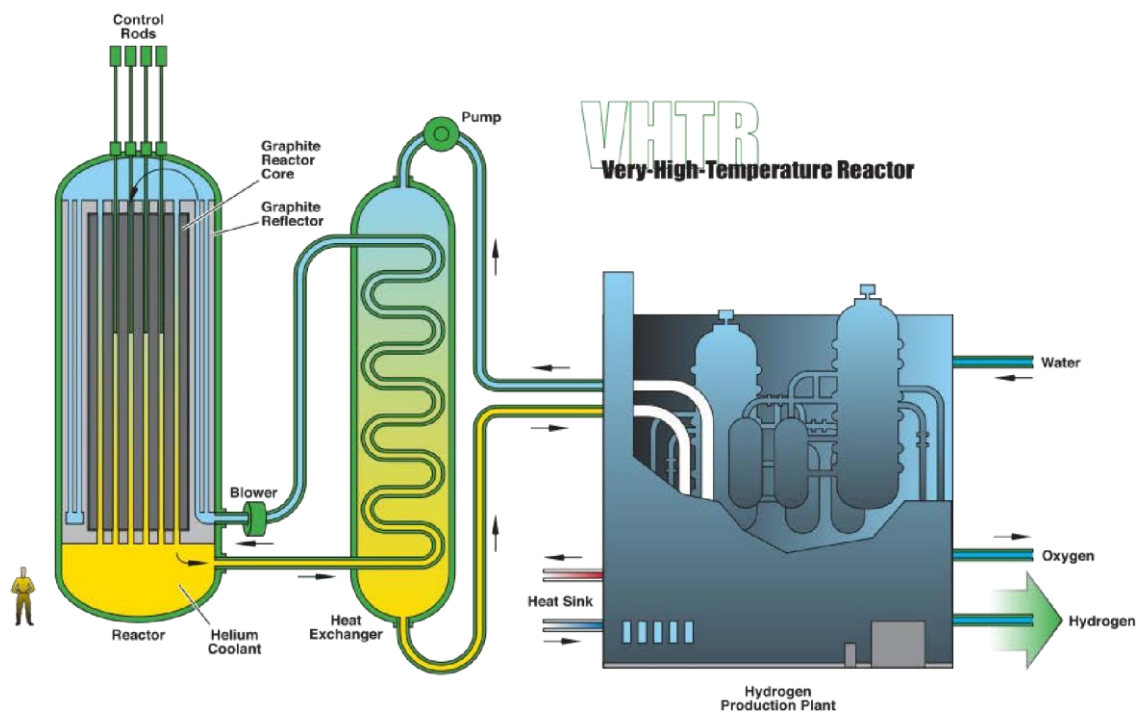


Figure 1.9 Conceptual schematic of a VHTR. Taken from source <sup>[17]</sup>

The hydrogen would be contained within water which allows extraction of such via various methods including thermal or electrolysis technique. A thermal process may be favoured as the heat from the outlet ( $\sim 1000^{\circ}\text{C}$ ) could be used for said extraction. This could potentially lead to a reliable and efficient source of hydrogen. Unlike LWR's, the VHT would employ liquid helium as a reactor core coolant which although would cool a reactor

core much quicker than water – and hence better temperature control – could be expensive. The fuel employed would be a micro particle with uranium oxide (UO) at its core, surrounded by several layers of porous and nonporous carbon coated in a carbon ceramic. This fuel has been coined TRISO (Tristructuralisotropic). <sup>[17]</sup>

#### 1.2.6. Nuclear fission waste

A nuclear site is obliged to have an approved waste management plan that minimises waste arising and reduces disposal costs. Certain materials that may have an intrinsic value such as uranium, plutonium and spent nuclear fuel have not been declared wastes by their owners in compliance with Government policy. Radioactive waste is assigned to three main categories; High Level (HLW), Intermediate Level (ILW) and Low Level Waste (LLW). HLW and ILW wastes after treatment are currently stored on reactor sites awaiting the provision of a deep geological repository (GDF). The treatment and disposal of spent nuclear fuel is detailed in section 1.2.7. The main deciding factors on the classification of nuclear waste are radioactivity and heat generation. The different classifications are described below.

##### 1.2.6.1 High Level Waste (HLW)

High Level Waste is derived from spent fuel dissolver liquor, which after reprocessing produces a liquid waste containing all the radionuclides except those of uranium and plutonium which is subsequently vitrified into a solid glass HLW <sup>[11]</sup>. This type of waste requires substantial shielding and cooling. Spent fuel dissolver liquors contain highly radioactive, short/medium lived fission products such as <sup>137</sup>Cs and <sup>90</sup>Sr, which decay to

$^{137}\text{Ba}$  and  $^{90}\text{Y}$  respectively, along with numerous  $\alpha$  emitting radionuclides such as U, Pu, Np, Am etc. Over 90% of radioactivity generated by waste from the nuclear fuel cycle is attributed to HLW. Storing HLW is expensive, requires strict control and heavy shielding as it is heat generating. <sup>[12]</sup>

#### 1.2.6.2 Intermediate Level Waste (ILW)

Intermediate Level Waste contains radionuclides that exhibit comparative high radioactivity but are not heat generating. Consequently, storage and encapsulation is not as demanding as HLW, with concrete encapsulation being the preferred option in the UK. ILW arises from reprocessing plants (Magnox swarf, stainless steel, zircaloy fuel pin cladding and graphite from AGR sleeves). In addition, sludges from reactors, ion exchange resins etc from other stages of the nuclear fuel cycle also require conditioning and treatment, i.e. encapsulation. <sup>[14]</sup>

#### 1.2.6.3 Low Level Waste LLW

The most common form of nuclear waste and considered the least harmful to life is Low Level Waste. This can be any form of nuclear waste that contains less than  $4\text{GBq/m}^3$   $\alpha$  emitting radionuclides and  $12\text{GBq/m}^3$   $\beta/\gamma$  emitting radionuclides. Over 92% of all nuclear wastes are classified as LLW. <sup>[15]</sup>

## 1.2.7 Waste management and Reprocessing

As explained previously, in a closed nuclear fuel cycle spent nuclear fuel is reprocessed as there is usable uranium present in spent fuel thus increasing the efficiency of the fission process. The current reprocessing technique used worldwide is the PUREX process and is described in the section 1.2.7.2. Much of the reprocessed and non-reprocessed spent fuel contains isotopes that must be transformed into a suitable waste form as explained in the next section.

### 1.2.7.1 Vitrification

In the nuclear industry, vitrification is the incorporation of liquid nuclear waste (usually HLW as it contains the most radioactive species) into a solid form that possesses long-term stability for storage. Typically, HLW has been transformed into borosilicate glass<sup>[11]</sup>. The process involves turning the liquid waste into a powder by calcining the liquor and then melting the resulting powder into a molten glass as is illustrated in figure 1.5.

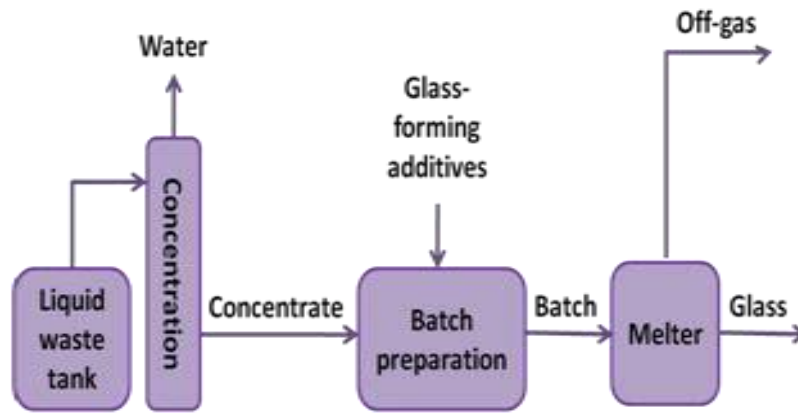


Figure 1 10 Illustration of the one-stage vitrification process <sup>[13]</sup>

Once the powder is a molten form, it is cooled rapidly after pouring to reach the glass transition temperature – that is, the temperature at which the molten material will start to turn into glass.

#### 1.2.7.2 Plutonium Uranium Redox Extraction PUREX

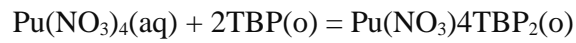
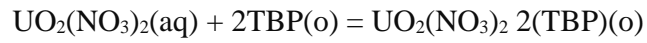
Throughout the world, reprocessing of nuclear fuels employs some form of the PUREX or THOREX solvent extraction processes using tri-n-butylphosphate (TBP) as the extracting agent.<sup>[3]</sup> Although no reprocessing of civil power reactor fuel has occurred and/or planned in the U.S., the Savannah River, Hanford, and Idaho Falls defence sites use TBP-based solvent extraction for military purposes. European, Japanese, Russian and Indian reprocessing facilities use PUREX or modified PUREX processes.

The PUREX process a solvent extraction process (figure 1.5) based on the use of tributyl phosphate (TBP, the extractant) dissolved in a suitable diluent. The TBP solvates the uranium and plutonium nitrate salts, which allows extraction from the aqueous to organic phase. In the UK, odourless kerosene (OK) is used, but dodecane is favoured in other

countries<sup>[3]</sup>. The species involved in the extraction process are highlighted in equation

1.1.

*Equation 1.1 Reaction of TBP with uranium and plutonium*



Where:

(aq) defines aqueous phase

(o) defines organic/solvent phase

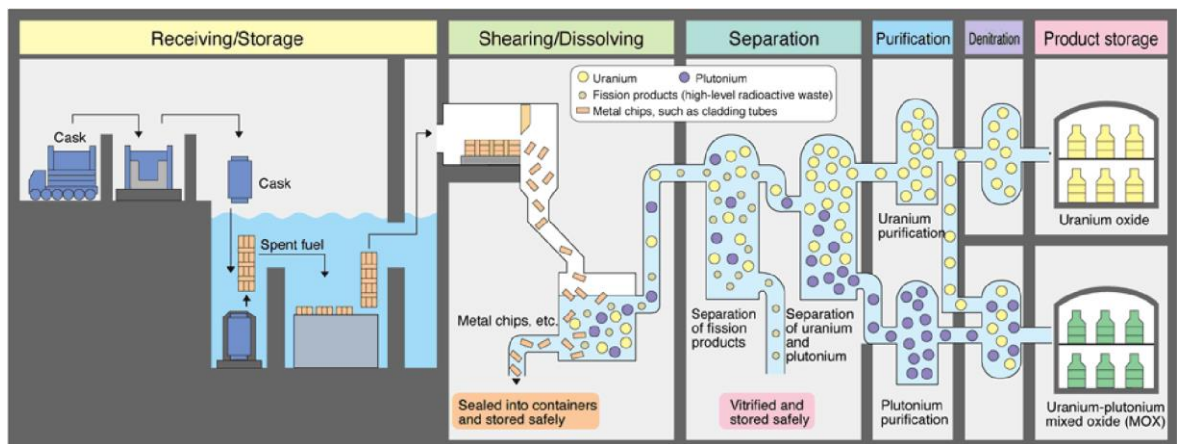


Figure 1.11 The PUREX process taken from source<sup>[16]</sup>



All other radioisotopes are ultimately left behind in the aqueous phase (raffinate).<sup>[3]</sup> The aqueous phase is obtained from the dissolution of the irradiated fuel (uranium metal rod or uranium dioxide fuel pellets) in hot 7M nitric acid<sup>[3]</sup>. Once the uranium and plutonium nitrate salts have been extracted in to the solvent phase and thus separated from the other radionuclides, they can then be back extracted into another aqueous phase. First plutonium nitrate as  $\text{PuO}_2(\text{NO}_3)_2$  and  $\text{Pu}(\text{NO}_3)_4$  is reduced to the lower oxidation state ( $\text{Pu}(\text{NO}_3)_3$ ) which back extracts into a ~1M nitric acid as the TBP affinity for the lower oxidation state is virtually zero. Having recovered the plutonium, the solvent phase, still containing the uranium nitrate, is contacted with warm dilute nitric acid (~0.01M at 60°C) which causes it to re-distribute in favour of the aqueous phase<sup>[3]</sup>. The TBP has a good affinity for both Pu(VI) and Pu(IV) but virtually no affinity for Pu(III). Both the higher oxidation states of Pu can be reduced with either ferrous sulphamate (Magnox reprocessing) or uranous nitrate (THORP reprocessing). The extracted uranyl nitrate in the solvent phase is unaffected by both these reducing agents as the redox cell energetics are unfavourable and hence remains in the solvent phase<sup>[3]</sup>. By using a very dilute nitric acid solution (~ 0.01M) the uranium can be back extracted into a separate aqueous phase thus accomplishing separation of Pu and U. Whilst uranium and plutonium coexist in the same phase the equipment employed has to meet certain criteria to prevent criticality, largely from the plutonium present. This can be achieved by use of soluble neutron poisons, neutron poisons fabricated into stainless steel or equipment that is safe by shape. The THORP uses both poisons and safe by shape equipment e.g. pulse columns. The TBP extractant is available comparatively cheap and from several sources, it has a low volatility and a high flash point making it safe under the operating conditions.

#### 1.2.7.2.1 Challenges of the PUREX process

Although the PUREX process achieves its primary objects to produce high purity U and Pu for recycling, it has some serious challenges and thus an alternative technique should be considered for future reprocessing. The degradation of both the extractant TBP and diluent (OK) by both hydrolytic and radiolytic reactions presents several challenges as these degradation products (dibutyl hydrogen phosphate and monobutyl dihydrogen phosphate) have an affinity for fission products and some minor actinides. <sup>[2]</sup> It is therefore a necessity for the extractant to be stable in the presence of radiation, especially when removing cesium and strontium from spent fuel dissolver liquor and/or High Level Waste (HLW).

A new reprocessing procedure (or development of the current technique) would therefore benefit from the removal of caesium and strontium, as these radionuclides produce the largest heat load, before separation of other ions thus reducing the radioactivity of the remaining waste liquor. <sup>[1]</sup>

In the past the ultimate aim of nuclear reprocessing was to recycle uranium and plutonium, but now nuclear waste management is the priority. UCLan's approach requires adsorbents to selectively remove fission products and ultimately minor actinides from uranium and plutonium. Ideally, the adsorbents should have high affinities for the target radionuclides as they will be present, in significantly lower concentrations than uranium and plutonium, for example ~ 20 Kg/te spent fuel for fission products compared with ~900 Kg/te of uranium and plutonium. In addition, the library of adsorbents that are stable in the presence of the high temperatures and radioactivity being emitted from short/medium lived fission products is small. Removing the high level of heat from decay of fission products allows

other, less stable, organic materials to be used for extraction of minor actinides such as commercially available resins.

#### 1.2.8 UCLan's Concept (ART)

It is envisaged that overcoming the challenges presented by PUREX could be eradicated by designing a new reprocessing technique that initially removes the major heat load; this will require materials with high efficiency and selectivity with ~100% uptake.

Our Alternative Reprocessing Technology concept (ART), Figure 1.7 [stage 4 & 5], is based on continuous chromatographic separation of fission products and minor actinides from uranium and plutonium isotopes in spent fuel dissolver liquor. The method development of stag 4 and 5 is presented by the results in Chapter 5.

Our process offers many advantages over the PUREX process as discussed later in this thesis. Elements of our proposed process could be, in the interim, incorporated into the existing PUREX flowsheet, with the potential to improve efficiency, safety and economy, whilst significantly reducing the volume of HLW. This would be a major improvement and one needed for the next generation (GEN IV) and subsequent generation of nuclear reactors. ART would encourage a greater proportion of spent fuel to be reprocessed compared with the current figure of less than 30% <sup>[17]</sup>, thus adding to the sustainability of the nuclear fuel cycle. Non-proliferation concerns are pacified, as U and Pu, if needed, are not separated until the final stages of our technology.

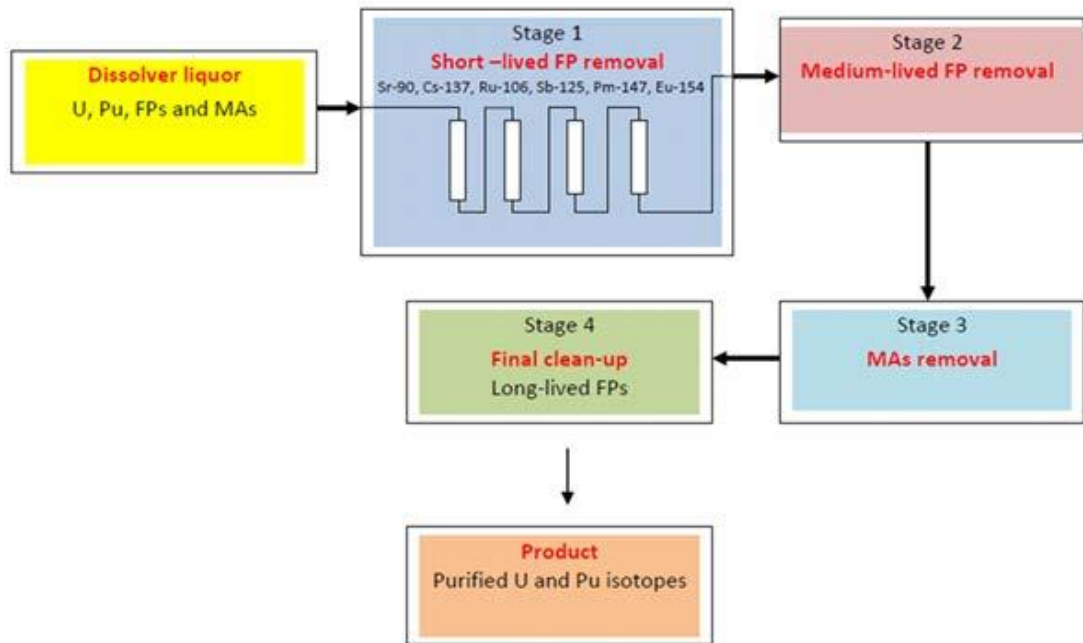


Figure 1.12 ART: UCLan's new reprocessing concept

Figure 1.7 depicts the short-lived fission products which produce the bulk of the heat/radioactivity would be removed first via continuous chromatography which is reviewed later. Cesium and Strontium are the two main contributors to heat decay in spent fuel, removal of these isotopes first could potentially eliminate Highly Active Waste and save the nuclear industry a substantial amount of money spent on waste management <sup>[18]</sup>. Table 1.1 shows the heat contribution of various isotopes, if all the cesium and strontium was removed from the spent fuel dissolver liquor, the final waste form would have heat load, lower than  $2\text{kW/m}^3$ , i.e. classed as Intermediate Level Waste (ILW) <sup>[1]</sup>. In addition, this removal of these fission products resulting in a less radioactive liquor would negate heavy shielding requirements, delay storage and eliminate the formation of cesium phosphomolybdate solids formation in the HALES evaporator and storage tanks; these solids cause blockages in transfer pipes <sup>[19]</sup>. The ART concept was developed circa 2012, but since then a considerable amount of work has been undertaken at UCLan which has resulted in the identification of AMP and its

potential to “specifically” remove cesium from nitric acid liquors thus negating a chromatographic separation.

*Table 1.1. Above values for 45GWd/t U burn up and 8 year cooling post reactor, data provided by NNL*

	Bq/tU	Heat Rating Factor	Heat Rating Contribution
	45GWd/tU	(W / Bq)	(W / tU)
Y-90	3.14E+15	1.50E-13	4.70E+02
Sr-90	3.14E+15	3.13E-14	9.84E+01
Rh-106	8.90E+13	2.60E-13	2.31E+01
Sb-125	4.65E+13	8.54E-14	3.97E+00
Cs-134	5.02E+14	2.75E-13	1.38E+02
Cs-137	4.38E+15	2.98E-14	1.31E+02
Ba-137m	4.14E+15	1.06E-13	4.39E+02
Ce-144	3.33E+13	1.78E-14	5.92E-01
Pr-144	3.33E+13	1.98E-13	6.60E+00
Eu-154	1.72E+14	2.42E-13	4.16E+01
Pu-238	3.34E+11	8.96E-13	2.99E-01
Pu-239	2.60E+10	8.40E-13	2.18E-02
Pu-240	3.82E+10	8.42E-13	3.22E-02
Pu-241	8.00E+12	8.59E-16	6.87E-03
Am-241	7.65E+13	9.04E-13	6.91E+01
Cm-242	9.93E+09	9.95E-13	9.88E-03
Cm-244	1.21E+14	9.46E-13	1.14E+02

There are few materials that have shown to take up cesium and strontium from very strong nitric acid (~3M) solutions with reasonable capacities. Equally their selectivity in the presence of other ions and their pH stability is questionable. Development of known materials and synthesis of possible new adsorbents for cesium and strontium is a fundamental part of designing our new reprocessing technique using continuous chromatography.

### 1.3 Continuous Ion Exchange Chromatography

Chromatography has suffered in the past as it was operated in batch mode resulting in an economic disadvantage. With the advent of simulated moving bed (SMB), chromatography is now established largely in the pharma industry and for large organic molecule separations<sup>[20][21]</sup>. SMB however, has not been adopted for inorganic molecule applications and certainly not by the nuclear industry. Simulated Moving Bed can offer a more efficient and selective separation process than conventional batch ion exchange methods. Our interest in chromatography for spent nuclear fuel reprocessing arose from the concentrations of the cesium and strontium and other fission products in spent fuel dissolver liquor. The comparatively low concentration of cesium and strontium (~1g/l) to that of Uranium (~300g/l)<sup>[22]</sup> in spent fuel liquors would suggest that the former two are amenable to separation via ion exchange chromatography. Selective separation via chromatography typically decreases with increasing concentration of ion, as is reported in work by Emmott<sup>[23]</sup>. This was true for Emmott's single column studies<sup>[23]</sup> but not necessarily for SMB as multiple columns and a fully customisable operation based on retention times offers several advantages such as the experimental protocols can be

modified to allow species to be separated in a specific order and more efficiently; this is addressed in more detail in chapter 5.

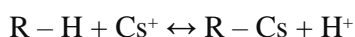
### 1.3.1 Principles of Ion Exchange

Ion exchange is a process in which ions in a solution are exchanged with suitable ions bound to a solid adsorbent material (resin). The process can occur via cationic or anionic exchange, whereby the exchanger ion bound to the resin is negatively charged or positively charged respectively. There are many factors contributing to an efficient ion exchange, most of which can be controlled and modified in order to achieve complete or near complete (99%) exchange.<sup>[24]</sup> These factors include but are not limited to:

- Kinetics;
- Surface area and porosity of the exchanger;
- Selectivity of the exchanger for specific ions;
- Capacity of the ion exchanger; - Temperature.

In addition, specific ions will have varying affinities for different exchange resins depending on the ionic group bound to the adsorbent. This can be used to great advantage if specific ions need to be separated from a multi-element solution. Therefore, the need for selective adsorbents is of paramount importance if ion exchange is to be employed in large-scale industrial processes. An example of a cationic exchanger involves the exchange of a hydrogen ion with a cesium ion viz:

*Equation 1.2 Exchange of hydrogen with cesium [24]*



R represents the insoluble part of the resin

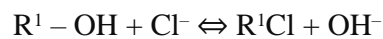
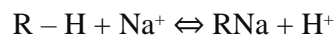
The overall charge is neutralised by the complete exchange of hydrogen with cesium. Ion exchangers can be classified as is presented in table 1.2

*Table 1.2 Types of ion exchangers*

Type of exchanger	Examples of functional groups	Effective pH range
Strong acidic	SO <sub>3</sub> H	0 - 4
Strong basic	N <sup>+</sup> (CH <sub>3</sub> ) <sub>3</sub>	Independent
Weak acidic	COO <sup>-</sup>	6, 14
Weak basic	NR <sub>2</sub>	0-7

If a solution contains cations and anions, then a mixed bed system can be employed whereby the system contains a mixture of cationic and anionic exchange resins. An example is displayed in equation 1.3.

*Equation 1.3 Ion exchange of sodium in a mixed bed system [24]*





Water is weakly dissociated and thus the exchange is driven to the right side of the equation.

As demonstrated by Emmott's work commercially available ion exchangers have poor affinities and selectivities for cesium in relatively strong nitric acid <sup>[23]</sup> which lead UCLan to develop new ion exchangers.

#### 1.3.1.1. Batch ion exchange

Batch ion exchange is largely limited to laboratory studies which can be subsequently compared with fixed bed studies. Batch processes employ a vessel which contain the ion exchange resin and solution of interest. This mixture is stirred or shaken at a specific speed to ensure efficient exchange but not to cause attrition of the resin beads. <sup>[25]</sup>

Separation of the resin and liquor is comparatively simple; decantation, gravity settling or if necessary centrifugation can be employed. Examples of batch uptake processes which employ such techniques would be the use of cellulose derivatives as ion exchangers for proteins <sup>[26]</sup>. In other ion exchange processes such as the de-mineralisation of water, the resin and water after equilibration are typically filtered to separate the two.

At laboratory scale the process is relatively simple but on scale-up becomes more complicated with the attrition of resin beads becoming a serious consideration, static columns overcome the attrition challenges but other considerations such as the physico-chemical characteristics of a resin need to be balanced to ensure an efficient and effective adsorption of ions from solution.

### 1.3.1.2. Ion Exchange equilibrium and selectivity

There are several terms that can describe the equilibrium of an ion exchange process: -

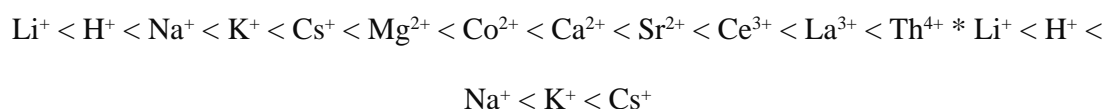
Distribution coefficient ( $K_d$ )

- Selectivity coefficient
- Separation factor (usually denoted ( $S_i$ ))
- Isotherm (typically Langmuir and Freundlich)

Some of these terms are described later in chapter 2 and are explored in more detail in work my

Helfferich <sup>[27]</sup>.

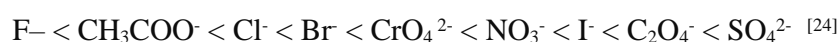
The selectivity of ion exchange resins and long term adsorption can be of paramount importance in ion exchange processes where specific species need to be separated. Ion exchange may be attributed to the ionic radii of a target ion and as such the affinity of an organic cationic exchange material for certain cations typically increases with increasing charge on the exchanging ion. <sup>[23]</sup> The work herein employs the use of hydrated materials thus the ionic radii is larger than that of the un-hydrated ion. A typical series of affinities for a cationic organic ion exchanger in order of increasing atomic number is as follows:



\*(Li+ is an exception, owing to its high hydration energy)

[24]

And for anions:



As mentioned, selectivity is one of the most important factors to be considered in an ion exchange process. Table 1.3 presents the selectivities of different ion exchange materials for cesium.

*Table 1.3 Selectivity of different media for cesium/sodium <sup>[24]</sup>*

Ion Exchange material	Concentration of sodium (mol/L)	Selectivity coefficient $k^{Cs/Na}$
Strong acid resin	1.00	<10
Cesium-selective resin	6.00	11400.00
Zeolite (mordenite)	0.10	450.00
Silico-titanate	5.70	18000.00
Hexacyanoferrate	5.00	1500000.00

### 1.3.2. Kinetics of ion exchange chromatography

For industrial scale processes, the rate of ion exchange is an important consideration as it will impact on running costs and the dimensions of the system. In most cases, fast kinetics are desired (as is much the case for the ART concept in this work) in order to achieve a quick separation of species. As spent fuel dissolver liquors contain highly radioactive species, they must be handled with extreme and lengthy safety procedures. A process with fast kinetics would reduce exposure time to the workers and also influence the design of a system (exposure to corrosive chemicals and radioactivity).

Ion exchange in a solid-liquid extraction relies on the diffusion of ions through the solution (described by  $K_d$ ). This can be broken down into several steps:

- Diffusion of soluble ions through the solution to the exchangeable site;
- Diffusion through a hydrated film surrounding exchangeable site;
- Diffusion through the exchangeable ion. [24]

High concentrations of ions in solution will typically result in fast kinetics depending on the nature of the exchanger. In this work, equilibration of the ion exchange has shown to be as quick as 1 hour for batch studies (chapter 3), of course this will be different for column studies where the resin is subject to flow rates as opposed to agitation.

### 1.3.3. Capacity

Ion exchange capacity describes the total available exchange ability of an ion exchange resin. This value should be constant for a given ion exchange material depending on conditions not limited to; concentration of solution and amount of resin per volume of solution and is given in milligrams per gram (mg/g). The equation for calculation of capacity is given in chapter 2.

The capacities of a resin for a specific ion obtained from batch studies cannot always be transferred to column techniques due to counter ions [24]. In terms of the nuclear industry, decontamination factors must be calculated (the ratio of radioactivity before and after the decontamination of contaminated objects)<sup>[28]</sup> so it is known when a resin must be replaced. For column techniques, a breakthrough curve (figure 1.8) must be obtained to gather information on elution behaviours of species within a liquor.

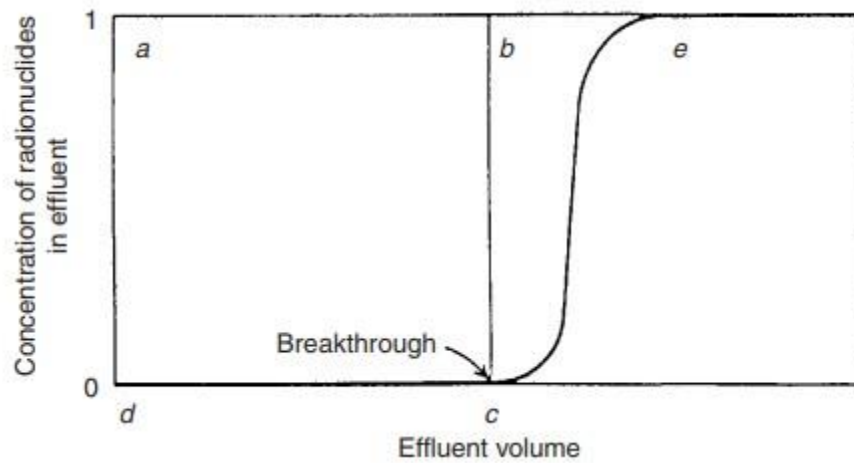


Figure 1.13 Typical breakthrough curve <sup>[24]</sup>

The breakthrough depends on several factors:

- Particle size of the resin;
- Flow rate;
- $K_d$  values.

A more detailed description of various ion exchange processes can be found in the references. <sup>[29, 30]</sup>

#### 1.3.4. Moving Bed Ion Exchange

Moving bed ion exchange/chromatography was evaluated some 40 years ago <sup>[31][32]</sup>. The technology i.e. column design was not widely implemented at the commercial scale largely due to the attrition of the resin beads. The fundamental of this chromatographic technique

was the counterflow of the packed bed to the flow of the solution. One account of this technique used commercially is the Higgins technique pictured in figure 1.9.

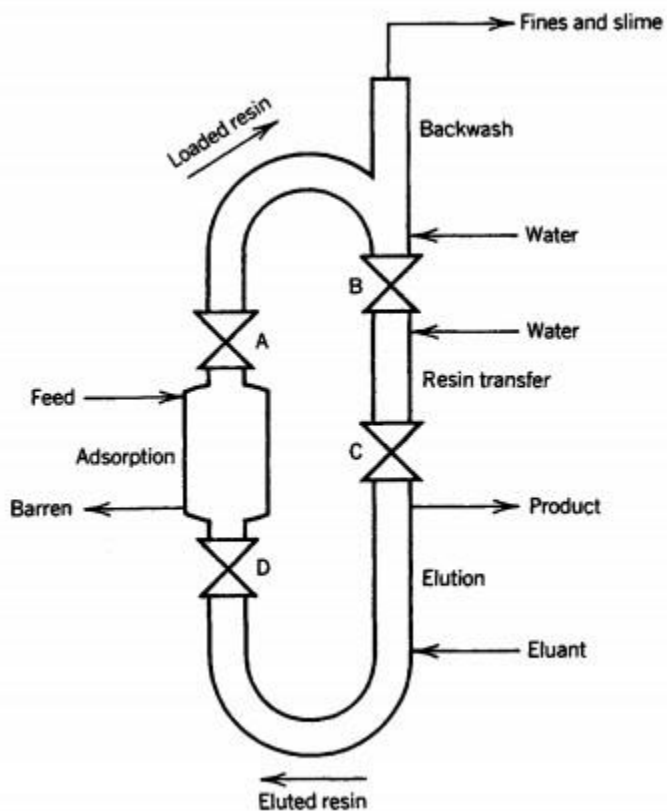


Figure 1.14 Higgins Loop, a packed moving bed technique <sup>[32]</sup>

The techniques comprised of a continuous loop an incremental flow of resin via displaced water. As mentioned, the use of moving bed systems leaves the resin liable to attrition, therefore limiting the effectiveness of a chromatographic separation. <sup>[31]</sup>

### 1.3.5. Simulated moving bed chromatography (SMB or SMBC)

Simulated Moving Bed (SMB) is a virtual replication of resins being moved from one column to another, as described in the previous section. Although some research has looked into continuous systems <sup>[21,33,34]</sup> like SMBC, there are no reports of work using this system and/or for experiments with nitric acid liquors as the feed solution. UCLan's concept (ART) would further develop SMBC technology in an arena hitherto unexplored. The benefit of SMBC is that it provides better results in terms of efficiency and selective separation than batch studies and reduces the labour, time spent and cost of materials. The solid and liquid phase is utilized more efficiently than in batch studies and other chromatography methods.<sup>[33]</sup> SMBC can utilise several columns with a counter-current flow of the liquid phase by simulating movement of the absorbent beds as opposed to fixed bed non-continuous systems. With batch and/or fixed bed systems, it is also difficult to achieve a high purity and yield without intense labour and high cost. <sup>[33]</sup>

A single column system does not make full use of the whole column as separation of materials occurs in a small part rather than across the whole length of the column bed. In SMBC, around 60% of the stationary phase is involved in in a separation with the other 40% ready for the next cycle. This continuous flow provides principally an infinite bed length but does not cost as much as large scale single columns due to less materials being used and does not require as much labour as batch experiments. <sup>[34]</sup> The efficient application of SMBC was first demonstrated in the oil (Ebex process) <sup>[35]</sup> and gas industry before being adopted by the pharmaceutical and food industries.

### 1.3.6. Continuous Annular chromatography

The use of Continuous Annular Chromatography (CAC) has seen employment in many applications and was initially explored for the separation of Hf from Zr by Oak Ridge Laboratory.<sup>[34]</sup> Other studies involved the separation of isotopes such as Uranium-238/235 and of boron isotopes using an anion exchange resin<sup>[35]</sup>. The work proved that CAC separations were more effective than batch column chromatography and CAC has been reported to operate quickly.<sup>[36]</sup> Although CAC has been used for the separation of zirconium and hafnium successfully in sulfate form and has produced pure zirconium<sup>[36]</sup>, neither CAC nor SMB have been previously considered for nuclear reprocessing.

### 1.3.7. Ion Exchange and chromatography in the Nuclear Industry

Ion exchange processes are not new to the nuclear industry. In fact it was the pioneering work of Kunin<sup>[37]</sup> that led to the development of more mechanically stable organic polymers now used for the extraction of uranium from dilute sulphuric acid (uranium mining/milling operations), cleaning up of spent decontamination liquors etc.<sup>[37]</sup> In more recent times natural occurring adsorbents such as zeolites (clinoptilolite) have found application for nuclear waste liquor clean up, e.g. BNFL's SIXEP for the removal of Cs/Sr from low-level liquid waste prior to discharge to the Irish Sea.<sup>[38]</sup>

In view of the introduction to this thesis, the ART concept described is a unique and novel approach to the reprocessing of nuclear waste with many advantages over the current technique. A large challenge remains however, in acquiring approval from regulatory authorities to employ ART into industry.



#### 1.4. References

- [1] Decay Heat data, National Nuclear Laboratory
- [2] Krishnamurthy, M. and Sipahimalani, A. (1995). Radiolytic degradation of TBP-HNO<sub>3</sub> system: Gas chromatographic determination of radiation chemical yields of n-Butanol and nitrobutane. *Journal of Radioanalytical and Nuclear Chemistry Letters*, 199(3), pp.197-206.
- [3] Hanford atomic product products operation (2017). The PUREX process - A solvent extraction reprocessing method for irradiated uranium. Richland, Washington.
- [4] A Ojovan, M.I., Lee, W.E. and Kalmykov, S.N. (2019) Chapter 6 - Power Utilisation of Nuclear Energy Elsevier.
- [5] MOUNT EVEREST OF THE OBVIOUS. 2020. Uranium Milling To Yellowcake To UF<sub>6</sub> Conversion. [online] Available at: <<https://mounteverestoftheobvious.com/welcome/credits/uranium-milling-to-uf6-conversion/>> [Accessed 29 July 2020].
- [6] Gnugnoli, G., Laraia, M. and Stegnar, P. (1996) 'Uranium mining & milling: assessing issues of environmental restoration', *IAEA Bulletin*, 38(2), pp. 22-26.

- [7] Web.evs.anl.gov. 2020. Conversion Of Yellow Cake To UF<sub>6</sub>. [online] Available at: <<https://web.evs.anl.gov/uranium/guide/prodhand/sld006.cfm>> [Accessed 29 July 2020].
- [8] World-nuclear.org. 2020. Conversion - World Nuclear Association. [online] Available at: <<https://www.world-nuclear.org/information-library/nuclear-fuel-cycle/conversion-enrichment-and-fabrication/conversion-and-deconversion.aspx>> [Accessed 29 July 2020].
- [9] Jeff C. Bryan. (June 17, 2015). Introduction to Nuclear Science, 1st ed. Boca Raton, FL, U.S.A: CRC Press, 2009
- [10] Wikimedia Commons. (June 17, 2015). Gas Centrifuge Cascade [Online]. Available: [https://commons.wikimedia.org/wiki/File:Gas\\_centrifuge\\_cascade.jpg#/media/File:Gas\\_centrifuge\\_cascade.jpg](https://commons.wikimedia.org/wiki/File:Gas_centrifuge_cascade.jpg#/media/File:Gas_centrifuge_cascade.jpg)
- [11] Nrl.mit.edu. (2019). *The Fission Process | MIT Nuclear Reactor Laboratory*. [online] Available at: <https://nrl.mit.edu/reactor/fission-process> [Accessed 30 Mar. 2019].
- [12] Hore-Lacy, I. (2007). NUCLEAR POWER. *Nuclear Energy in the 21st Century*, pp.37-53.
- [13] Rufus, A., Kumar, P., Jeena, K. and Velmurugan, S. (2018). Removal of gadolinium, a neutron poison from the moderator system of nuclear reactors. *Journal of Hazardous Materials*, 342, pp.77-84.

- [14] Hyperphysics.phy-astr.gsu.edu. (2019). *Light Water Nuclear Reactors*. [online] Available at: <http://hyperphysics.phy-astr.gsu.edu/hbase/NucEne/ligwat.html> [Accessed 30 Mar. 2019].
- [15] Nucleus.iaea.org. (2019). *Open Knowledge Wiki - General Design and Principles of the Advanced Gas-Cooled Reactor (AGR)*. [online] Available at: [https://nucleus.iaea.org/sites/graphiteknowledgebase/wiki/Guide\\_to\\_Graphite/General%20Design%20and%20Principles%20of%20the%20Advanced%20GasCooled%20Reactor%20\(AGR\).aspx](https://nucleus.iaea.org/sites/graphiteknowledgebase/wiki/Guide_to_Graphite/General%20Design%20and%20Principles%20of%20the%20Advanced%20GasCooled%20Reactor%20(AGR).aspx) [Accessed 30 Mar. 2019].
- [16] Archive.uea.ac.uk.(2019).[online]Available at [https://archive.uea.ac.uk/~e680/energy/energy\\_links/nuclear/How\\_an\\_AGR\\_power\\_station\\_works.pdf](https://archive.uea.ac.uk/~e680/energy/energy_links/nuclear/How_an_AGR_power_station_works.pdf) [Accessed 30 Mar. 2019].
- [17] (VHTR), V. (2019). *GIF Portal - Very-High-Temperature Reactor (VHTR)*. [online] Gen-4.org. Available at: [https://www.gen-4.org/gif/jcms/c\\_42153/very-hightemperature-reactor-vhtr](https://www.gen-4.org/gif/jcms/c_42153/very-hightemperature-reactor-vhtr) [Accessed 30 Mar. 2019].
- [18] World Nuclear Association. (2019). *Treatment and Conditioning of Nuclear Waste*. [online] Available at: <https://www.world-nuclear.org/information-library/nuclear-fuelcycle/nuclear-wastes/treatment-and-conditioning-of-nuclear-wastes.aspx> [Accessed 30 Mar. 2019].
- [19] World-nuclear.org. (2019). *Radioactive Waste Management | Nuclear Waste Disposal - World Nuclear Association*. [online] Available at: <http://www.world-nuclear.org/information-library/nuclear-fuel-cycle/nuclear-wastes/radioactive-wastemanagement.aspx> [Accessed 30 Mar. 2019].
- [20] Ojovan, M. and Lee, W. (n.d.). *An introduction to nuclear waste immobilisation*.
- [21] *Managing the Nuclear Legacy A strategy for action*. (2019). national archives.

- [22] (<http://www.forepoint.co.uk>), F. (2019). *What are the main waste categories? / UKRWI (tools)*. [online] Ukinventory.nda.gov.uk. Available at: <https://ukinventory.nda.gov.uk/about-radioactive-waste/what-is-radioactivity/what-arethe-main-waste-categories/> [Accessed 30 Mar. 2019].
- [23] Jnfl.co.jp. (2019). *Reprocessing / Business - JNFL*. [online] Available at: <http://www.jnfl.co.jp/en/business/reprocessing> [Accessed 30 Mar. 2019].
- [24] World-nuclear.org. (2019). *Processing of Used Nuclear Fuel - World Nuclear Association*. [online] Available at: <http://www.world-nuclear.org/informationlibrary/nuclear-fuel-cycle/fuel-recycling/processing-of-used-nuclear-fuel.aspx> [Accessed 30 Mar. 2019].
- [25] Berry, S. and Tolley, G. (n.d.). *Nuclear Fuel Reprocessing: Technological, Social, and Economic Problems*. [ebook] Chicago: Chicago University. Available at: <http://franke.uchicago.edu/energy2013/group6.pdf> [Accessed 30 Mar. 2019].
- [26] Neepa Paul, Robert B. Hammond, Timothy N. Hunter, Michael Edmondson, Lisa Maxwell, Simon Biggs, Synthesis of nuclear waste simulants by reaction precipitation: Formation of caesium phosphomolybdate, zirconium molybdate and morphology modification with citratomolybdate complex, *Polyhedron*, Volume 89, 2015, Pages 129141,
- [27] A. J. Ragauskas, “ "The Path Forward For Biofuels And Biomaterials".,” *Science* , vol. 311.5760 , pp. 484-489. , 2006.
- [28] Yi Xie, Sungyong Mun, Chim Yong Chin, Nien-Hwa Linda Wang, “Simulated Moving Bed Technologies for Producing High Purity Biochemicals and Pharmaceuticals,” *Frontiers in Biomedical Engineering* , pp. 507-52.
- [29] Fedorov, Y.S., Zilberman, B.Y., Kopyrin, A.A. et al. *Radiochemistry* (2001) 43: 166.

- [30] Emmott J, " Chromatographic Separation of Metals" PhD. University of Central Lancashire, 2016.
- [31] IAEA (2002). *APPLICATION OF ION EXCHANGE PROCESSES FOR THE TREATMENT OF RADIOACTIVE WASTE AND MANAGEMENT OF SPENT ION EXCHANGERS*. Vienna: IAEA.
- [32] ARMENANTE, P. (n.d.). *Ion Exchange*. [PDF] New Jersey: New Jersey Institute of Technology. Available at: [https://sswm.info/sites/default/files/reference\\_attachments/ARMENANTE%20000%20Ion%20Exchange.pdf](https://sswm.info/sites/default/files/reference_attachments/ARMENANTE%20000%20Ion%20Exchange.pdf) [Accessed 17 Feb. 2019].
- [33] Weaver, V.C. Z. *Anal. Chem.* (1968) 243: 491.
- [34] HELFFERICH, F., *Ion Exchange*, McGraw Hill, New York (1962).
- [35] Sehgal, B. (2012). *Nuclear safety in light water reactors*. Amsterdam: Elsevier/Academic Press.
- [36] Bibler J.P. (1990) *Ion Exchange in the Nuclear Industry*. In: Williams P.A., Hudson M.J. (eds) *Recent Developments in Ion Exchange*. Springer, Dordrecht
- [37] IAEA (1986). *ION EXCHANGE TECHNOLOGY IN THE NUCLEAR FUEL CYCLE*. [online] Austria: IAEA. Available at: [https://inis.iaea.org/collection/NCLCollectionStore/\\_Public/17/054/17054131.pdf](https://inis.iaea.org/collection/NCLCollectionStore/_Public/17/054/17054131.pdf) [Accessed 31 Mar. 2019].
- [38] Streat, M. and Cloete, F. (n.d.). *Ion Exchange*. [PDF] Available at: <https://pdfs.semanticscholar.org/ce74/414838cdad875018c26b0f8458201fef3abe.pdf> [Accessed 20 Mar. 2019].
- [39] I. R. Higgins and J. T. Roberts, *Chem. Eng. Prog. Symp. Ser.*, 50(14), 87 (1954)
- [40] S. Bio, "Simulated Moving Bed Chromatography," [Online]. Available:

<http://sembabio.com/simulated-moving-bed-chromatography/>. [Accessed 15th March 2016].

- [41] Zhou, Lihua et al, ""Separation Characteristics Of Boron Isotopes In Continuous Annular Chromatography".," Science China Chemistry , vol. 58.7 , pp. 1187-1192, 2015.
- [42] A. Chauvel, " Petrochemical Processes.," Paris: Éd. Technip, 1989.
- [43] Begovich, J. and Sisson, W. (1983). Continuous ion exchange separation of zirconium and hafnium using an annular chromatograph. Hydrometallurgy, 10(1), pp.11-20.
- [44] Kunin, R., "Ion Exchange Resins," John Wiley & Sons, Inc., New York, NY (1958). [38] Colloidal Processes in SIXEP Streams. (n.d.). .NNL

## Chapter 2 Experimental methodology and Materials

Table 2.1 Analytical Equipment

Type of analysis	Equipment	Manufacturer and model	Software
Surface Area and Pore Size /volume	Gas sorption	Micromeritics ASAP 2010 and 2020	ASAP 2010 v5.02 and ASAP 2020 PLUS
Morphology	SEM	Jeol JCM - 6000 plus	SMILEVIEW
Functional groups	FT-IR	Jasco FT-IR 410	OMNIC
Thermal decomposition	TGA	Mettler Toledo TGA 1	STARe V13.00
Cation uptake measurements	ICP-MS	Thermo Fisher X series	PlasmaLab
pH measurements	pH meter	Hanna Instruments HI2215	-
Retention times of ions in solution	HPLC	Jasco FP15-20 and Dionex AD20	-

Table 2.2 Experimental and other equipment

Equipment	Manufacturer and Model
Water bath with shaker	Jaluba SW22
Table top shaker	IKA KS 260
Vacuum oven	Binder
Overhead stirrer	IKA RW basic
Peristaltic pump	Watson Marlow
Centifuge	Sprout
Micro-pipette	VWR
Glass pipette	Hirschmann Instruments bulb pipette
Glass nozzle	Made according to the literature <sup>[1]</sup>
Refined jet nozzle	Built with Swagelock parts
Dual nozzle	Linari Nanotech 2-Layer sealed coaxial needle
Hot plate with stirrer	IKA C-MGG HS7
Water bath	Clifton
Centrifuge	Sprout mini
Balance	VWR LA314i



## 2.1. Analytical equipment

### 2.1.1. Surface area and pore size analysis

The surface area, pore volume and pore size of materials can dictate their physical properties and this analysis is crucial to understanding how the migration of candidate ions onto and within the materials in this thesis relate to their diffusion mechanisms. Gas adsorption was employed in these studies due to the microporous nature of the materials. The use of gas adsorption allows for a vast array of pore sizes in the mesoporous and microporous range to be analysed.

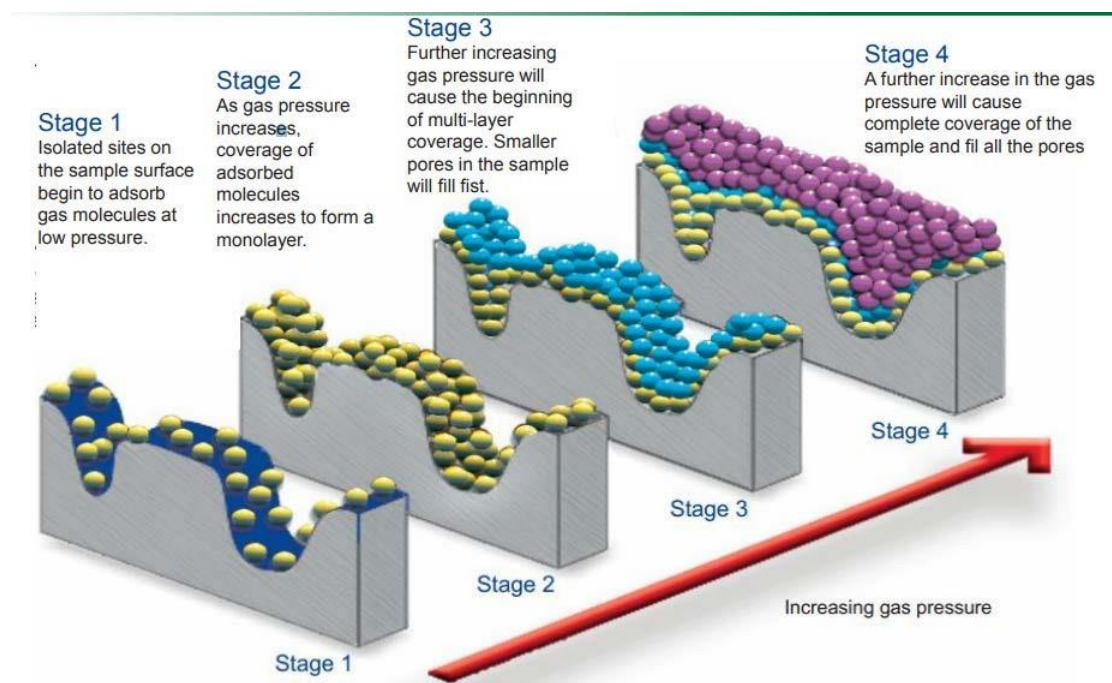


Figure 2.1 Gas adsorption stages. Take from source [1]

The technique involves the adsorption of nitrogen gas onto the surface and into the material being analysed. Figure 2.1 shows the different stages explained by Micromeritics – the

manufacturer of the gas sorption equipment used in this thesis. An isotherm is produced at the end of the experiment which can display information about the type of adsorption and how much gas is adsorbed. The different types of isotherm are explained in the subsections to follow.

#### 2.1.1.1 Types of isotherm

Brunauer classifies 5 different types of isotherms for gas sorption onto solid materials, named type I to type V (figure 2.2). These isotherms can explain the type of sorption and provide information about pore size distribution.

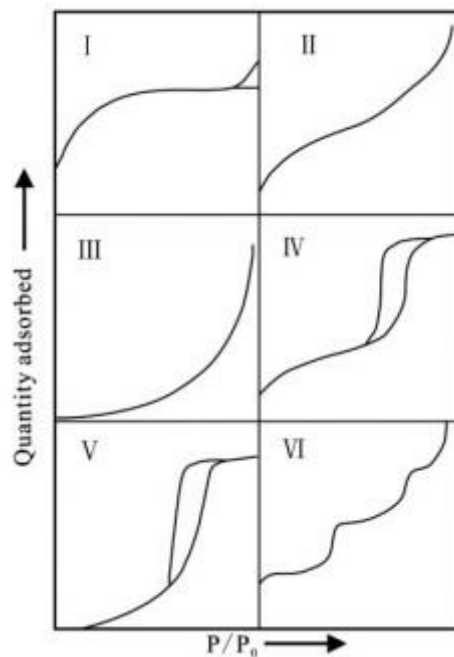


Figure 2.2 Typical curves of each of the five isotherm models. [2]

The most common types of isotherm are type I, II and IV. Type I isotherms indicate that the adsorption is complete when a single monolayer of gas molecules are adsorbed onto the adsorbent surface. [2] This applies to microporous materials whose pore sizes are similar in size to the diameter of an adsorbate molecule. The other 4 types do not limit

adsorption completion to a monolayer. For type I, II and III isotherms the sorption is reversible, meaning desorption of the adsorbate re-traces the adsorption curve. [2][3]

Type II isotherms portray the stacking of monolayers to form multi-layers of adsorbate. Typical substances that exhibit type II isotherm model have varied pore sizes and are macroporous (pore size 50-200nm<sup>[4]</sup>) or non-porous. The volume of gas adsorbed for type II increases faster than type I at lower relative pressures (<0.01). [3] This is attributed to the interaction of the gas molecules initially with the high-energy region of the adsorbent. [3] The characteristic curve of type II isotherms is due to the multi-layer formation once the monolayer adsorption is complete. Type III and type V isotherm models explain stronger adsorbate-adsorbate molecule interaction as opposed to type II and type IV for which the adsorbate-adsorbent interactions are stronger. Type IV and V are a result of capillary condensation after monolayer formation. As is seen in figure 2.3.[5]

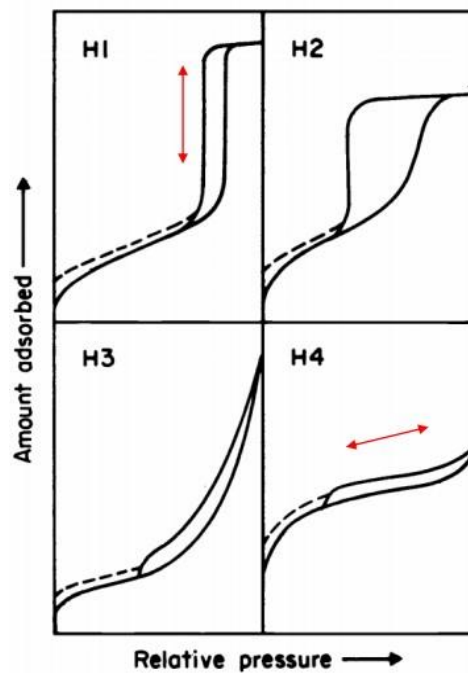


Figure 2.3 Figure 2.3 Types of hysteresis loop. H1 defines uniform spherical particles and subsequent pore size uniformity. H2 is characteristic of “ink-bottle” shaped pores with a pore network. H3 is attributed to slit shaped pores. H4 also defines slit shaped po

### 2.1.1.2 Brunauer-Emmett-Teller (BET)

The fundamentals of BET theory describe infinite layers of gas molecules adsorbing onto the surface of an adsorbent with no interactions between each layer. The method works on the basis of Langmuir's theory which relates the gas pressure to the amount adsorbed onto a solid surface and is represented by equation 2.1.

*Equation 2.1 BET method of gas sorption*

$$\frac{1}{V(P/P_0 - 1)} = \frac{C}{V_m C} + \frac{1}{V_m C} \frac{P_0}{P}$$

P = pressure

P<sub>o</sub> = saturation pressure

V = total volume adsorbed

V<sub>m</sub> = volume of gas needed to form the monolayer

C = constant

Using this equation, a graph can be plotted using  $P/\sqrt{P(P_0 - P)}$  against volume adsorbed and an isotherm model can be generated. Accumulative pore volume and pore diameter is measured via

Barrett-Joyner-Halenda method and is explained in more detail in reference [6]

### 2.1.1.3 Sample preparation and experimental procedure

The sample was dried in an oven at 80°C prior to analysis to remove any moisture. Around 200mg of dry sample was de-gassed in a round bottom tube at 110°C for 4 hours. The weight after de-gassing was entered into the software and the sample tube was placed into the analysis chamber. Using the pre-programmed protocol for mesoporous/microporous materials from the Micromeritics software, the analysis was started according to the manufacturer's procedures. The results provided are single experiments due to the nature of the machine, and the maintenance it required.

### 2.1.2 Thermo Gravimetric Analysis (TGA)

TGA was used in this research to determine the relative thermal stability of our composites.

This technique can provide information on the decomposition temperatures of different parts of a material and is particularly useful when analysing compounds containing several volatile components. A typical TGA graph is illustrated in figure 2.4.

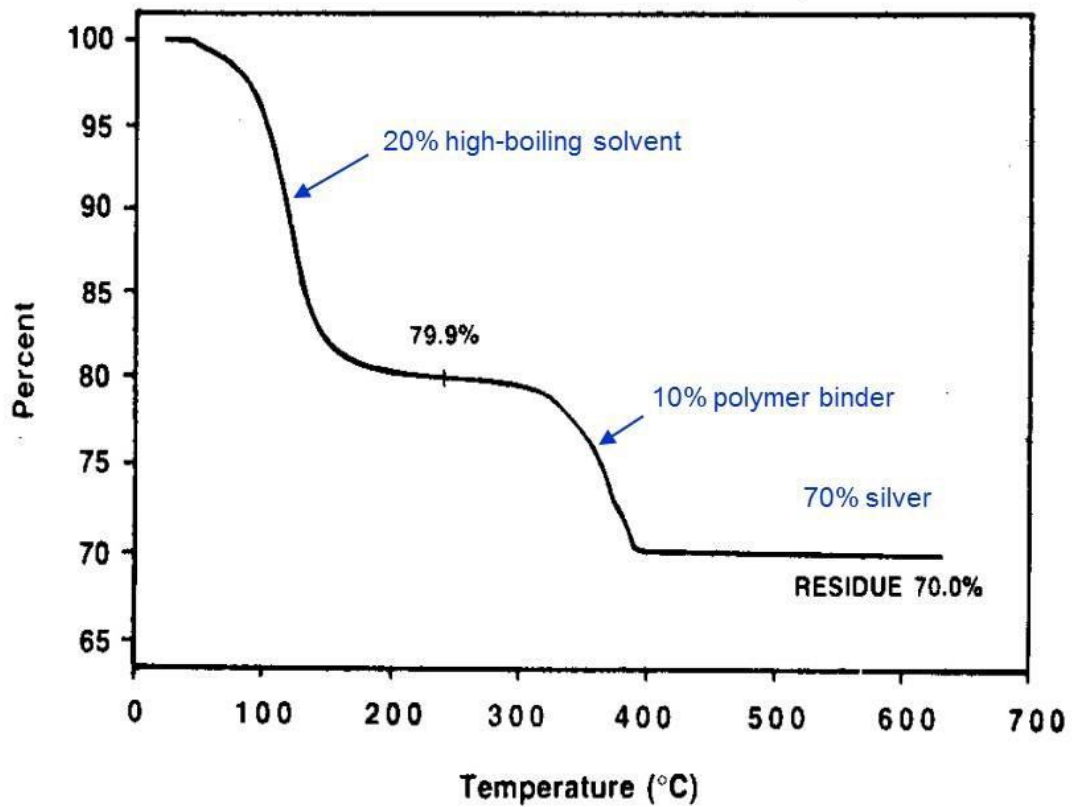


Figure 2.4 TGA plot of silver-filled thermosetting ink. [7]

There are several functions of the analytical technique that can be controlled such as; ramp time/temperature, atmosphere and set point. All materials within this thesis were subject to a high set point of 1000°C with a heating rate of 10°C/minute and performed under an atmosphere of air (15ml/min). TGA records the change in mass of materials under these set conditions and reports the mass loss as a function of temperature or time. The decrease in weight at the different stages of the analysis represents different fragments of our composites decomposing and thus their stability and potential application for the task under investigation can be partially concluded.

### 2.1.2.1 Sample preparation and experimental procedure

A sample (~0.2g) was loaded onto an alumina pan crucible and covered with a lid before being loaded on to the sample stage and entering the furnace; the furnace was then sealed. Using the PC software the desired protocol was selected, for the required atmosphere.

### 2.1.3 Inductively Coupled Plasma –Mass Spectroscopy (ICP-MS)

A Thermo Scientific X series ICP-MS instrument with auto-sampler was employed to measure the concentration of ions in solution. The system performs under inert gas and is cooled by a chiller unit. The instrument is connected to a computer, which is operated by Plasmalab software.

Before running samples, a calibration curve must be obtained; this requires a range of standards that contain a known concentration of the target ion. To obtain a reliable curve, 4 or more standards are usually prepared and run concurrently with the test samples. For samples, which may contain up to 5mM Cs (around 660ppm) a suitable range for the standard solutions would be 1,3,5,7 ppm as the samples should be diluted 100x as to accommodate for the sensitivity of the instrument. The standards should also contain an internal standard.

The ion concentrations obtained by ICP-MS analysis were used to calculate the results in the tables that follow. The capacity, distribution coefficient ( $K_d$ ) and selectivity values were of most interest and crucial to the composite performance as a highly selective cesium adsorbent.

In regards to the nuclear industry, the distribution coefficient describes the exchangeability of radionuclides in spent fuel liquors. The  $K_d$  value is sensitive to certain variables such as concentration of cesium, acidity and in some instances, temperature. The  $K_d$  is calculated using the following equation:

*Equation 2.2 Calculation of distribution coefficient*

$$kd = \frac{C_0 - C_e}{C_e} \times \frac{v}{m} \text{ ml/g}$$

The capacity values measure the amount (in mg) of cesium that can be adsorbed per amount of composite (in g). It can be denoted as “q” and is calculated as follows:

*Equation 2.3 Calculation of capacity*

$$q = \frac{C_0 - C_e}{1000} \times \frac{v}{m} \text{ mg/g}$$

Selectivity can be represented by the ratio of the  $K_d$  values measured under the same conditions i.e. acid concentration, viz:

$$K_{dCs}/K_{dCe}$$



### 2.1.3.1 Sample preparation and experimental procedure

Table 2.3 Materials used for analysis by ICP-MS

Material	Role	Supplier
70% Nitric Acid	Diluted for acidic matrix of experiments	Fisher Scientific
De-ionised water	For dilutions	Nanopure purifier
Cesium Analytical standard 1000pm	Used for calibration standards	Fisher Scientific
Strontium Analytical standard 1000pm	Used for calibration standards	Fisher Scientific
Zirconium Analytical standard 1000pm	Used for calibration standards	Fisher Scientific
Molybdenum Analytical standard 1000pm	Used for calibration standards	Fisher Scientific
Cerium Analytical standard 1000pm	Used for calibration standards	Fisher Scientific
Barium Analytical standard 1000ppm	Used as an internal standard	Fisher Scientific

Initial and equilibrated aliquots (100µl) were taken from sample solutions and placed into separate 10ml centrifuge tubes along with an internal standard (Ba used for Cs samples) of concentration 1ppm and then diluted to 10ml with 1% HNO<sub>3</sub>. These were placed onto the autosampler in the corresponding position chosen by the software.

Once the plasma had ignited, the instrument was ready to operate; prior to analysing the samples a 15-30 minute 1% HNO<sub>3</sub> flush was completed. A bank containing only the internal standard and 1% HNO<sub>3</sub> was also prepared and analysed. Once completed, the standards were run consecutively and an acid wash was undertaken between each test sample. On completion an analysis report was generated with concentrations of appropriate ions.

#### 2.1.4 Scanning Electron Microscopy (SEM)

Analysis of internal morphology and composite bead size was performed using SEM. The sample chamber was kept under vacuum when the electron beam was turned on. The machine was connected to SEM imaging software that produced live images of the subject using an electron beam as a light source.

##### 2.1.4.1 Sample Preparation and experimental procedure

Sample preparation involved using a sticky carbon paper on a SEM pin stub. The sample for analysis was placed on the carbon sticky paper which served as a stable support and a black background. The sample was always placed into the sample stage using the measurement gauge as an indicator to how high the stub should be. The chamber was vented before the sample was placed inside and then re-pumped under vacuum once the chamber was closed.

Magnification for composite beads of 1mm in size never exceed 2400x due to loss of clarity of the image. A cross section of a bead was placed on the same sample stage in order to

view exterior and internal morphology on the same screen. Once images were saved, the chamber was vented and sample discarded.

### 2.1.5 Fourier Transform – Infrared Spectroscopy (FT – IR)

Modern Infrared Spectroscopy is a type of vibrational spectroscopy that works in the infra-red radiation spectrum (700nm-1mm) of which the values are typically displayed in wavenumbers ( $\text{cm}^{-1}$ ). The equipment used for IR analysis operates in the range of 500-4000 $\text{cm}^{-1}$ . The sample is exposed to a controlled laser of infra-red radiation which specific functional groups will absorb. The bonds of the functional groups undergo vibrations which adversely affect either the length or angle of said bonds; if the bond length is affected, this is known as a stretching vibration and if the bond angle is affected this is known as bending vibration. These absorptions are translated into peaks plotted onto a graph of absorbance vs wavenumber and subsequently display information on functional groups present in the material. A typical IR spectrum can be seen below with common peaks of interest designated by arrows.

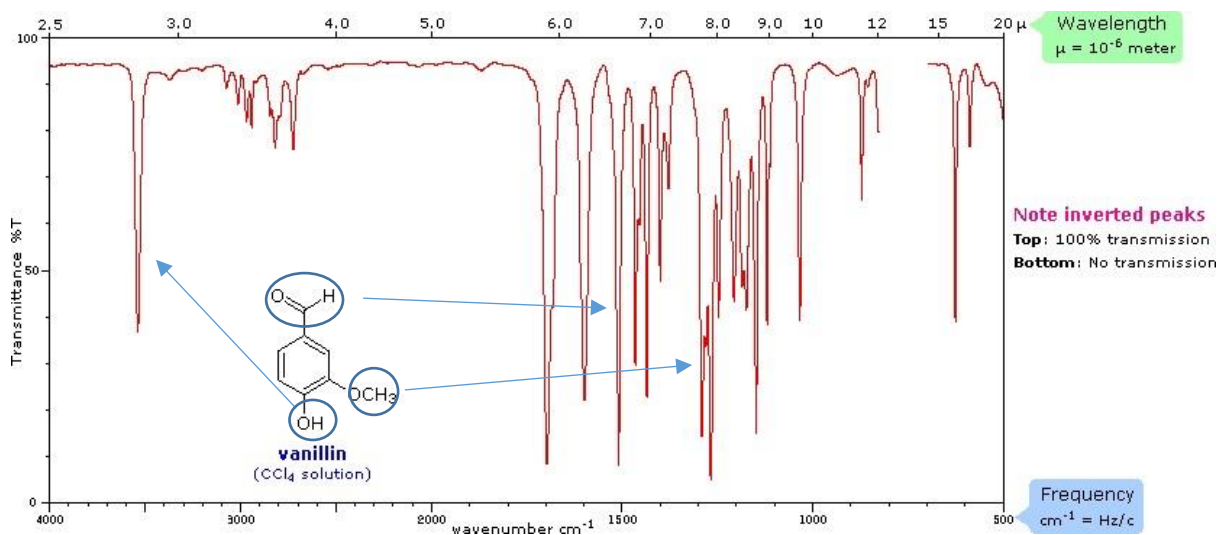


Figure 2.5 IR spectrum of vanillin [8]

### 2.1.5.1 Sample Preparation and experimental procedure

The initial stage of sample analysis must be calibrated with a blank to subtract from the sample spectra. Upon calibration, a small amount of sample was placed onto the instrument and the computer software was used to start the analysis.

### 2.2 Cation uptake experiments

*Table 2.4 Materials used in the make-up of stock solutions*

Material	Role	Supplier
Sodium Molybdate	Molybdenum Source for Stock solution	Sigma Aldrich
Zirconium oxynitrate hydrate	Zirconium source for stock solution	Sigma Aldrich
Cesium nitrate	Cesium source for stock solution	Sigma Aldrich
Strontium Nitrate	Strontium source for stock solution	Sigma Aldrich
Cerium(III) Oxide	Cerium (III) source for stock solution	Sigma Aldrich
Ammonium Cerium(IV) Nitrate	Cerium (IV) source for stock solution	Sigma Aldrich
70% Nitric Acid	Diluted for acidic matrix of experiments	Fisher Scientific
De-ionised water	For dilutions	Nanopure purifier

In a 100 ml Duran glass bottle a 0.5 g of adsorbent was contacted for 24 hours with 50 ml of the candidate solution on the table top shaker at room temperature set at 300 rpm. Samples of liquor were taken at initial concentration ( $C_o$ ) and after assumed equilibrium ( $C_e$  at 24 hours) and centrifuged before assay. For kinetics studies aliquots were taken at 10, 20, 30, 60, 180, 360 and 1440 minutes and analysed by ICP-MS (Thermo; X series, Software; Plasma Lab.). Triplicate analytical data points were obtained for all ICP MS samples in Chapter 3 and 4 with average standard deviations from  $\sigma$ 0.001 to 0.047 which are reported in the figure captions or their respective table (denoted by  $\sigma$ ). The standard deviations were obtained from the ICP-MS automatically.

## 2.3 Composite adsorbent bead formation

### 2.3.1 Synthesis of AMP/PAN

All chemicals were purchased from either Sigma Aldrich, Fisher Scientific or GoodFellow and were of ANALAR grade.

*Table 2.5 Materials used in the synthesis of AMP/PAN*

Material	Role	Supplier
Ammonium molybdophosphate hydrate	Synthesising AMP/PAN	Fisher Scientific
Polyacrylonitrile Mw 150,000	Synthesising AMP/PAN	Sigma Aldrich
Polyacrylonitrile Mw 85,000	Synthesising AMP/PAN	GoodFellow
Dimethyl sulfoxide	Solvent for AMP/PAN synthesis	Fisher Scientific

Tween 80	Surfactant to make AMP/PAN microporous	Sigma Aldrich
De-ionised water	For gelation	Fisher Scientific

The synthesis of AMP/PAN 70 composite was achieved by dissolving 0.4 g of Tween 80 in 200 ml of dimethylsulfoxide (DMSO) and mixed at 50°C by overhead stirrer at approximately 250 rpm. 10 g of ammonium phosphomolybdate (AMP) was added to the solution and the mixture was stirred for a further 1 hour at 50°C. After one hour, a homogeneous yellowish green colour mixture was obtained, to which 4 g of polyacrylonitrile (PAN) powder was added and the solution was maintained at 50°C with constant stirring (~250 rpm) for 3 hours. The composite mixture was dispensed gravimetrically via a 1 mm (int. dia.) bore tube into ~400 ml of deionised water. The spheres were left overnight in deionised water and thereafter washed 3 times with fresh deionised water every 30 minutes. The washed beads were separated and dried in air at room temperature then stored in a poly(propylene) bottle to retain the moisture content.

The moisture retention of these materials is reported in chapter 3.

For AMP/PAN 50 the ratio of AMP: PAN was adjusted accordingly. Several modifications to this synthesis is also reported in the same chapter.

### 2.3.2 Synthesis of strontium adsorbent composites

Starting adsorbent materials were prepared via a fast flow synthesis reported in work by Holdsworth. <sup>[9]</sup>

The synthesis of strontium adsorbents was almost identical to the synthesis of AMP/PAN. The difference with this experimental method is the replacement of AMP with one of the adsorbent powders in table 2.6. In addition, the amount of starting reagents was reduced as is detailed further on.

*Table 2.6 Strontium adsorbent powders*

Material name	Composition
XP	$\text{Ti}_{0.66}\text{W}_{0.33}$
HT51	$\text{Ti}_{0.8}\text{Zr}_{0.2}$
HT52	$\text{TiZr}$
YP	$\text{Zn}(\text{NH}_4)_3$
HT50	$\text{Ti}_{0.4}\text{Zr}_{0.6}$

Upon dissolution of tween 80 (0.2g) in 50ml of dimethylsulfoxide (DMSO) and mixed at 50°C by overhead stirrer at approximately 250 rpm. 2.5 g of adsorbent powder (AMP) was added to the solution and the mixture was stirred for a further 1 hour at 50°C. After one hour, a homogeneous white mixture was obtained, to which 1.5 g of polyacrylonitrile (PAN) powder was added and the solution was maintained at 50°C with constant stirring (~250 rpm) for 3 hours.

### 2.3.3 Bulb Pipette Nozzle

Using clear tubing (diameter 5-10mm) and a peristaltic pump (~10rpm), the reaction mixture

was fed through the pump into a 25ml glass pipette fitted with a 200 $\mu$ l pipette tip on the exit. The mixture was allowed to drop under gravity into a beaker of DI water (~500ml).

The solution was kept in the water bath at a constant reaction temperature of 50°C throughout bead formation. A photograph of the experimental setup can be seen in figure

2.6.



Figure 2.5 Synthesis of AMP/PAN beads by gravity dropping. Taken from P. Kavi. [10]



### 2.3.4 Confined Jet

Swage lock piping (1/2 inch thickness) was used to build the confined jet nozzle (figure 2.7) with 1/4inch diameter stainless steel pipe used for the mixture to flow through. A blanket of nitrogen gas surrounds the feed nozzle and accelerates the speed in which the mixture exits the nozzle. The setup of the bead formation is the same as in figure 2.8 but the confined jet replaced the glass pipette. An attempt to control the bead size was achieved by altering the flow of nitrogen to the nozzle. The water used for gelation is used in the same conditions as the conventional method.

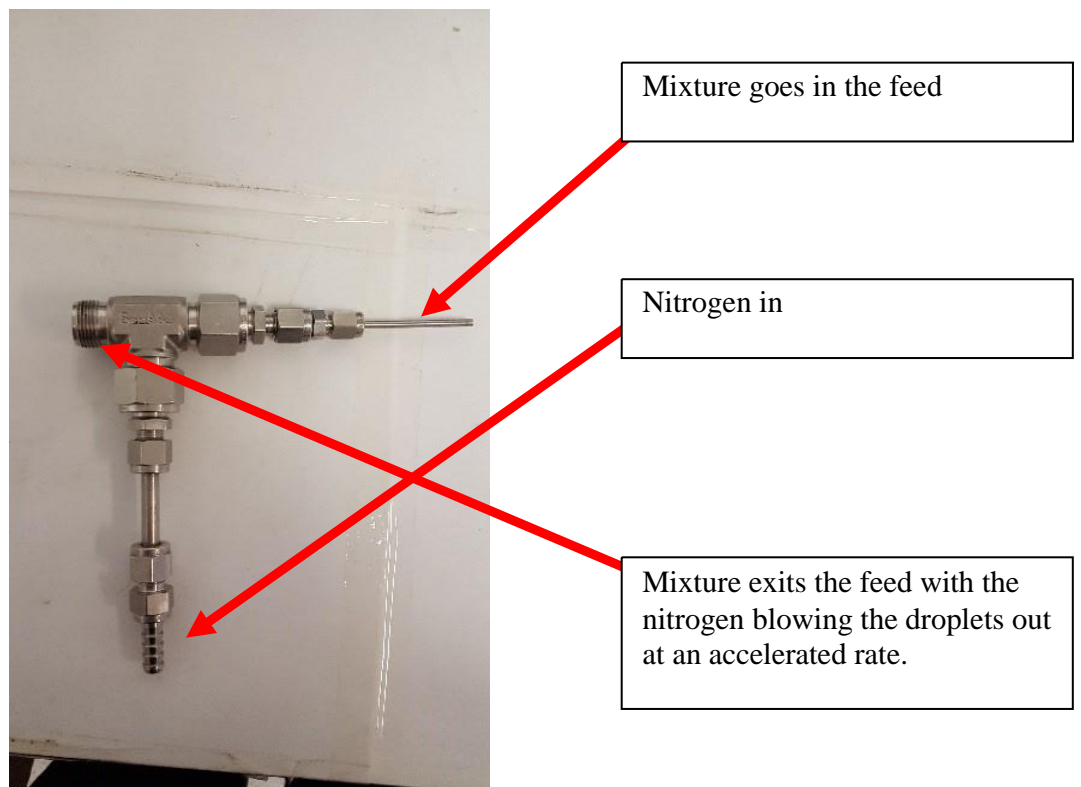


Figure 2.6 Confined jet design

### 2.3.5 Dual Glass nozzle

The glass nozzle used was custom made according to the drawing in the literature <sup>[1]</sup> It was used in the same way as the confined jet but offered greater accuracy and provided a more uniform bead size and higher throughput (roughly 30 minutes faster) due to less blockages and shorter feed nozzle. The de-ionised water used as the gelation agent was stirred at around 200rpm and the nozzle was positioned so the droplets made contact with the edge of the vortex. This reduced shear with the aim of making more spherical beads. The height of the nozzle from the vortex was around 2cm and in close accordance to the literature. Altering the nitrogen flow to the glass nozzle allowed better control of bead size and spray angle.



Nitrogen in

Mixture exits into spinning water

Mixture Feed in

Figure 2.7 Glass Nozzle setup

### 2.3.6 Dual stainless steel nozzle

The equipment setup was near identical to the dual glass nozzle with the difference being the type of nozzle used. A 2-layer stainless steel sealed coaxial needle from Linari Nanotech (figure 2.9) was used as a replacement to the glass nozzle.



*Figure 2.8 2-Layer sealed coaxial needle with threaded luer lock fastenings for gas and mixture feed inlets*

The feed exit had an internal and outer needle measuring 0.83mm and 1.83mm in diameter respectively. This was significantly smaller than the ~2.5mm glass nozzle exit diameter, which combined with the low adhesion of stainless steel and anti-stick properties, allowed for small droplets to be formed. This nozzle was used as the latest experimental technique for bead formation.

## 2.4 Simulated Moving Bed Chromatography

The Octave Chromatography System by Semba Biosciences involves the use of multiple columns set up in tandem and can operate in two different modes; isocratic and step (detailed in Chapter 5). The purpose of this work focussed on isocratic mode in order to achieve an initial understanding of the instrument. The protocols for the instrument can be modified extensively to achieve the desired outcome. The fundamentals are detailed in chapter 5 and more information can be retrieved from Semba Biosciences' website <sup>[12]</sup>

### 2.4.1 Materials and procedure

The Purolite resins used throughout the SMBC experiments were of commercial grade in the form of spherical beads possessing an average bead diameter of ~300µm. The details of each resin can be seen in table 2.7.

Table 2.7 Commercial ion exchange materials used for SMB taken from source [13]

Name	Manufacturer	Functional Group	Form Shipped	Polymer Structure	Particle Size ( $\mu\text{m}$ )	Uniformity Coefficient
C100H	Purolite	Sulfonic Acid	H <sup>+</sup>	Gel Polystyrene crosslinked with 8 % DVB	300 - 1200	1.3
C100X10MBH	Purolite	Sulfonic Acid	H <sup>+</sup>	Gel Polystyrene crosslinked with 10 % DVB	425 - 1200	1.6
S910	Purolite	Amidoxime	Freebase	Polyacrylic crosslinked with DVB	300 - 1200	1.7

Prior to each SMB experiment, single column studies were performed to obtain retention times for ions. A single column was packed with the specific resin and the stock feed solution and desorbent was run through HPLC at 5ml/min. The desorbents used for each experiment were 1M and 3M HNO<sub>3</sub>. The composition of the stock solution used for chromatographic studies can be seen in table 2.8

Table 2.8 Stock solution composition for SMBC experiments

Element	Concentration (ppm)
Ce	515
Zr	47
Mo	42

For each experiment four 10cm x1cm columns obtained from Semba Biosciences were packed with an adsorbent material listed in in table 2.7 according to the manufacturer's procedure. The protocol parameters for each experiment were calculated using data obtained from single column results that was entered into the pre-programmed SMB parameter calculator. The parameters for each experiment and the subsequent modification of these are discussed in more detail in chapter 5. Aliquots were taken every 10 minutes to perform kinetic measurements.

Stripping profiles obtained from work performed by Emmott, J. were used as guidance when regenerating the resin acid groups so that the materials could be recycled. The stripping was performed using the required amount of 5M HNO<sub>3</sub> fed through the system.

## 2.5 References

- [1] Gas Adsorption Theory.(n.d). [pdf] Micromeritics. Available at:  
[https://www.micromeritics.com/Repository/Files/Gas\\_Adsorption\\_Theory\\_poster.pdf](https://www.micromeritics.com/Repository/Files/Gas_Adsorption_Theory_poster.pdf) [Accessed 14 Mar. 2019].
- [2] Yang, Shuang & Chen, Guojun & Lv, Chengfu & Li, Chao & Yin, Na & Yang, Fei & Xue, Lianhua. (2017). Evolution of nanopore structure in lacustrine organic-rich shales during thermal maturation from hydrous pyrolysis, Minhe Basin, Northwest China. *Energy Exploration & Exploitation*. 36. 10.1177/0144598717723647.
- [3] Adsorption types and kinetics. (n.d.). Available at  
<https://nptel.ac.in/courses/103103026/module1/lec3/2.html> [Accessed 11 Mar. 2019]
- [4] Li, Y., Gao, F., Wei, W., Qu, J., Ma, G. and Zhou, W. (2010). Pore size of macroporous polystyrene microspheres affects lipase immobilization. *Journal of Molecular Catalysis B: Enzymatic*, 66(1-2), pp.182-189.
- [5] Sing et.al, *Pure & Appl. Chem.*, 1985, 57, 603-619
- [6] Valenzuela-Muñiz, A. (2012). *ABC's of Electrochemistry series Materials Characterization techniques: Surface Area and Pore Size Distribution*.
- [7] Prime (1992) *poly.eng.sci.* 32, 1286 menczel/prime fig 3.17
- [8] [www2.chemistry.msu.edu](http://www2.chemistry.msu.edu). (n.d.). *Infrared Spectroscopy*. [online] Available at:  
<https://www2.chemistry.msu.edu/faculty/reusch/virttxtjml/spectrpy/infrared/infrared.htm> [Accessed 25 Jan. 2019].



- [9] Alistair F. Holdsworth, Harry Eccles, Alice M. Halman, Runjie Mao, and Gary Bond  
Low-Temperature Continuous Flow Synthesis of Metal Ammonium Phosphates,  
Nature Sci Rep. 2018; 8: 13547
- [10] P. Kavi, "The Preparation And Characterisation Of Highly Selective Adsorbents For Fission Product Removal From Acid Solutions". PhD. University of Central Lancashire, 2016.
- [11] Moon, Jei-Kwon & Kim, Ki-Wook & Jung, Chong-Hun & Shul, Yong-Gun & Lee, EilHee. (2000). Preparation of Organic-Inorganic Composite Adsorbent Beads for Removal of Radionuclides and Heavy Metal Ions. *Journal of Radioanalytical and Nuclear Chemistry.* 246. 299-307. 10.1023/A:1006714322455.
- [12] Available from: <http://sembabio.com/>. Accessed 12/05/2018
- [13] Emmott J, " Chromatographic Separation of Metals" PhD. University of Central Lancashire, 2016.

## **Chapter 3 Selective cesium separation from spent fuel dissolver liquors.**

### 3.1 Review of selective cesium adsorbents.

The research into extracting cesium from HLW liquors is vast and a wide range of materials have been synthesised and developed over the past few decades (some materials reviewed in the next sub section). Many of the widely used materials have a good affinity for cesium and good selectivity over competing ions. Some of the materials have desirable uptake properties but undesirable characteristics such as their instability in acidic media and susceptibility to radiolytic damage. There are no adsorbent materials that offer all the desirable properties in addition to operating with maximum efficiency, hence the need for the development of known materials and synthesis of new extractants for cesium. For the purpose of this work, different types of materials in different applications are reported, however ion exchange is the most attractive method and is the underlying experimental technique for this project due to its ability to be applied to chromatography, with preliminary results presented in chapter 5.

#### 3.1.1 Crown ethers.

Crown ethers are usually employed for solvent extraction, which involves transferring the target material into the organic phase leaving the unwanted ions in the aqueous phase. This is a proven method of extraction, e.g. the PUREX process, provided the extractant and cation complex are readily soluble in the organic phase.

Crown ether research for cesium extraction has seen them incorporated into a PUREX style system that uses kerosene and tributyl-phosphate. When used alone, the crown ether did

not extract a substantial amount of cesium <sup>[1]</sup>. Increasing the solubility of the cesium ions in the organic phase was achieved by introducing other soluble organic molecules, which in turn allowed the cesium to complex with the crown ether and thus extraction increased. The application of some of the organic anions into the nuclear industry would not be viable, e.g. bis (2-ethylhexyl) phosphate, or HDEHP has an acid dissociation value too low for use in acidic media and spent nuclear fuel is dissolved in strong nitric acid (5 to 7M acid)<sup>[2]</sup>. Other organic anions such as the didodecyl naphthalenesulfonic acid anion (HDDNS) have a higher  $K_d$  value and have proven to be stable in 3M  $\text{HNO}_3$ <sup>[3]</sup>. It does however have a limited selectivity when zirconium is introduced and increasing the amount of HDDNS would reduce its solubility in the organic phase. <sup>[4]</sup> These organic anions show some potential, provided their inclusion has no detriment to the selective uptake of ions. The inclusion of TBP would be detrimental as explained earlier (chapter 1), it is not a highly selective extractant (flowsheet conditions for PUREX are tightly controlled to allow only U and Pu nitrates to be extracted), other cations such as zirconium would also be extracted along with cesium.

### 3.1.2 Phosphotungstic acid.

The application of phosphotungstic acid (PTA) precipitation has been evaluated for the treatment of the raffinate from the PUREX process. The process involved the precipitation of cesium by adding PTA to the raffinate via several steps and the separation of the precipitate and liquor using centrifugation.<sup>[5]</sup> This method has been developed over the past 40 years and is valued almost as much as ion exchange processes for the separation of waste products from radioactive waste liquors. PTA is stable in acidic media and allows for almost complete extraction (~98%) of the cesium from the supernatant. The PTA

process is fairly complex when compared to ion exchange and requires a longer operation, for complete reaction to be achieved.<sup>[5]</sup> The final waste form produced is low level, however, as all PUREX raffinates in American flowsheet were neutralised with sodium hydroxide, the initial waste must be acidified, if not already done so as was the case with the West Valley waste <sup>[6]</sup>. Re-adjustment of the pH value of the now low level waste to neutral/slightly alkaline is required before being passed to the appropriate downstream facility.

The PTA must be in excess to achieve an effective precipitation of cesium and the PTA concentration is nitric acid dependent, up to 1.5M HNO<sub>3</sub>. A major advantage of this precipitation method is that it also exhibits fast kinetics and, especially with increasing temperature (<5 minutes at 60°C). The solubility of the Cs bound PTA is also temperature dependent, precipitation is favoured at a higher temperatures <sup>[5]</sup>.

### 3.1.3 Ammonium Molybdophosphate.

Ammonium molybdophosphate has replaceable ammonium ions which exchange with cesium in our case. Ion exchange represents the most developed area of separating cesium from HLW. Ion exchange has to satisfy several attributes before application to the reprocessing industry, namely kinetics, susceptibility to radiolytic damage and their ability to regenerate (not necessary for all applications). Selectivity of the target ions is also of paramount importance so as discard unwanted materials. Solid phase ion exchange will occur between a solid composite and a solution containing the target ions for extraction<sup>[7]</sup>. The process could be pH sensitive depending on the adsorbent used as the exchangeable ions in the solid will be replaced with the appropriate ion(s) in solution, effectively binding with the solid and allowing them to be separated from other ions. New solid phase ion

exchangers can be synthesised for HLW treatment with chromatographic separations in mind.

Ammonium molybdophosphate is a versatile microcrystalline powder which has exchangeable ammonium that can be used for ion exchange studies; the investigation of AMP as an ion exchanger dates back to 1959<sup>[8]</sup>. The supporting research is now very extensive, mainly due to its selective uptake of cesium and high theoretical capacity (213g Cs/kg AMP)<sup>[9]</sup>. In addition, it is stable in a wide range of acidities and less acidic media such as seawater<sup>[10]</sup>.

The mechanism behind its ion exchange properties lies with the exchangeable ammonium ions; although there are three ammonium ions available only two take part in the exchange<sup>[11]</sup> hence why the original theoretical capacities are much higher than practical, measured capacities for cesium.

AMP is also stable in high doses of irradiation<sup>[12]</sup> up to around 2MGy and therefore has incredibly attractive properties, some reports have exposed AMP to doses of up to 200MGy where it was found that it degraded to molybdate<sup>[13]</sup>. Although AMP has many of the attributes required for an ion exchanger for the nuclear industry, its microcrystalline form would negate its application for commercial processes due to its inability to be applied to column processes (overpacking would occur) and the difficulties of separating it from a liquid are more substantial the smaller the particle (filtration becomes more difficult). Although attempts to incorporate modified AMP into columns have been performed, other secondary problems arose. Many researchers have bound AMP to porous supports<sup>[14]</sup> in an effort to allow AMP to be used in column applications. The selectivity and capacity for cesium decreased however, which could be due to a reduced amount of cesium per gram of material and a reduced surface area. The decreased selectivity could have resulted from the porous support having an affinity for other ions in solution in preference to cesium.

In order for laboratory studies to have commercial significance, it is important that the AMP is of an appropriate particle size and hence should be bound to and/or incorporated into some sort of porous support, such as polyacrylonitrile. This composite is discussed later in this chapter along with the capability of PAN as a support.

#### 3.1.4 Titanosilicates.

As with AMP, the use of crystalline titanosilicates (CSTs) have shown promise as efficient cesium adsorbents but have not exhibited the same stability in nitric acid <sup>[15]</sup>. They have a high selectivity compared to other materials such as ferrocyanides, in the presence of certain competing ions such as potassium. In our envisaged application, there is little potassium in spent fuel dissolver liquor. The selectivity was proven by the adsorption of cesium in the presence of sodium ( $\text{NaNO}_3$  as a source) and the CSTs exhibited good uptake of cesium in pH values ranging from 7-12 <sup>[16]</sup>, CSTs, would therefore, be more suitable for capturing cesium from seawater.

#### 3.1.5 Polyacrylonitrile as a support.

Polyacrylonitrile (PAN) is a versatile copolymer that usually comes in the form of a fine powder and high molecular weight (typically ~150,000Mw). It offers much of the same qualities that AMP has in terms of its application to the nuclear industry. PAN can be easily made into beads for use in practical applications without losing any of its chemical properties/characteristics. It is chemically stable in a range of pH values and is stable to high doses of radiation up to 1MGy<sup>[17]</sup>. When exposed to 1M  $\text{HNO}_3$  and 1M  $\text{NaOH}$

separately over the course of almost a month, the PAN beads only started to degrade in the alkaline solution when  $\text{NaNO}_3$  was introduced into the solution.<sup>[17]</sup> The stability in alkaline solution in the presence of increasing concentration of salts, would limit its applications, however its stability in acidic media remains high. There is apparent cross-linking in PAN when exposed to high doses of radiation in high alkaline solutions<sup>[18]</sup>. This is advantageous as the polymer becomes stronger and more durable, increasing its stability when exposed to nuclear waste solutions for an extended time scale.

The stability of PAN is not the only desirable characteristic; it has universal applications as a support material for many adsorbents and provides added protection from radiation and drastic changes in pH.<sup>[12][17]</sup> Due to the swelling nature of PAN during the preparative stage, many fine powders can be encapsulated and hence used in practical applications where larger particles are required. Many adsorbents are microcrystalline powders which, when bound to/into PAN, gives them the potential to be used in column work.

### 3.1.6 AMP/PAN composite.

In recent studies, AMP/PAN composite has been developed and undergone extensive evaluation. The current research has encompassed selectivity, kinetics and capacities evaluated for different shaped and sized beads.<sup>[12]</sup> The synthesis is simple, requires a surfactant dissolved in a suitable aprotic polar solvent such as dimethyl sulfoxide. The AMP is added and stirred for a set time with PAN being the final addition, it is a 'one pot' synthesis.

Many publications report the selectivity over competing ions such as sodium and potassium that may be present in some radioactive waste liquors <sup>[14]</sup>. In addition, high cesium capacities have been reported in the region of 150mg/g Cs/AMP <sup>[9]</sup> but are derived from the actual quantity of AMP that has been incorporated into PAN.

AMP-PAN composites exhibit very fast cesium uptake kinetics and almost reach maximum capacity within 10 minutes in acidic media. <sup>[9]</sup>

The challenge for UCLan's concept is the selectivity of AMP for cesium in a background of uranium and plutonium. In our case cerium is used as the simulant of these actinides as UCLan does not have an appropriate radioactive authorisation.

As both AMP and PAN have inherent stability to nitric acid and radiation, it is not surprising that composites of these reagents have similar properties.. In acidic simulated liquors and exposed to radiation doses of up to 1MGy, neither PAN or AMP exhibited any decomposition and therefore any negative effect on each other <sup>[12][17]</sup>. Nether the cesium adsorption capacities nor the uptake kinetics were hindered.

The results of countless experiments using AMP/PAN to extract cesium from strong acidic conditions, in particular from HLW, demonstrated that the inclusion into a PAN polymeric matrix had little or no effect on loading capacities. Although some research has been devoted to improving the cesium capacity, the majority of studies have involved exploring how capacity changes with differing variables such as competing ions<sup>[19]</sup>. Even the most efficient extractions are still below 99% of theoretical, with efficiency up to 98% <sup>[20]</sup> in studies relating to clean up of seawater on the Japanese coast. In addition, although various different size beads of AMP/PAN have been produced, there has been little modification to the composite in order to optimise surface area and porosity thus improving Cs uptake capacity and kinetics.



It was envisaged that the synthesis of AMP/PAN could be refined to optimise ion exchange performance via various experimental modifications, such as the refining of a confined jet nozzle to produce smaller, uniform beads. Even the most recent work on AMP/PAN was unable to improve the cesium capacities and kinetic uptake values reporting a much lower capacity than the theoretical (<30mg/g) [21] and thus significantly more work is needed to improve the uptake capabilities of AMP/PAN.

### 3.2 Characterisation of materials.

Various techniques detailed in chapter 2 were used to characterise the materials herein this chapter. These are outlined in table 3.1

*Table 3.1 Material Characterisation techniques*

Type of analysis	Analytical technique
Surface Area and Pore Size/volume	Gas sorption
Morphology	SEM
Functional groups	FT-IR
Thermal decomposition	TGA
Cation uptake measurements	ICP-MS

### 3.3 Results and Discussion.

The rationale developed during this project was to concentrate on the most promising composite, thus most of the data relates to AMP PAN 70. It should be emphasised that with further development and more extensive studies this rationale may be modified.

Ammonium phosphomolybdate has been identified previously as a highly selective adsorbent with a high capacity for cesium, but largely for HLW, i.e. liquors which have had the uranium and plutonium isotopes removed by the PUREX process. The readily replaceable ammonium ions is the underlying reason for these traits. Their ease of exchange for cesium ions is attributed to their hydrated ionic radii, 0.331nm and 0.329nm respectively. <sup>[21][22]</sup>

If the assumption that energetics, i.e. stability is dependent on ionic radii, based on Wells' work<sup>[23]</sup>, then other phosphomolybdate complexes that have ionic radii similar to that of cesium should be exchangeable. Rubidium for example has an identical hydrated ionic radius on the nanometer scale to cesium <sup>[24]</sup> A rubidium phosphomolybdate has been previously isolated and characterised, <sup>[25]</sup> and would no doubt compete with cesium if present in the same solution. Fortunately rubidium is not produced as a fission product in significant quantities in a nuclear reactor.

If the size of hydrated ionic radii is a key factor in AMP selectivity then the ions present in spent fuel dissolver liquor will be of significant interest and influence in selectivity. Cerium(III) and ceric(IV) have hydrated ionic radii of 0.120nm and 0.107nm respectively <sup>[26]</sup>. The difference in size of hydrated ionic radii should affect the likelihood of exchange

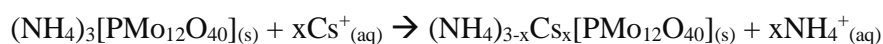
with ammonium ions, cf. cesium ions. Rubidium for example has an identical hydrated ionic radius to cesium [24]

It should be emphasised that the measured hydrated ion radii quoted are for a simple aqueous phase, i.e. water, the exchange of ion in our experiments is taking place in nitric acid solutions. Cerium however and zirconium ions are capable of forming mono-valent nitrate-complexes in nitric acid such as  $\text{Ce}(\text{NO}_3)_3^+$  [27][28] but it is highly unlikely such ions have the respective size to displace the ammonium ions from the phosphomolybdate lattice. Cesium ions in solution are relatively simple and exhibit little or no affinity to form complex ions. This debate is addressed later when discussing the selectivity and the  $K_d$  values for Cs and Ce ions.

If as discussed the selectivity of AMP is largely dependent on hydrated ionic size of exchangeable cations, then the surface area and porosity of AMP will greatly influence both capacity and kinetics of exchange. As reported earlier the surface area of microcrystalline AMP is high per unit weight, due largely to the small particle size of AMP. It is this small size that requires AMP to be incorporated into suitable matrices for practical applications. It is desirable that this surface area is not compromised when incorporated into for example PAN. In fact it is the porosity of PAN that will directly influence the kinetics and capacity of the composite. Optimising the surface area and porosity of AMP/PAN is fundamental to achieving high uptake capacity for cesium with fast uptake kinetics. This is addressed later when examining/analysing the SEM data.

AMP adsorbs caesium ions from aqueous solution by exchange with the ammonium ions in the crystal structure (phosphomolybdate anion pictured in Figure 2.1), as per Equation below,

where  $0 \leq x \leq 3$ , through pores in the crystal structure.[29]



Equation 2.1 Ion exchange of cesium with ammonium in AMP

Caesium phosphomolybdate ( $\text{Cs}_3[\text{PMo}_{12}\text{O}_{40}]$ , CsMP,  $x = 3$ ) can be prepared synthetically and has been studied,<sup>[30]</sup> although in ion exchange environments, only about two thirds of the  $\text{NH}_4^+$  ions in AMP ( $x = 2$ ) are typically replaced with  $\text{Cs}^+$ ,<sup>[31][32]</sup> though the theoretical capacity of AMP is 220 mg/g Cs at  $x = 3$ .

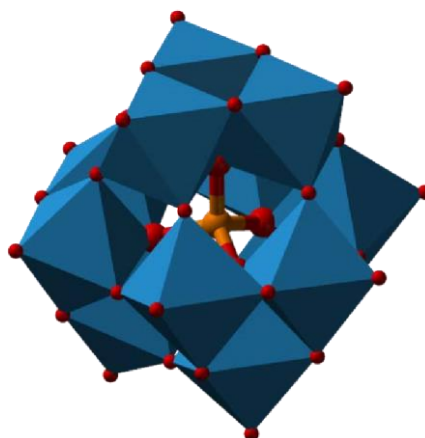
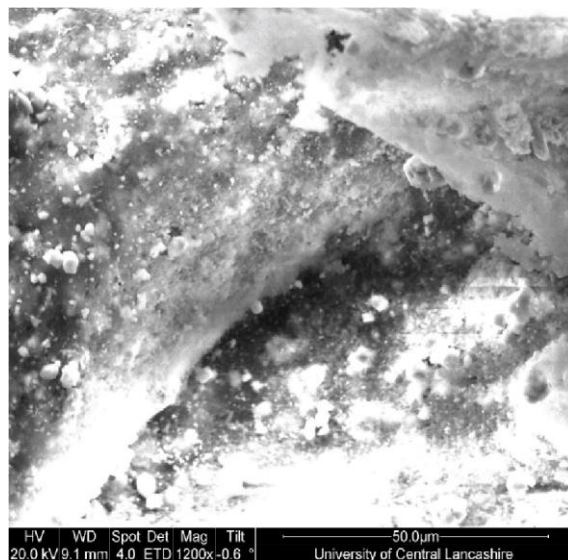


Figure 3.2.1 Keggin structure of the phosphomolybdate anion ( $\text{PMo}_{12}\text{O}_{40}^-$ ).

*MoO6 octahedra: blue; P: orange; O: red. open source image.*

Upon examination of the internal structure of AMP/PAN beads at high magnifications (x1200), particulate can be observed as encapsulated within the PAN. Figure 3.2 displays small particles within the internal structure of the AMP/PAN bead that are assumed to be the AMP particles. As proposed previously in the review of AMP, the AMP does not appear to dissolve in the reaction mixture, but rather is highly dispersed within the DMSO

containing the surfactant (hence the 1 hour stirring time). Once the PAN is added and swells upon contact with DMSO, the AMP is then encapsulated within the PAN and contained in the droplets used to form the beads.



*Figure 3.2 Internal Morphology of an AMP/PAN 70 bead displaying encapsulated AMP particulate*

### 3.3.1 Cesium uptake with AMP PAN composite - high and low concentration of cesium.

The AMP/PAN composite used for these experiments was synthesised according to the first method and the beads formed were gravity dropped and had a size range of 1-2mm. Initial studies were performed in 1M HNO<sub>3</sub> with AMP/PAN 70. The cesium uptake is reported in table 3.2 for high and low concentrations of the cation in solution. Values for  $K_d$  not only vary greatly between contaminants, but also vary as a function of aqueous and solid phase chemistry. Mechanistic models explicitly accommodate the dependency of  $K_d$  values on cation concentration, competing ion concentration, exchangeable sites on the absorbent, and solution species distribution. In our case only cation concentration and exchangeable sites predominate in this series of experiments, hence both the  $K_d$  and capacity values reported are influenced by cation concentration and the maximum capacity

of the AMP composite. A lower cation concentration favoured a high  $K_d$  value and conversely a high cation concentration favours a high capacity value. Table 3.2 clearly shows that AMP/PAN 70 exhibited limited capacity and uptake at higher concentrations of cesium due to the low surface area of beads,  $3.92\text{m}^2/\text{g}$ . A higher surface area and hence greater porosity will result in higher cesium uptake and diffusivity of cesium into/within the composite is significantly improved as reported later.

Table 2.2 Effect of differing cesium concentrations in 1M HNO<sub>3</sub> on capacity and  $K_d$  values

3ppm initial  $\sigma$  0.019, 514ppm initial  $\sigma$  0.043

	Cs (ppm)		Uptake		Capacity
	Initial	24 hrs	(%)	$K_d$ (ml/g)	(mg/g)
AMP/PAN 70	3	0.05	98	6154	0.3
AMP/PAN 70	514	271	47	89	24

### 3.3.2 Modifications to the synthesis of AMP/PAN

Each modification to the variables discussed in the sections to follow was changed independently of the others unless otherwise stated in their relevant sub sections.

#### 3.3.2.1 Uptake of Cs – altering the ratio of AMP: PAN

Differing the amount of AMP added to the mixture has previously affected the uptake of cesium in acidic solution [20]. For comparative studies AMP/PAN with 50% AMP and 70% AMP were synthesised separately as per the method in chapter 2.

Table 2.3 Effect of AMP concentration on cesium uptake from 1M HNO<sub>3</sub>. AMP/PAN 70  $\sigma$  0.046, AMP/PAN 50  $\sigma$  0.044

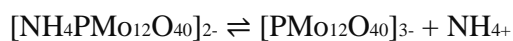
	Cs (ppm)		Uptake (%)	K <sub>d</sub> (ml/g)	Capacity (mg/g)
	Initial	24 hrs			
AMP/PAN 70	514	272	47	89	24
AMP/PAN 50	599	440	27	36	16

As expected, increasing the concentration of AMP in the composite resulted in a higher uptake of cesium (table 3.3), not surprising as a 50% AMP composite will have a theoretical cesium capacity of ~133mg/g, whilst the 70% composite 186mg/g (factor of 1.39) these values based on two exchangeable ammonium ions. Interesting the cesium uptake improvement ratio is 1.52 (24/16mg/g) which would suggest that other factors than AMP concentration cannot be disregarded.

Previous work <sup>[20]</sup> however has shown that there is an upper threshold concentration for AMP in PAN. An AMP concentration of 70% in the composite had a reduced effect on the cesium uptake <sup>[20]</sup>, this again may be due to the morphology of the bead. The results in this report differ from the previous results. This aspect is discussed later.

In most of the experiments the nitric acid concentration was 1M, but it is known that higher concentrations improve cesium  $K_d$  values <sup>[20]</sup>. Increasing acidity of the aqueous phase would suppress the dissociation of AMP and thus make it less likely to adsorb cesium in strong nitric acid. Obviously other factors are participating.

Equation 2.2 Theoretical dissociation of AMP

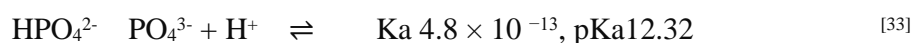


Unfortunately, although there is a wealth of information on cesium extraction by AMP, there is little or no mechanistic/thermodynamic data on the extraction reaction. One can



therefore only draw comparisons with phosphoric acid and phosphomolybdic acid. The dissociation of  $\text{H}_3\text{PO}_4$  is well documented and understood, and can be represented by;

Equation 2.3 Dissociation of Phosphoric Acid



Above values measured at 25°C

Replacing the final proton in phosphoric acid requires a strong base in order to overcome the energetics. We present here that there is a similar behaviour with AMP. The replacement of the third ammonium ion is difficult and exacerbated when the adsorbent is in the presence of stronger acid such as nitric, generally regarded as fully dissociated. Our theory would appear to be underpinned as previous work with AMP has suggested that only two of the ammonium ions are replaceable <sup>[31][32]</sup>.

This position may be further complicated on increasing nitric acid concentration with the potential to form phosphomolybdic acid (HMP) ( $\text{H}_3\text{PMo}_{12}\text{O}_{40}$ ) and as such AMP and HMP could co-exist in acid solutions employed in this study.

### 3.3.2.2 Effect of Gelling Temperature.

PAN produces a polymeric gel which is a three-dimensional network, formed by flexible molecule chains either through chemical cross-linking or physical phase transformation<sup>[40]</sup>. During gelation, a polymer liquid (in this case PAN in DMSO) gradually solidifies, and the liquid solution behaves more like an elastic solid beyond a critical point in terms of either aging time, polymer concentration, or temperature.<sup>[40]</sup> The study of gelling temperature on composite formation has been studied previously for many systems, but few have actually addressed the effect of temperature on the morphology of the composite. One paper noteworthy of mention with some applicability to this project involved the study of PAN fibres produced by electro spinning<sup>[34]</sup>. The workers demonstrated that increasing the gel bath temperature with a higher concentration of solvent in the bath resulted in more circular fibers and smoother fiber surface, not that dissimilar to the morphological structure found in this study but with AMP PAN beads, as is displayed in figure 3.3.

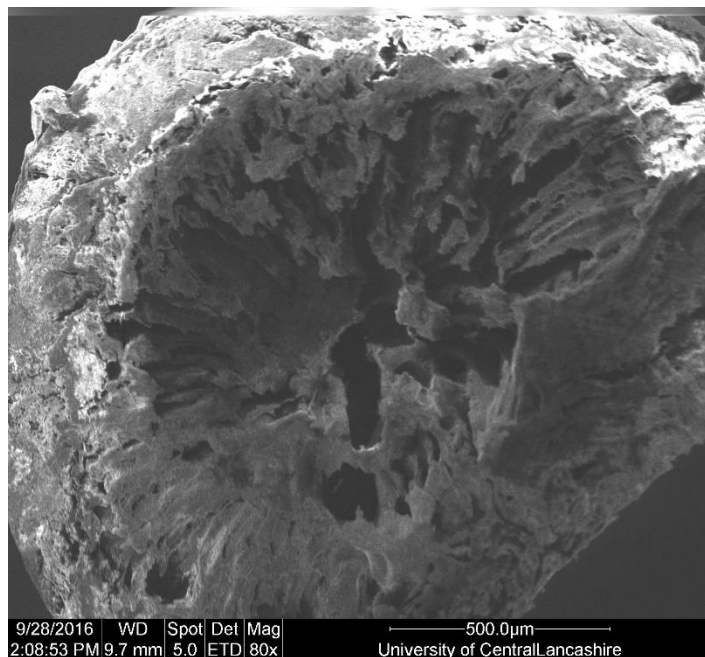


Figure 2.3 Cross section of AMP/PAN bead of 1-2mm in diameter synthesised with a reaction temperature of 80°C

The experimental conditions and techniques were kept the same with temperature of the reaction mixture being the only variable changed. Table 3.4 shows the uptake results of the temperature change.

There was no noticeable difference in uptake of cesium. The only observable difference was that the droplets of mixture formed discs instead of spherical beads when the gel solution made contact with water, possibly due to the different viscosities of the AMP PAN gel solution at 50<sup>o</sup> and 80°C.

Table 2.4 Effect of gel temperature of cesium uptake in 1M HNO<sub>3</sub>. 80°C  $\sigma$ 0.042, 50°C  $\sigma$ 0.027

	Gel temp °C	Cs (ppm)		Uptake (%)	K <sub>d</sub> (ml/g)	Capacity (mg/g)
		Initial	24 hrs			
AMP/PAN 70	80	514	272	46	88	24
AMP/PAN 70	50	514	271	47	89	24

Despite no considerable change in cesium uptake the SEM studies displayed less porous channels compared to previously synthesised beads at a lower temperature <sup>[20]</sup>. The disc shaped composites produced exhibit some voids close to the centre of the cross section but an apparent loss of voids and channels near to the surface suggests a decrease in porosity. The flat nature of these discs could explain the reason for a small discrepancy in cesium uptake. There is less distance between the surface and the internal voids, making the AMP easily accessible despite the reduced porosity.

### 3.3.2.3 Reducing molecular weight of PAN

A potential debating point with the PUREX process compared with UCLan's ART process could be the appropriate price of the extractant, i.e. TBP vs AMP PAN. Undoubtedly, TBP is significantly cheaper than AMP PAN, even though the composite could be manufactured at scale in a one-pot process. In addition, TBP is recycled whereas cesium loaded AMP PAN will be vitrified. This latter consideration may not be too drastic as the quantity of cesium to be extracted from a litre of spent fuel dissolver liquor

is around 600ppm and hence the quantity of AMP PAN required would not be substantially high <sup>[35]</sup>. A further cost saving with UCLan's envisaged flowsheet would be accrued from the reduced hardware/equipment needed once the bulk of the radioactivity had been removed from the spent fuel dissolver liquor. This aspect is under consideration for a future publication. Nonetheless producing a most cost effective composite by either reducing the AMP concentration and/or cheaper polymeric support material was undertaken. PAN with Mw 150,000 was used for the initial synthesis (3.3.2.1) and temperature variation experiment (3.3.2.2) but for this series of experiments a reduced molecular weight of PAN (Mw 85,000) was used. The cost of Mw 85,000 PAN is half the price of 150,000 Mw. It should be emphasised that comparing costs from small chemical suppliers such as Sigma Aldrich can be misleading as prices are significantly influenced by bulk buying and under contract.

Although it was appreciated that a lower Mw PAN could significantly reduce the cost of AMP PAN synthesis, the impact on cesium uptake was unknown. Previous studies but not in the context of cesium extraction have shown that reducing the Mw of PAN from 87K to 30K influences bead quality and size. <sup>[36]</sup>

PAN with Mw 150,000 was used for the initial synthesis and hence when varying the experimental temperature as this was the first condition variable to be changed. The Mw of PAN used was reduced to 85,000 and reduced the experimental cost by almost half.

Table 2.5 Effect of PAN molecular weight on cesium uptake from 1M HNO<sub>3</sub>. 150kPANσ  
0.035, 85k PAN σ 0.004

Mw	Cs (ppm)				K <sub>d</sub> (ml/g)	Capacity (mg/g)
	Initial	24 hrs	Uptake (%)			
AMP/PAN 70 150k						
PAN	514	271	47		89	24
AMP/PAN 70 85K						
PAN	514	282	47		81	23

Although from the work previously cited <sup>[36]</sup> using PAN of different Mws had an impact on bead quality the workers did not address morphology of the internal structure. The results in table 3.5 indicate that reducing the Mw of PAN had no substantial effect on the uptake of cesium and the difference (<5%) is too small to be considered otherwise. This PAN (85K) was therefore used in the production of beads using the glass nozzle and confined jet techniques.

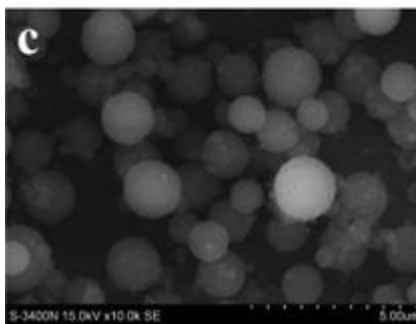
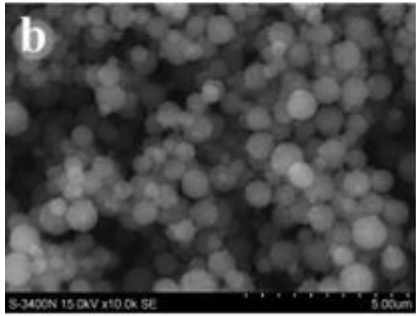
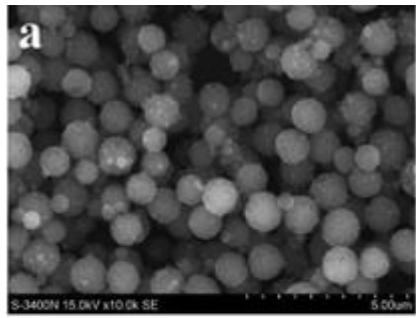


Figure 2.5 SEM images of the electrospinning products from PAN ( $M_w = 30,000$ )/DMF solutions at different concentrations: (a) 2 wt.%, (b) 3 wt.%, and (c) 4 wt.%. Taken from source [36]

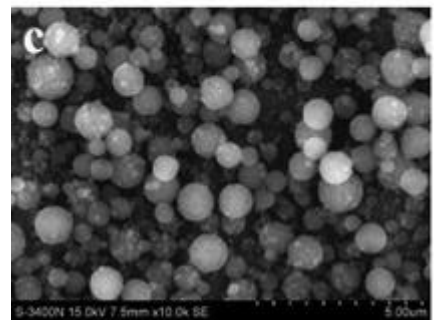
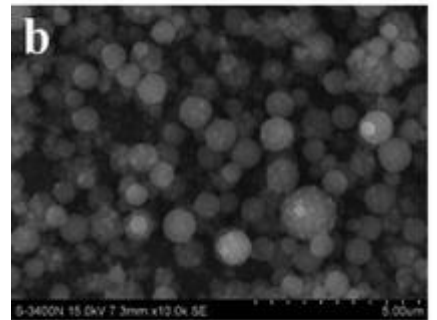
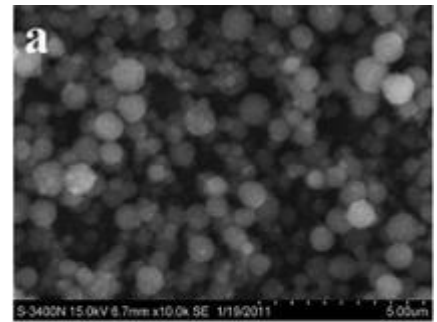


Figure 2.4 SEM images of electrospinning products from PAN ( $M_w = 87,000$ )/DMF solution at different concentrations: (a) 2 wt.%, (b) 3 wt.%, and (c) 4 wt.%. Taken from source [36]

### 3.3.2.4 Reducing solvent volume.

From the previous cited work [36] the impact of increasing PAN concentration of the DMSO i.e. reducing solvent volume appeared to have marginal visible effect on the bead quality (figures 3.4 and 3.5). The concentration of PAN in DMSO affects the viscosity and therefore the dispersion of AMP and as shown with the data in Table 7 results in an increased cesium uptake.

Table 2.6 Effect of reducing solvent volume on uptake of cesium in 1M HNO<sub>3</sub>. 50ml of solvent was used as opposed to 100ml. reduced solvent  $\sigma 0.006$ , original  $\sigma 0.035$

	Cs (ppm)				
	Initial	24 hrs	Uptake (%)	K <sub>d</sub> (ml/g)	Capacity (mg/g)
AMP/PAN 70 reduced solvent	645	269	58	139	37
AMP/PAN 70 original	514	282	47	81	23

As presented in table 3.6, halving the amount of DMSO added to AMP/PAN 70 almost doubled the cesium capacity at similar concentrations (4 - 5mM). This increase in cesium capacity can be attributed to the concentration of PAN and AMP in the DMSO thus affecting the morphology of the beads.

The newly synthesised composite with reduced solvent is superior to previous composite beads [20]. As a result of the increased cesium capacity of AMP/PAN 70 with a reduced



solvent volume, 50ml DMSO was used as opposed to 100ml, for the preparation of the beads in section 3.3.3 onwards.

### 3.3.2.5 Changing Surfactant concentration.

The morphology and size of the particles have been shown to be dependent on the type of surfactant and solution used. The size range of the particles was about 75–160 nm and their molecular structure has been studied by using Fourier-transform infrared spectroscopy. Which showed that the intensities of the peaks were dependent on the nature of the surfactant. [37]

The supposed role of the surfactant is to make the composite beads more microporous which results in their high malleability. In theory, an increase in surfactant concentration, within limits, should increase porosity of the beads and therefore give the cesium ions better access to the AMP. This however, turned out not to be the case as can be seen in table 3.7.

Table 2.7 Effect of increasing surfactant concentration on cesium uptake x1 tween  $\sigma 0.012$ , x5 tween  $\sigma 0.003$

	Cs (ppm)				Capacity (mg/g)
	Initial	24 hrs	Uptake (%)	$K_d$ (ml/g)	
AMP/PAN 70 x1 Tween	514	271	47	89	24
AMP/PAN 70 x5 Tween	514	366	28	40	14

The increase in surfactant concentration slightly decreased the cesium uptake. Currently there is no satisfactory explanation as the surface area increased to  $6.58\text{m}^2/\text{g}$  from around  $3\text{m}^2/\text{g}$  which should in theory have increased cesium uptake. This requires further investigation.

#### 3.3.2.6 Reducing bead size.

The optimisation of surface area of the composites can increase the uptake capabilities due to the increased amount of composite available to the cations. Reducing bead size significantly would increase the surface area per gram and even the total surface area/g of material but could also reduce the amount of AMP encapsulated within the beads. As the results of decreasing solvent volume experiment were positive, subsequent experiments aimed to reduce bead size and followed the default method of AMP/PAN synthesis but with half the amount of solvent.

##### 3.3.2.6.1 Confined Jet.

The confined jet was a relative crude concept and provided little uniform size of beads. The reaction mixture appeared to be too viscous resulting in poor hydrodynamics within the jet thus producing AMP PAN “strings” but with some small beads  $<1\text{mm}$  salvageable for use in batch experiments.

Table 2.8 Comparison of cesium uptake as a function of bead size.  $\sigma < 1\text{mm}$  0.028, 1-2mm  $\sigma$  0.042

		Cs (ppm)				Capacity (mg/g)
Bead size (mm)	Initial	24 hrs	Uptake (%)	$K_d$ (ml/g)		
AMP/PAN 70 beads	<1	645	255	60	151	38
AMP/PAN 70 beads	1-2	514	282	47	81	23

Table 3.8 shows that the larger beads produced using the conventional gravitational dropping method have a much lower uptake of cesium and adsorption capacity than the smaller beads prepared using the confined jet. The increase of surface area is one explanation for these results, the outer surface areas of a 1mm and 2mm diameter sphere are 3.14 and 12.60 mm<sup>2</sup> respectively. The BET data also substantiated this as the total surface area had almost tripled in value to 9.16m<sup>2</sup>/g.

#### 3.3.2.6.2 Glass Nozzle.

A custom made nozzle that was produced according to the literature drawing <sup>[38]</sup> provided a much more reliable way to produce small beads of AMP/PAN. As appropriate equipment was not available producing precise parameters for optimal bead production was difficult, but there was a reduction in ‘stringer’ production with more uniform size bead control

(~200 – 500 microns) compared with the confined jet (300 – 1000 microns). With this improvement bead examination was expanded to include cesium uptake experiments in 3M HNO<sub>3</sub>.

Table 2.9 Cesium uptake of composite produced using the glass nozzle technique. 1M  $\sigma$  0.047, 3M  $\sigma$  0.010

	Nitric Acid concn	Cs (ppm)		Uptake (%)	K <sub>d</sub> (ml/g)	Capacity (mg/g)
		Initial	24 hrs			
AMP/PAN 70	1 M	574	305	46	88	26
AMP/PAN 70	3 M	634	44	93	1322	58

Previous work has shown that the concentration of nitric acid influences the cesium K<sub>d</sub> value [20], these experiments confirmed that early work. In 1M HNO<sub>3</sub>, the small beads did not perform as well as expected, but did show a slight increase in cesium capacity compared to the original sized beads, but this may have been due to the slightly more concentrated cesium solution used.

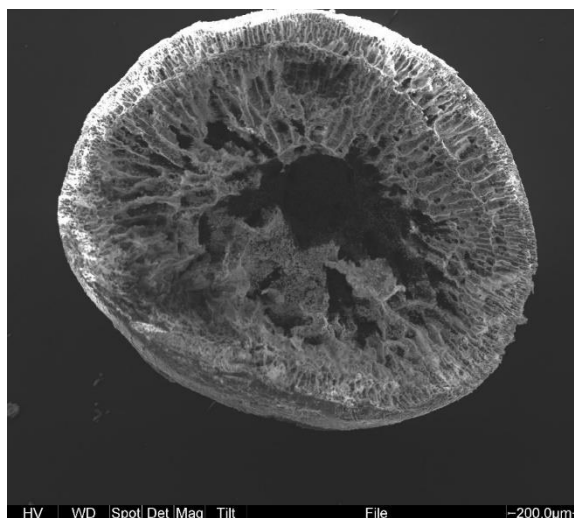


Figure 2.6 Cross section of a single bead of AMP/PAN 70 produced using the glass nozzle method.

The SEM image of a single bead produced by this new glass nozzle technique can be seen in figure 3.6. The bead displayed a greater amount of voids present, as opposed to the ordered channel structure of previously synthesised AMP/PAN 70 [20]. A greater amount of voids within the beads could possibly mean a greater amount of AMP within the PAN composite and easier access for the cesium ions to diffuse through the composite, hence the increase in cesium uptake.

This method has drastically improved the capacity and uptake of cesium from stronger nitric acid; further refinement of the material should result in even higher capacity composites which could be appropriate for column work.

### 3.3.3 Selectivity of AMP/PAN.

Although AMP/PAN has shown to be selective for cesium in the presence of other cations such as K, Na, Ca, there is no recorded evidence of its performance for cesium isotopes

when in the presence of uranium and plutonium. Demonstrating this performance will be crucial to UCLan's alternative reprocessing technology (ART). In the PUREX process decontamination values ( $D_f$ ) of at least  $10^6$  are achieved but require a multi-stage extraction process. To put this  $D_f$  value into context then our chromatographic process would require to reduce the cesium concentration from 1g/te U to 1 $\mu$ g/te U. AMP/PAN is capable of extracting low concentrations of cesium even in 1M HNO<sub>3</sub> as reinforced by results in table 3.2. Although this efficiency may fall short of the required  $D_f$ , it should be emphasised that batch experiments are indicative and more superior results would be achieved in column studies.

As UCLan's radio-lab is not equipped to handle uranium and the university's radioactive authorisation currently excludes the use of alpha emitting radionuclides, simulant cations were used, i.e. cerium ions instead of for both uranium and plutonium ions due to similar cationic radii. <sup>[23]</sup>

The superior cesium uptake of the newly synthesised AMP/PAN beads using the glass nozzle warranted these to be used in the selectivity experiments. The results were compared to previously produced material. <sup>[20]</sup>

Table 2.10 Selectivity of AMP/PAN in the presence of high concentrations of cerium in 3M HNO<sub>3</sub>.  
Cs:Ce(iv) ratio of 1:50.

AMP/PAN 50 1- 2mm beads Cs  $\sigma$  0.047, Ce  $\sigma$ 0.009, AMP/PAN 70 Glass Nozzle <1mm beads Cs  $\sigma$ 0.014, Ce  $\sigma$ 0.043.

	Cs (ppm)		Ce(iv) (ppm)		Uptake (%)		K <sub>d</sub> (ml/g)		Capacity (mg/g)	
	Initial	24hrs	Initial	24hrs	Cs	Ce	Cs	Ce	Cs	Ce
Parthiv's AMP/PAN 50	14.44	0.267	713	700.2	98.1	1.8	5305.1	1.8	1.4	1.2
AMP/PAN 50 1-2mm beads	14.44	0.184	713	677.0	98.7	5.1	7752.5	5.3	1.4	3.6
AMP/PAN 70 Glass Nozzle <1mm beads	14.44	0.148	713	708.0	98.9	0.7	9670.3	0.7	1.4	0.5

Data in table 3.10 indicates that in addition to the high cesium uptake the majority of the cerium was not extracted from solution, confirming the selectivity of AMP/PAN and strengthening the case that the material could have potential for UCLan's reprocessing idea. The results of the beads synthesised by P. Kavi<sup>[20]</sup> can be seen in the first row. Although of similar performance, the newly synthesised AMP/PAN 70 using the glass nozzle are slightly superior and have an even lower affinity for cerium. These levels of cerium do not replicate the concentration of U and Pu in real spent fuel and thus further experiments were undertaken with much increased cerium ratio (table 3.11).

Table 2.11 Selectivity of AMP/PAN in the presence of high concentrations of cerium in 3M

HNO<sub>3</sub>. Cs:Ce(iv) ratio of 1:450

Parthiv's AMP/PAN 50 Cs  $\sigma$  0.031, Ce (iv)  $\sigma$ 0.022, AMP/PAN 50 Cs  $\sigma$  0.027, Ce(iv)  $\sigma$ 0.005, AMP/PAN 70 Cs  $\sigma$ 0.011, Ce (iv)  $\sigma$ 0.26

	Cs (ppm)		Ce(iv) (ppm)		Uptake (%)		K <sub>d</sub> (ml/g)		Capacity (mg/g)	
	Initial	24hrs	Initial	24hrs	Cs	Ce	Cs	Ce	Cs	Ce
Parthiv's AMP/PAN 50	1.242	0.027	555.4	536.2	99.9	3.4	4502.7	3.5	0.1	1.9
AMP/PAN 50	1.242	0.029	555.4	549.4	99.9	1.0	4187.8	1.0	0.1	0.6
AMP/PAN 70	1.242	0.025	555.4	545.1	99.9	1.8	4871.9	1.8	0.1	0.1

The results in table 3.11 show that selectivity for cesium is maintained even with a much higher excess of cerium present. This data demonstrates the good cesium selectivity; its low capacities from these solutions should not be seen negatively as capacity is a function of the cation in solution. Although the cerium uptake increased slightly, the selectivity ratio (table 3.13) was still significantly high to effect a good cesium/cerium separation.



### 3.3.4 Effect of Ce oxidation state on cesium uptake.

The selectivity of AMP PAN under these different cation conditions are presented in table 3.12.

It is noticeable that the cesium selectivity is hindered by cerium being present in its 3+ oxidation state (table 3.12). The smaller beads produced from the glass nozzle in this experiment did not perform as well as previously synthesised AMP/PAN, the reasons for this are under review. Although the cesium uptake decreased by around 10% with a slight increase in cerium uptake this trend would not reflect column studies as cesium has the far greater  $K_d$  value and would subsequently dislodge cerium from the AMP PAN.

The separation factors ranged from ~1500 to >13,000 (table 3.13) depending on the AMP PAN beads employed and the ratio of Cs:Ce in solution and for Ce(IV) ions, but with Ce(III) impairing the selectivity. It can only be deduced with some confidence from the data reported in table 3.13 that cerium oxidation state had a significant impact on the selectivity value.

Table 2.12 Selectivity of AMP/PAN in the presence of high concentrations of cerium in 3M HNO<sub>3</sub>.

Cs:Ce(III) ratio of 1:225

Parthiv's AMP/PAN 50 Cs  $\sigma$  0.016, Ce (iii)  $\sigma$ 0.017, AMP/PAN 50 1-2mm beads Cs  $\sigma$  0.032, Ce(iii)  $\sigma$ 0.018, AMP/PAN 70 Glass Nozzle Cs  $\sigma$ 0.019, Ce (iii)  $\sigma$ 0.042

	Cs (ppm)		Ce(iii) (ppm)		Uptake (%)		$K_d$ (ml/g)		Capacity (mg/g)	
	Initial	24hrs	Initial	24hrs	Cs	Ce	Cs	Ce	Cs	Ce
Parthiv's AMP/PAN 50	0.627	0.068	140.3	138.7	89.1	1.1	822.1	1.1	0.05	0.1
AMP/PAN 50 1-2mm beads	0.627	0.161	140.3	133.1	74.3	5.1	289.4	5.4	0.04	0.7
AMP/PAN 70 Glass Nozzle	0.627	0.099	140.3	136.9	84.2	2.4	533.3	2.4	0.05	0.3

The possible reason for impairment is the hydrated ionic radii of the two oxidation states of cerium. Cerium (III) has a more similar hydrated radius to ammonium than cerium (IV), making it feasible that ion exchange between the former may occur. The ability of cerium (IV) to form nitrate-complexes can also be attributed to this change in selectivity as mentioned previously, i.e. this hydrated complex ionic radii may be too large to be accommodated in the transferring ammonium ions hole. Kinetics studies may provide information that can substantiate the selectivity behaviour of cerium ions.

It should again be emphasised that these values were measured for batch studies i.e. one contact. Depending on the number of theoretical plates in a column a much superior separation would be expected.

Table 2.13 Cesium selectivities

Table No	AMP PAN	Oxidation state of Ce	Acidity (M)	Cs: Ce ratio	Separation factor
11	AMP PAN 50 Parthiv's	+4	3	1:50	2900
	AMP PAN 50 1-2 mm beads				1457
	AMP PAN 70 glass nozzle				13620
12	AMP PAN 50			1:450	1258
	AMP PAN 50				3842
	AMP PAN 70				2578
13	AMP PAN 50 Parthiv's	+3		1:225	715
	AMP PAN 50 1-2 mm beads				53
	AMP PAN 70 glass nozzle				215

### 3.3.5 Kinetics of cesium uptake.

The extraction rate is the second most important criteria for ion exchange/adsorption, only capacity is more important. The detailed reaction kinetics for AMP PAN cesium are largely unknown, and hence identification of the rate-limiting step is still doubtful and this lack of knowledge is of great concern for developing and improving a separation process based on chromatography. The results reported in the section may assist in this identification, but it is considered that further kinetic studies will be necessary with the various components, in particular bead morphology, surface area and bead size requiring greater scrutiny. Column studies should complement these further batch studies.

The kinetic studies for AMP/PAN were performed using composite material synthesised using the dual stainless steel nozzle as these performed best in terms of uptake in 3M HNO<sub>3</sub>. Table 3.14 presents the results over 48 hours.

Table 2.14 Kinetics of cesium uptake using AMP/PAN 70 produced using glass nozzle

Time (mins)	Total (%)	Uptake (%)	Kinetics (%)	uptake K <sub>d</sub> (ml/g)	Capacity (mg/g)	Cs (ppm)	SD (σ)
0		0		0		635	0.004
10		90.		69.	907	57	0.010
30		91		75	984	57	0.004
60		91		78.	1035	58	0.027
180		93		97	1304	59	0.022
360		93		9	1317	59	0.015
1440		93		98	1323	59	0.036
2880		93		100	1349.99	58.84	0.030

The rate of uptake results in table 3.14 displays that >90% of the total cesium in solution was achieved within the first 10 minutes equilibrium in 3M nitric acid. This value is consistent with previous recorded data <sup>[9][39]</sup>. In addition, uptake continued over the next 1-48 hours but only an additional 3% was adsorbed and the cesium capacity similar remained relatively constant at ~59mg/g. This number is approximately 42% of the theoretical capacity (~142mg/g equivalent to the exchange of two ammonium ions). As previously discussed capacity is a function of the aqueous phase conditions.

The newly prepared beads exhibited much faster kinetics compared to the composite beads prepared by P. Kavi as illustrated in figures 3.7 and 3.8. <sup>[20]</sup> Although these composite beads were inferior to beads produced in this study they did demonstrate that neither temperature nor acidity affected the kinetics. The former result is somewhat confusing and requires further examination whilst the independence of acid concentration fits with previously published data.

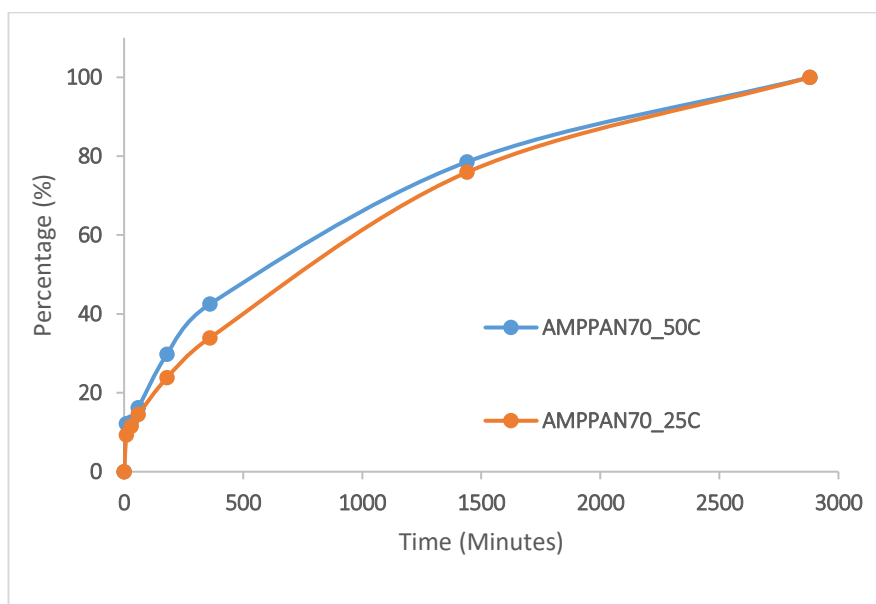


Figure 2.7 Cs ions rate of uptake at different temperature in 1 M HNO<sub>3</sub>

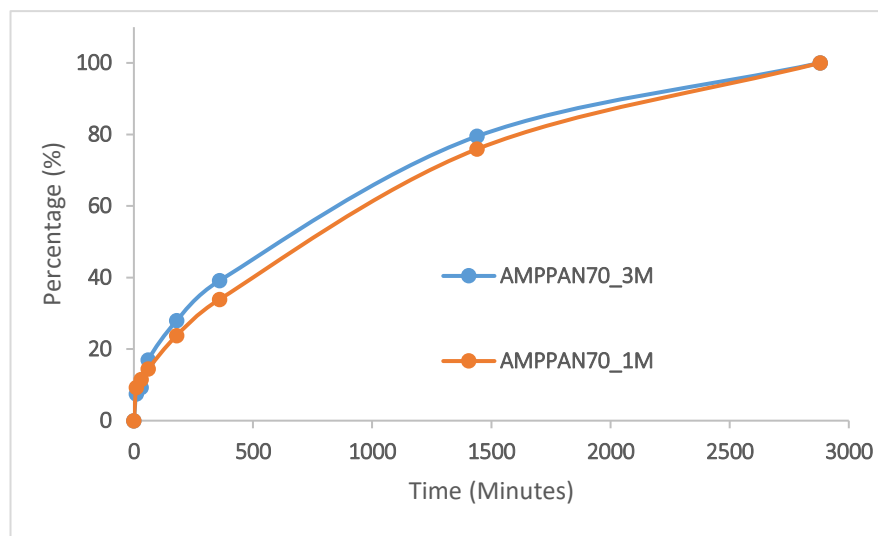


Figure 2.8 Cs ions rate of uptake at 25 °C in different acidity

The kinetics showed positive results and reinforced the fast uptake of cesium that AMP/PAN exhibits. Over 90% of all the cesium present was taken up in 10 minutes of contact time with

5mM cesium solution. Despite this, uptake continued over the next 48 hours but only an extra 3% was adsorbed. The results show there was no leaching of cesium over this time, proving the stability of the material.

### 3.3.6 Irradiation studies with varying cesium concentration.

Dry AMP powder and AMP-PAN 70 (composite beads formed via dual stainless steel nozzle) were both irradiated in sealed vials with gamma radiation (1.173 MeV and 1.333 MeV) at a rate of 60 Gy/min, to an exposure of 100 kGy using a using a Foss Therapy 812-self-shielded <sup>60</sup>Co irradiation source located at the Dalton Cumbrian Facility, Whitehaven, UK.

### 3.3.6.1 Kinetics.

The most profound visible effect observed following irradiation, however, is a marked colour change (AMP from yellow to green, AMP-PAN from lime green to dark green, shown in Figure 3.9, reminiscent of literature references,<sup>[40][41][42]</sup> and theorised as a result of  $\text{Mo}^{\text{VI}}$  to  $\text{Mo}^{\text{V}}$ . We explored the rate of uptake and capacity of  $\text{Cs}^+$  for virgin and irradiated AMP and AMP-PAN using two different  $\text{Cs}^+$  concentrations in 3M  $\text{HNO}_3$ : 5.0 and 10.0 mM, replicating the acidity<sup>[43]</sup> and  $\text{Cs}^+$  concentration<sup>[44]</sup> for spent fuel recycling of present and future, higher-burnup fuels respectively. The observed  $\text{Cs}^+$  uptake is shown as capacity as a function of time in Figures 3.9AD, and the associated distribution coefficients ( $K_d$ ) of each sample after 24 h are shown in Figure 3.11.

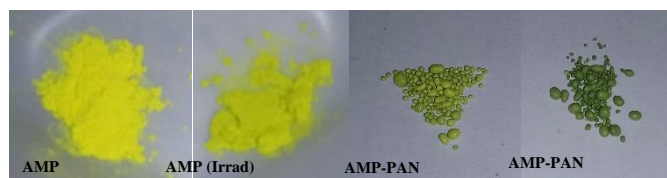
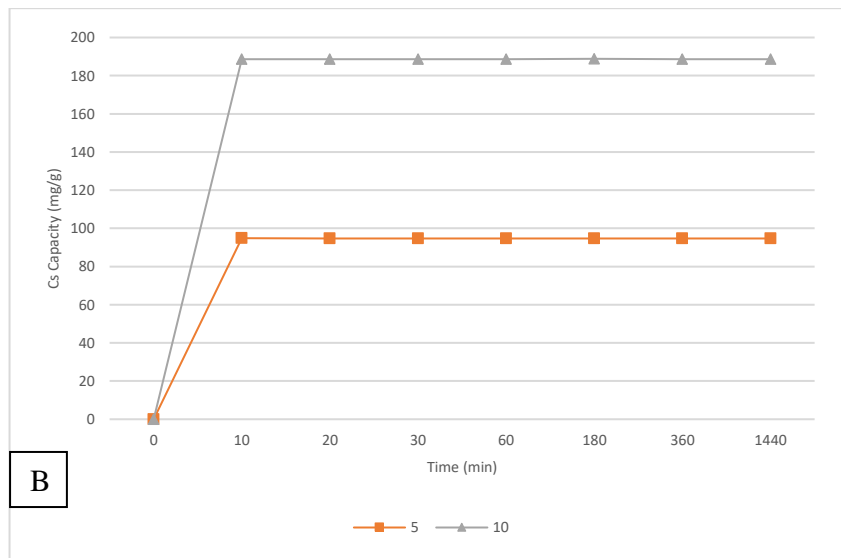
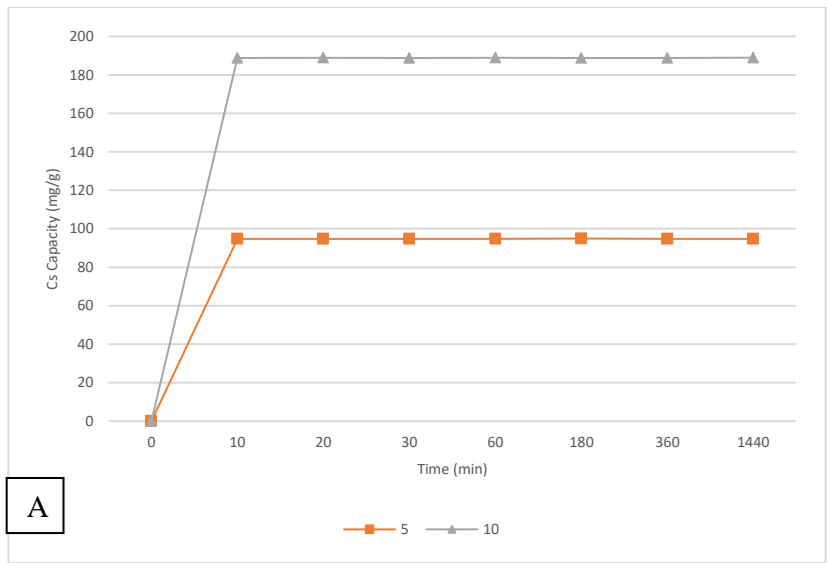


Figure 2.9 Optical images of virgin and irradiated AMP powder and AMP-PAN composite beads.



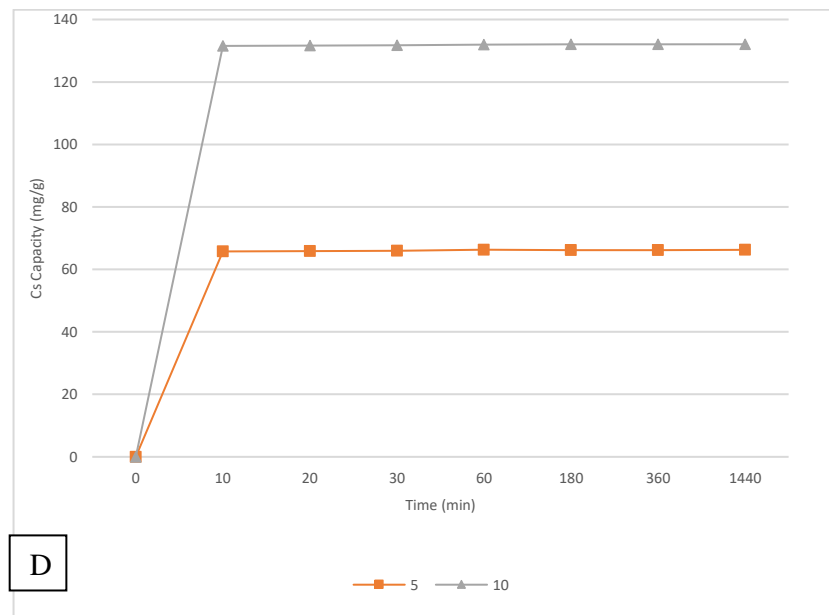
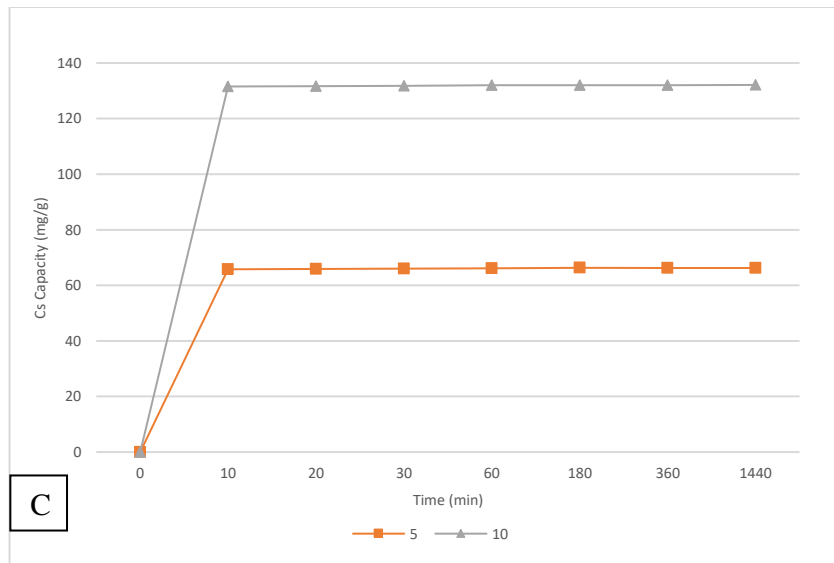


Figure 2.10A to D: Measured Cs<sup>+</sup> capacities (mg/g) over time (min) and with Cs<sup>+</sup> concentration (mM) for virgin AMP (3.10A), irradiated AMP (3.10B), virgin AMP-PAN (3.10C) and irradiated AMP-PAN (3.10D) from 3 M HNO<sub>3</sub> solution.



The uptake of Cs<sup>+</sup> by AMP (Figure 3.10A and 3.10B) is rapid, achieving near complete uptake (> 98%) within 10 minutes, independent of the Cs<sup>+</sup> concentration. Capacity is proportional to the concentration of Cs present in the solution, reaching near the theoretical maxima for AMP: 5.0 mM: 95 mg/g; and 10 mM: 190 mg/g. Irradiation has no discernible effect on either the rate of uptake or capacity by AMP.

The Cs capacity AMP-PAN composites (Figures 3.10C and 3.10D) is similarly proportional to the Cs<sup>+</sup> concentration used. Uptakes at both Cs<sup>+</sup> concentrations are rapid, as per AMP, reaching a maximum within 10 minutes of exposure for both virgin and irradiated AMP-PAN samples; the theoretical maxima of capacity: 5.0 mM: 66 mg/g; and 10 mM: 133 mg/g is approached. As the AMP-PAN composite is 70% by weight AMP, the resulting capacities are hence c.a. 70% lower than AMP. The slight increase in the Cs<sup>+</sup> capacity of AMP induced by β<sup>-</sup> irradiation reported by Rao et al,<sup>[41][45]</sup> was not observed here.

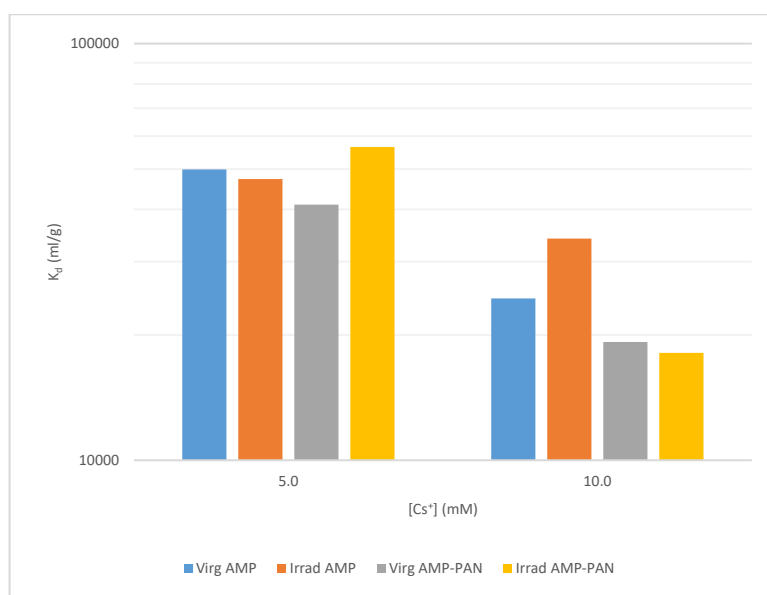


Figure 2.11 Variation of Cs<sup>+</sup> K<sub>d</sub> values and capacity after 24 h exposure to AMP and AMP-PAN.

Due to the sensitivity of Equation 2.2 (for the calculation of distribution coefficients) at near complete  $Cs^+$ , small variations in the observed uptake result in significant variations in the value of the distribution coefficient ( $K_d$ ): at complete (100%) uptake,  $K_d = \infty$ . Figure 3.11 highlights the affinity of AMP for  $Cs^+$  is maintained<sup>28</sup> across the range of concentrations tested, with irradiation having negligible impact on the uptakes.

### 3.3.6.2 Isothermal analysis.

The Langmuir and Freundlich isotherms are expressed as equations 3.4 and 3.7.<sup>[46]</sup> Rearranged these equations give straight line plots for pseudo first order Langmuir (Equation 3.5) or second order Langmuir or Freundlich (Equation 3.6 and 3.8) processes.<sup>[46]</sup>  $Q^0$  and  $K_l$  are the Langmuir constants for absorption capacity (mg/g) and energy of adsorption (L/g), and  $K_f$  and  $n$  are the Freundlich constant (mg/g) and the adsorption intensity constant, respectively.<sup>[46-49]</sup>

$$q_e = (Q^0 \cdot K_L \cdot C_e) / (1 + K_L \cdot C_e)$$

Equation 2.4 Langmuir Isotherm

$$1/q_e = 1/Q^0 + (1/K_l \cdot Q^0 \cdot C_e)$$

Equation 2.5 Pseudo first order Langmuir

$$C_e/q_e = 1/K_l \cdot Q^0 + C_e/Q^0$$

Equation 2.6 Second Order Langmuir

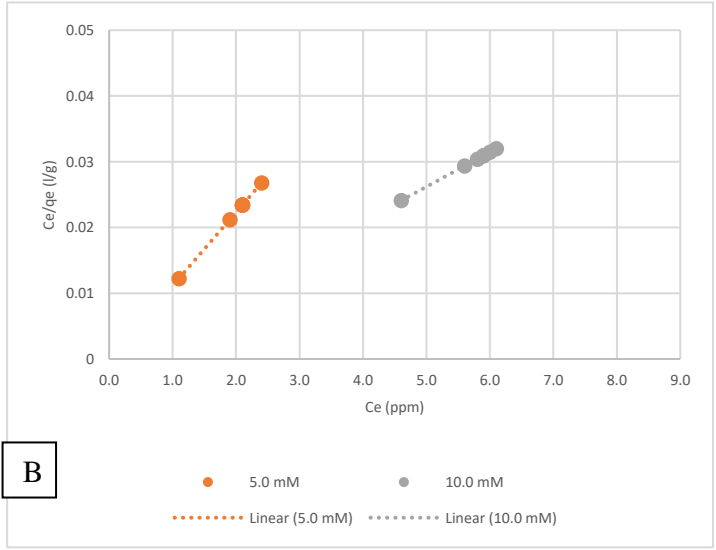
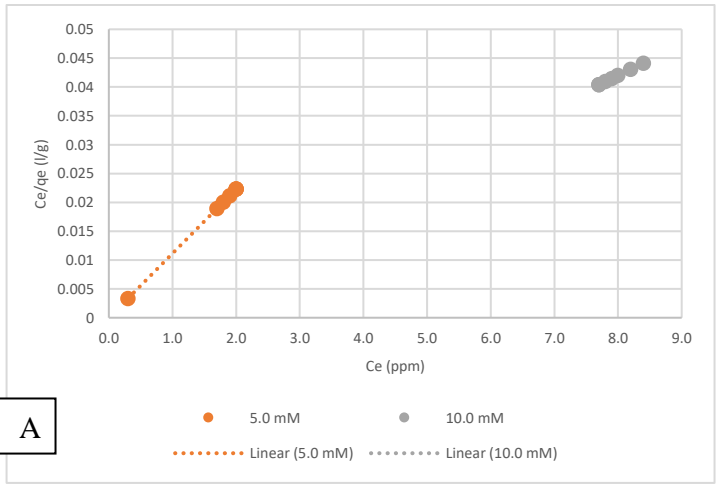
$$q_e = K_f \cdot C_e^{1/n}$$

Equation 2.7 Freundlich Isotherm

$$\log q_e = \log K_f + 1/n \cdot \log C$$

Equation 2.8 Second Order Freundlich

Figure 3.12A to 3.12D shows Langmuir (Equations 3.4-3.6) isotherm plots for virgin and irradiated AMP and AMP-PAN exposed to 5.0 and 10.0 mM Cs<sup>+</sup>. The isothermal parameters and regression coefficients calculated from this data and the equivalent Freundlich isotherm interpretation<sup>[46]</sup> are presented in Table 3.15.



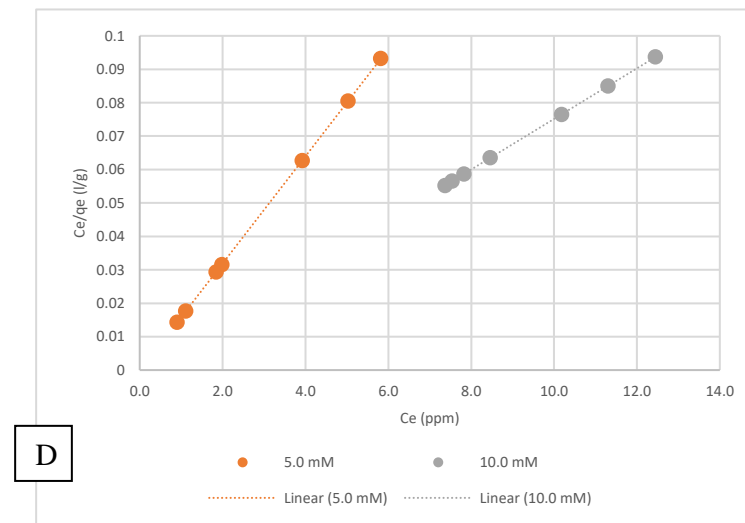
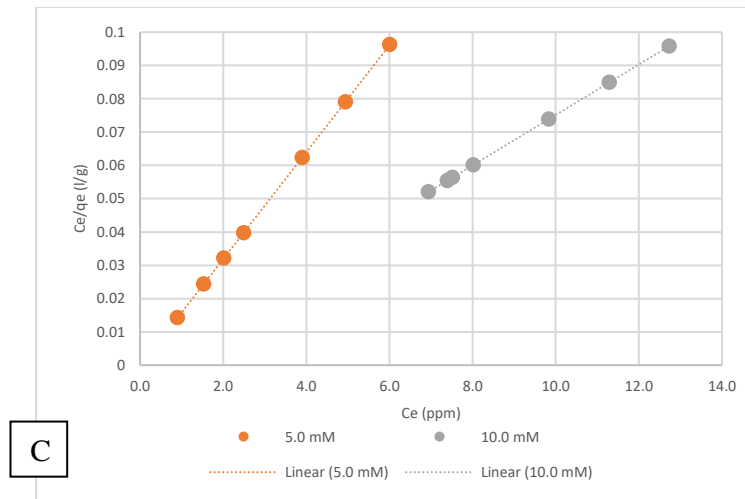


Figure 2.12A to D: Pseudo-second order Langmuir isothermal plots for virgin and irradiated AMP (3.12A and 3.12B), and virgin and irradiated AMP-PAN (3.12C and 3.12D), calculated from the data in Figure 3.12A to 3.12D

Table 2.15 Comparison of calculated Langmuir and Freundlich isothermal parameters.

Isotherm	Parameter	AMP		AMP (Ir)		AMP-PAN		AMP PAN (Ir)	
		5 mM	10 mM	5 mM	10 mM	5mM	10 mM	5 mM	10 mM
Langmuir	$Q_0$ (mg/g)	89.28	188.68	89.28	188.68	62.50	131.57	62.50	131.57
	$R^2$	1.000	1.000	1.000	1.000	1.000	1.000	1.000	1.000
	Freundlich	$K_F$ (mg/g (l/mg) $1/n$ )	89.81	192.83	89.86	192.08	62.95	135.27	62.93
	$R^2$	0.990	0.999	0.991	0.999	0.935	0.995	0.952	0.996

As the data presented in Figure 3.12 demonstrates, the observed uptake of  $Cs^+$  by AMP and AMPPAN fits the pseudo second-order Langmuir isotherm with a high regression coefficient ( $R^2$ ), mirroring the previous work of Mahendra, Herbst, and Ding.<sup>[47][50][51]</sup> While the regression coefficients ( $R^2$ ) for the Freundlich isotherm are close to 1, slopes of the lines produced by this method were negative, indicating a poor fit to the technique. Despite this, the calculated Langmuir absorption capacity constants ( $Q_0$ ) and the Freundlich constants are in close agreement for the AMP and AMP-PAN system, and the  $Cs^+$  concentrations investigated. No variation is observed between the virgin and irradiated material, indicating that irradiation does not negatively affect ion exchange performance,  $Cs^+$  capacity or the mechanism of uptake.

The Langmuir isotherm represents a dynamic equilibrium balance of the surface covered with the relative rates of adsorption and desorption for monolayer coverage. Adsorption is proportional to the fraction of the surface of the adsorbent that is open while desorption is proportional to the fraction of the adsorbent surface that is covered. This may be

applicable for gas adsorption but not necessarily valid for ion exchange. The Langmuir constant which is related to capacity and can be correlated with the variation of the suitable area and porosity of the adsorbent is valid with the data produced in this project i.e. a large surface area and pore volume favours higher adsorption capacity. The Freundlich isotherm, an empirical construct, has greater degrees of freedom, i.e. not restricted to mono layer adsorption, and defines the surface heterogeneity and the exponential distribution of active sites and their energies. It is largely applicable to adsorption processes that occur on heterogenous surfaces such as our composites.

### 3.3.7 Morphology.

SEM results show the internal morphology at different zoom levels. Figure 3.13 is taken from work by Kavi, P for comparison with newly synthesised materials. Figures 3.14 – 3.17 are of

AMP/PAN 70 synthesised using the glass nozzle route with the reduced solvent volume. Figure 3.14 shows the new beads and the difference in internal structure is substantial. There are much more voids present and less ordered channels in the glass nozzle beads. This however is proven to be the much better structure due to the uptake results associated with these materials. The explanation for a better performing material could be due to the increased amount of voids, more AMP can be encapsulated within the bead. Figure 3.17 shows possible AMP particulate within the bead and figure . shows the particulate that sits on the surface of the bead, making it available for ion exchange with cesium ions. Previously it was suggested that the AMP dissolves in the reaction mixture however upon analysis by SEM, it can be seen that particulate – presumed to be AMP – sits on the surface and within the bead in an encapsulated form. This partially explains the high uptake values

associated with the composites as the AMP is readily available for exchange providing the diffusion of ions is efficient.

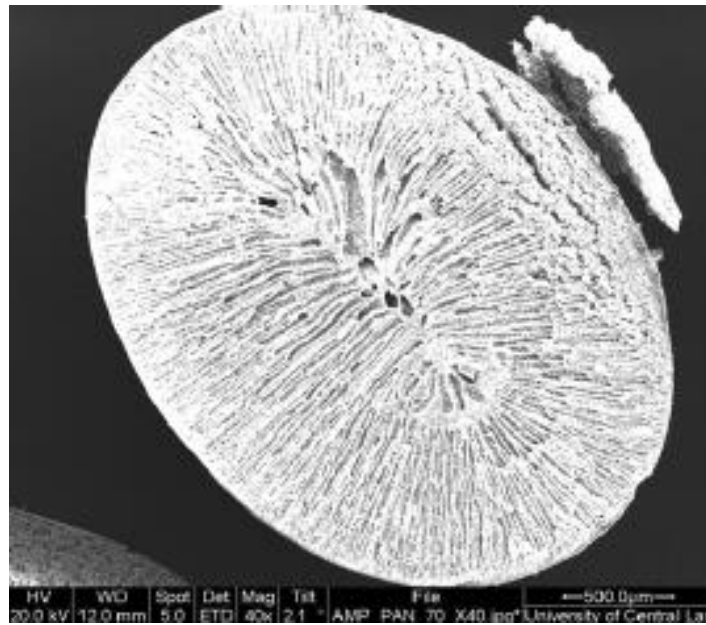


Figure 2.13 Cross section of AMP/PAN 70 taken from Kavi, P

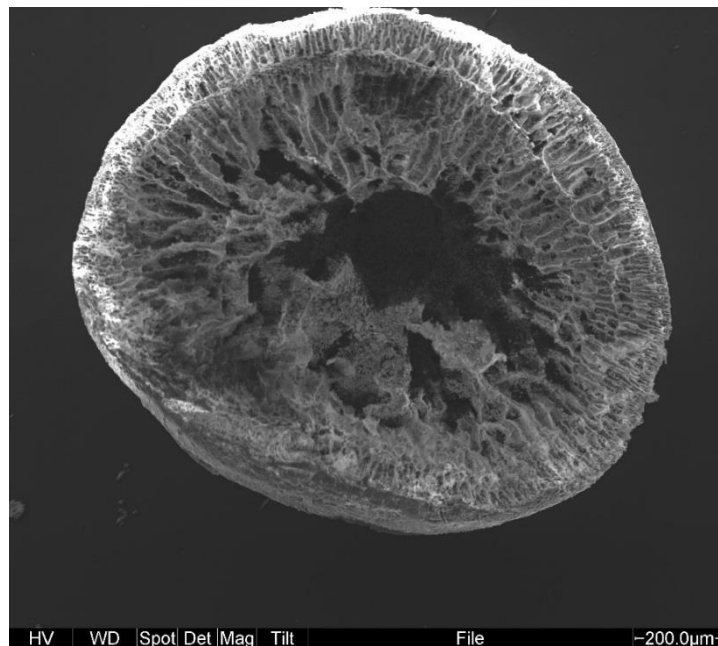


Figure 2.14 Cross section of AMP/PAN 70 1-2mm bead diameter

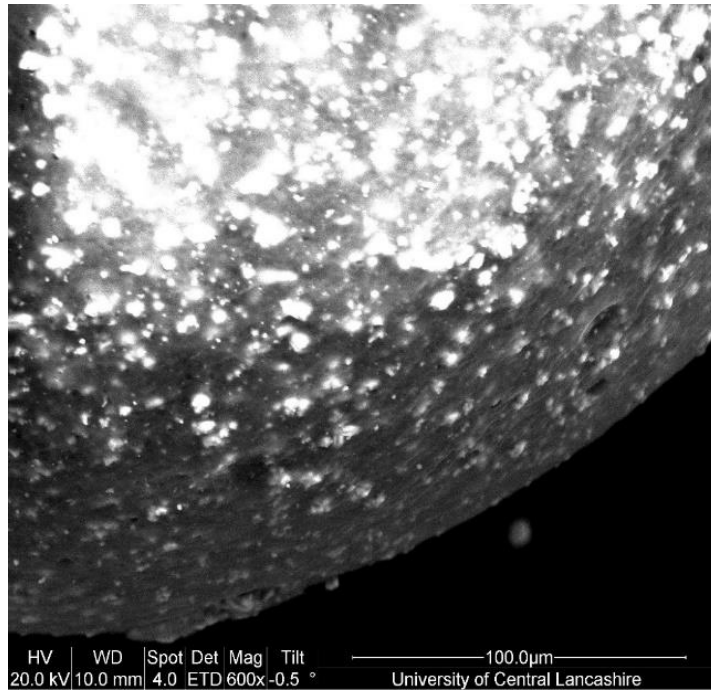


Figure 2.15 External surface of AMP/PAN 70 1-2mm bead

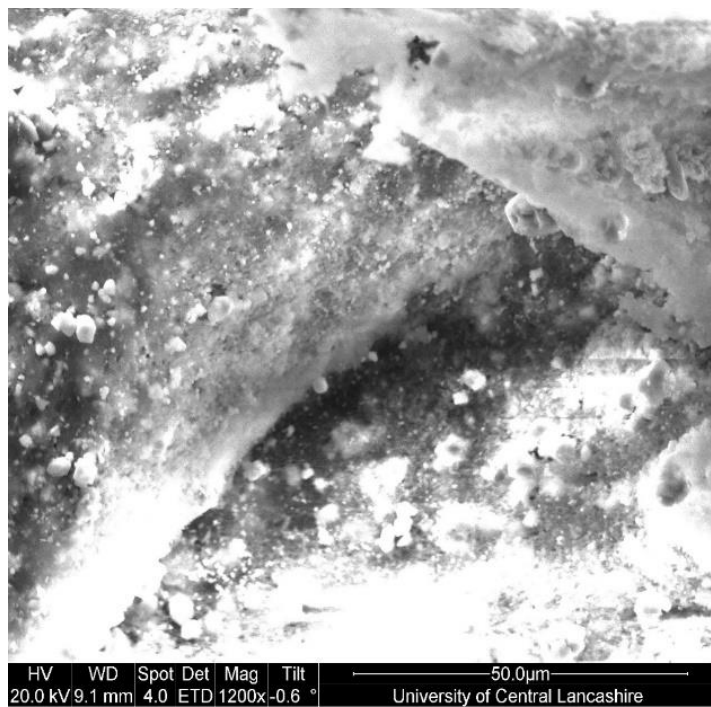


Figure 2.16 Internal section of AMP/PAN 70 1-2mm bead diameter



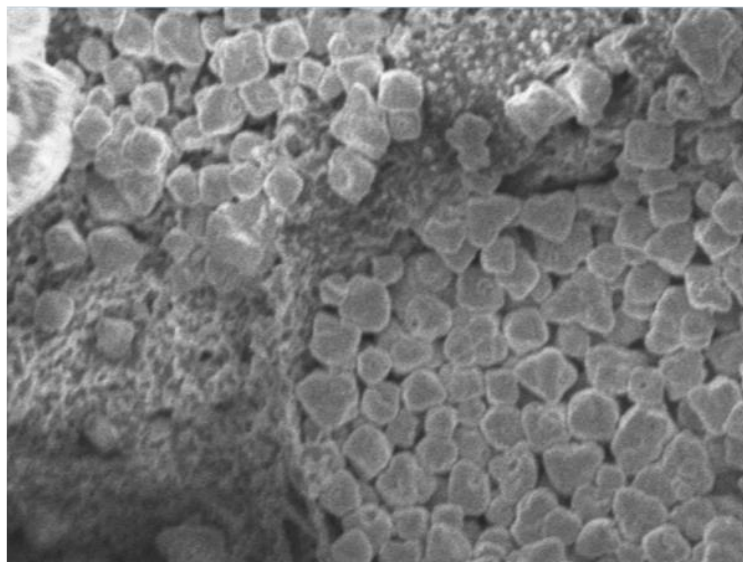


Figure 2.17 Internal section of AMP/PAN 70 ~400 $\mu$ m beads. The polyhedral particulate is suggested to be AMP particles.

### 3.3.8 Thermal Stability.

Upon initial analysis of the starting adsorbent material - AMP - by TGA, it was observed that there was no substantial denaturing below 800°C and thus confirming the expected high thermal stability. This stability is one of the properties of AMP that makes the material suitable for ion exchange in spent fuel dissolver liquors, where high temperatures are present.

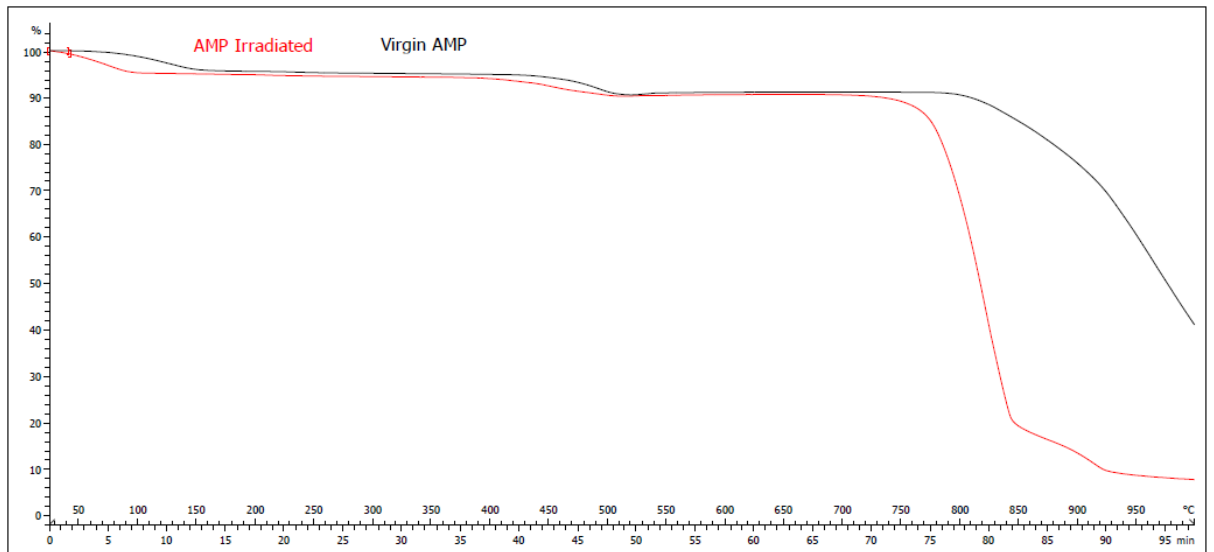


Figure 2.18 TGA spectrum of virgin and irradiated AMP

The radiolytic stability of AMP was also confirmed as can be seen in figure 3.17 which displays an almost identical spectrum to that of the virgin material. The decomposition at ~800-920°C will not alone impact on its effectiveness as an ion exchanger in real spent fuel liquors as is confirmed by heat decay factors displayed earlier in table (1.1) which suggests the temperature of the liquors will not reach this high.

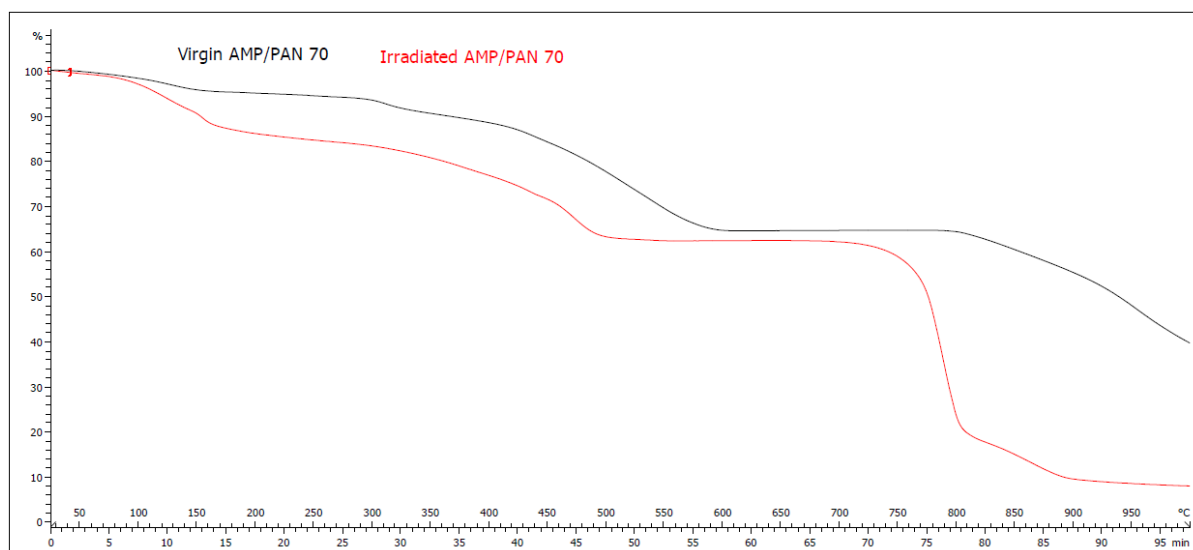


Figure 2.19 TGA spectra of virgin and irradiated AMP/PAN 70

The results of virgin and irradiated AMP/PAN 70 concur with the similarities observed for AMP as is seen in figure 3.18. Irradiation did not have any negative impacts on the thermal stability of the composite materials thus suggesting that exposure to radiation also did not compromise the structural integrity of said materials. Initial mass decreases at around 100°C can be attributed to water loss with a further decrease in mass between 150°C and 250°C attributed to the evaporation of residual DMSO.

An interesting property of PAN is the degradation begins at 300°C, however providing the heating rate is lower than 50°C/min, it will not melt until much higher temperatures. The spectra confirms the initial denature at 300°C and the further decomposition with most significant mass change occurring at 550°C and 750°C. It can be argued that a higher decomposition ‘safety net’ would be needed in spent fuel dissolver liquors to safely ensure that the material does not begin to denature before its purpose has been served. With this being said, PAN offers diversity as a polymeric support with relatively high stability by its ability to encapsulate possibly most micro-crystalline powder materials.

The use of PAN with a reduced Mw (~85,000) was obviously anticipated to decompose faster than the high Mw (150,000) material and was one of the major concerns with trying to reduce the cost of AMP/PAN by this method. Figure 3.19 presents the decomposition of these two materials.

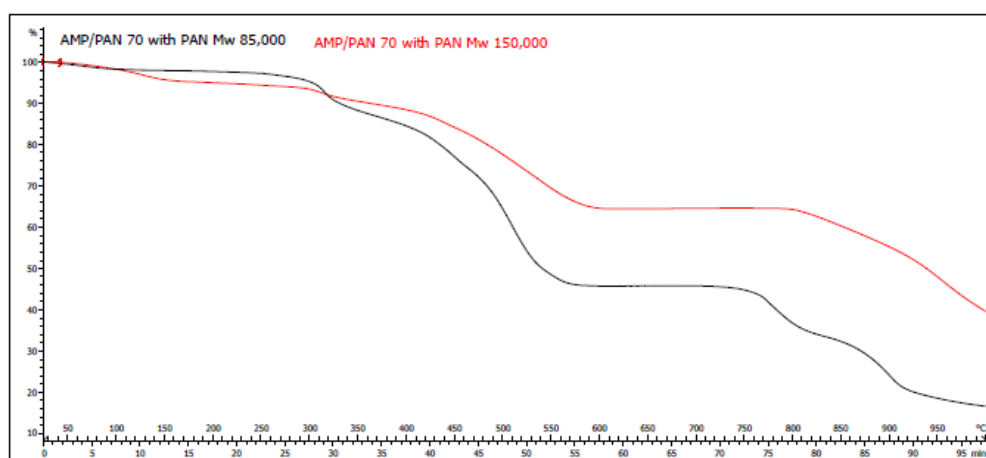


Figure 2.20 TGA spectra of AMP/PAN 70 with 85,000Mw PAN and 150,000Mw PAN.

The aforementioned thermal stability of PAN is not as highly dependent on the Mw as was initially thought (figure 3.20). The degradation of PAN still occurs at around 300°C but the reduced rate of mass loss suggests the higher Mw PAN is slightly more stable than the lower Mw. For industrial application however, it is not envisaged that the lower Mw of PAN would cause the material to degrade at a low enough temperature to impact on the ion exchange performance and stability in spent fuel dissolver liquors.

### 3.3.9 Surface area.

The surface areas of some of the modified AMP/PAN materials are discussed in previous sections. Table 3.16 presents the surface areas of the AMP/PAN varieties of most interest.

Table 2.16 Surface area of various AMP/PAN materials and AMP alone. Bead size measurements refer to the diameter.

Material	BET Surface area (m <sup>2</sup> /g)
AMP/PAN 70 ~1-2mm beads	3.48
AMP/PAN 70 ~400-600m beads	21.6
AMP/PAN 70 ~400-600m beads Irradiated	19.87
AMP/PAN 70 ~400-600m beads increased surfactant	21.05
AMP	121.04
AMP irradiated	111.4

As was confirmed previously, the surface area dramatically decreases when AMP is composited with PAN and when bead size increases due to less particles per gram of sample. This decrease in surface area is analogous to the decrease in cesium uptake capacity despite kinetics being relatively the same for both AMP and its composite.

The small difference in surface area between the original material and an increased amount of surfactant is expected due to the bead size similarity. The uptake of cesium is however dramatically affected which was previously attributed to the over saturation of surfactant within the reaction mixture. The porosity in the next section offers more conclusions surrounding this phenomenon.

The results of the irradiation studies confirmed the stability and resistance of these materials to radiolytic damage. Surface area analysis suggests that irradiation had some effect on the physico-chemical properties of the materials in table. Although the literature reports that AMP is stable up to 2Mgy<sup>[12]</sup>, some shrinkage of the particle size – however slight – may have occurred. The slight effect of radiation on these materials is reinforced by the change in hue of the characteristic green colour due to the change in oxidation state of molybdenum.

### 3.3.10 Pore size/volume distribution.

Table 2.17 Average pore diameter of various materials. Measurements of bead sizes refer to the diameter.

Material	BET Average Pore diameter (nm)
AMP/PAN 70 ~1-2mm beads	4.3
AMP/PAN 70 ~400-600µm beads	5.2
AMP/PAN 70 ~400-600µm beads increased surfactant	5.3
AMP/PAN 70 ~400-600µm beads Irradiated	10.7

An increase in pore diameter after irradiation was not expected as the physical properties were theorised to not change under exposure to certain levels of radiation. As the only noticeable change was the colour of the materials before and after irradiation, a lack of pore uniformity amongst the sampled beads may be attributed to this increase in pore size. As cesium uptake performance was not affected by radiation, the change in pore

diameter was not considered as a relevant change in the physico-chemical properties of AMP/PAN.

The uptake performance of AMP/PAN when using an increased volume of surfactant significantly decreased despite the average pore diameter remaining relatively constant. It was expected that the size of the pores would not change as an increased volume of surfactant could theoretically produce an increased amount of pores within the composite material as opposed to changing the size of individual pores.

The accumulative volume of pores was of most interest in AMP/PAN composites as it gives an insight into the overall porosity of a composite bead. Providing there are no other negative influential factors, a higher pore volume should result in a higher distribution coefficient of a particular material and hence increased ion exchange performance for cesium. The results of several composites are displayed in table 3.18

Table 2.18 Accumulative pore volume of AMP/PAN 70

Material	Accumulative Pore volume ( $\mu\text{m}^3/\text{g}$ )
AMP/PAN 70 ~1-2mm beads	52.8
AMP/PAN 70 ~400-600m beads	172.8
AMP/PAN 70 ~400-600m beads Irradiated	161.3
AMP/PAN 70 ~400-600m beads increased surfactant	273.5

As expected, a similar pore size between irradiated and virgin samples was characteristic of the adsorbents' radiolytic stability. A lack of bead uniformity can be attributed to the small discrepancy between these two samples.

As mentioned previously, the increase of surfactant in the reaction mixture concurred with a proposed increase in porosity as is portrayed by the higher accumulative pore volume when compared to other composites in table 3.18. The use of varying amounts of surfactant warrants further investigation but was not the focus of further study in this work due to the already high performing materials developed.

The larger AMP/PAN beads showed surprisingly low pore volume which suggests the lack of individual pores present. SEM images confirm this as there is a large void in the centre of the bead as opposed to the ordered porous channels of AMP/PAN composites in work by P.Kavi<sup>[20]</sup> The smaller, ordered channels did not result in higher ion exchange performance possibly due to the lower saturation of AMP within each individual bead compared to newer materials.

### 3.4 Conclusions

Although AMP PAN composites have received previous attention, but for nuclear high level waste treatment, little is known of its capability to replace the PUREX process for reprocessing spent nuclear fuel. The data reported in this report are the first tranche that will be required to engineer this ambitious project.

1. These studies have demonstrated that AMP PAN is a highly selective adsorbent for cesium from acid solutions.



2. The preparation of AMP PAN composite is comparatively simple, easy with great flexibility.
3. Several injection techniques have been employed to prepare different size beads, the double nozzle arrangement has produced the most consistent and smaller beads. Further refinement of the method could result in smaller diameter beads suitable for column studies.
4. The gel composition i.e. using a lower molecular weight PAN (150K to 85K) had little impact on cesium uptake, in contrast to changing surfactant concentration five-fold reduced cesium capacity. This was unexpected, as generally surfactant concentration, within limits, increases porosity. It is unlikely that increased surfactant influenced the solubility of AMP in PAN as on addition of the gel to the deionised water no colouration, i.e. the water having a yellow tinge was observed. Unlike previous studies with PAN, but not involving AMP, reducing the solvent volume (DMSO) had only marginal effect on cesium capacity.
5. Increasing the gelation temperature from 50 to 80°C had little impact on the cesium capacity of the composite beads.
6. All of the cesium and cesium/cerium adsorption studies were carried out under batch equilibration conditions, with different acid, cesium and cerium concentrations. The evidence from these studies indicate that:
  - The capacity for cesium was dependent on its solution concentration. A precise correlation between solution concentration and total capacity is difficult to compute at this stage as the morphology of the bead appeared to have a greater impact.
  - The extraction of cesium from solution is nitric acid dependent, 3M favouring better extraction.
  - The rate of extraction of cesium is comparatively fast with ~ 80% achievement in less than 10 minutes, after which the rate reduces significantly. This may suggest that within the first 10 minutes the surface

and near surface AMP particles in the composite bead are participating. This requires further consideration as it will influence the optimum size of bead.

- The selectivity of cesium was affected by the oxidation state of the cerium ion. The AMP PAN composite having a greater affinity for higher oxidation state +3 (selectivity value of about 50) compared with cerium (+4), AMP having a much lower affinity and hence a selectivity for cesium in excess of 10,000 when present in 3M nitric acid.
7. The SEM scans have shown that the bead morphology comprise of a comparatively smooth surface but with large fissures/pores within the bead. Increasing the AMP composition of the composite influences the internal morphology, but not appreciably. Correlation of the pore structure with cesium rate of uptake still requires more evidence.
  8. The morphology, i.e. SEM scans was underpinned by BET analysis indicating that ~ 1mm diameter beads (~3m<sup>2</sup> outer surface area) have a total surface area of ~9 m<sup>2</sup>/g.
  9. The synthesis of AMP/PAN has been made more cost efficient providing that the reduced molecular weight of PAN is stable to high doses of radiation present in spent fuel liquors.

These studies have provided sufficient data that the preparation of AMP PAN composite beads can be optimised. Initially literature searches for a suitable strontium extraction have identified candidate composite which is based on PAN encapsulation. Combination of two adsorbents into one polymer structure would be novel. This would be compared to individual adsorbent PAN composites.

### 3.5 References

- [1] Cunha, I. and Sakai, L. (1989). Determination of cesium-137 in water by ion exchange. *Journal of Radioanalytical and Nuclear Chemistry Articles*, 131(1), pp.105-109.
- [2] I. Komasaawa, T. Otake, Y. Higaki, Equilibrium studies of the extraction of divalent metals from nitrate media with di-(2ethylhexyl) phosphoric acid, *Journal of Inorganic and Nuclear Chemistry*, Volume 43, Issue 12, 1981, Pages 3351-3356,
- [3] Lumetta, G., Moyer\*, B., Johnson, P. and Wilson, N. (1991). EXTRACTION OF ZINC(II) ION BY DIDODECYLNAPHTHALENESULFONIC ACID (HDDNS) IN CARBON TETRACHLORIDE: THE ROLE OF AGGREGATION. *Solvent Extraction and Ion Exchange*, 9(1), pp.155-176.
- [4] Orth, R. and Kurath, D. (1994). Review and Assessment of Technologies for the Separation of Strontium from Alkaline and Acidic Media. U.S. Department of Energy.
- [5] Orth, R., Brooks, K. and Kurath, D. (1994). Review and Assessment of Technologies for the Separation of Cesium from Acidic Media. U.S Department of Energy.
- [6] Hannum, W. (1983). Analysis of the terminal waste form selection for the West Valley Demonstration Project. West Valley, N.Y.: West Valley Nuclear Services Co.
- [7] Högfeltd, Erik & I. Kuvaeva, Zoya & Soldatov, Vladimir. (1978). On the properties of solid and liquid ion exchangers—V.

- [8] van R. Smit, J., Robb, W. and Jacobs, J. (1959). Cation exchange on ammonium molybdophosphate—I. Journal of Inorganic and Nuclear Chemistry, 12(1-2), pp.104-112.
- [9] Carla J. Miller, Arlin L. Olson & Calvin K. Johnson (1997) Cesium Absorption from Acidic Solutions Using Ammonium Molybdophosphate on a Polyacrylonitrile Support (AMP-PAN), Separation Science and Technology, 32:1-4, 37-50, DOI: [10.1080/01496399708003185](https://doi.org/10.1080/01496399708003185)
- [10] Pike, Steven & O. Buessler, K & Breier, C & Dulaiova, Henrieta & Stastna, K & Sebesta, Ferdinand. (2012). Extraction of cesium in seawater off Japan using AMPPAN resin and quantification via gamma spectroscopy and inductively coupled mass spectrometry. Journal of Radioanalytical and Nuclear Chemistry. 296. 10.1007/s10967012-2014-5.
- [11] Boeyens, J., McDougall, G. and Smit, J. The Mechanism of Ion Exchange on Ammonium 12-Molybdophosphate (AMP), Recent developments in ion exchange pp.291-299.
- [12] Šebesta, F. and Štefula, V. (1990). Composite ion exchanger with ammonium molybdophosphate and its properties. Journal of Radioanalytical and Nuclear Chemistry Articles, 140(1), pp.15-21.
- [13]
- [14] Ding, D., Zhang, Z., Chen, R. and Cai, T. (2017). Selective removal of cesium by ammonium molybdophosphate – polyacrylonitrile bead and membrane. Journal of Hazardous Materials, 324, pp.753-761.

- [15] Milyutin, V., Nekrasova, N., Yanicheva, N., Kalashnikova, G. and Ganicheva, Y. (2017). Sorption of cesium and strontium radionuclides onto crystalline alkali metal titanosilicates. *Radiochemistry*, 59(1), pp.65-69.
- [16] Bortun, A., Bortun, L. and Clearfield, A. (1996). Ion Exchange Properties of a Cesium Ion Selective Titanosilicate. *Solvent Extraction and Ion Exchange*, 14(2), pp.341-354.
- [17] Sebesta, F., John, J., Motl, A. and Stamberg, K. (1995). Evaluation of Polyacrylonitrile (PAN) as a Binding Polymer for Absorbers Used to Treat Liquid Radioactive Wastes. Albuquerque, New Mexico.
- [18] Sayed M. Badawy and Ahmed M. Dessouki, Cross-Linked Polyacrylonitrile Prepared by Radiation-Induced Polymerization Technique *The Journal of Physical Chemistry B* 2003 107 (41), 11273-11279 DOI: 10.1021/jp034603j
- [19] Bruno R Figueiredo, Simão P Cardoso, Inês Portugal, João Rocha & Carlos Manuel Silva (2018) Inorganic Ion Exchangers for Cesium Removal from Radioactive Wastewater, *Separation & Purification Reviews*, 47:4, 306-336.
- [20] Pike, Steven & O. Buessler, K & Breier, C & Dulaiova, Henrieta & Stastna, K & Sebesta, Ferdinand. (2012). Extraction of cesium in seawater off Japan using AMPPAN resin and quantification via gamma spectroscopy and inductively coupled mass spectrometry. *Journal of Radioanalytical and Nuclear Chemistry*. 296. 10.1007/s10967012-2014-5.
- [20] P. Kavi, "The Preparation And Characterisation Of Highly Selective Adsorbents For Fission Product Removal From Acid Solutions". PhD. University of Central Lancashire, 2016.
- [21] Liu, J., Li, X., Rykov, A., Fan, Q., Xu, W., Cong, W., Jin, C., Tang, H., Zhu, K., Ganeshraja, A., Ge, R., Wang, X. and Wang, J. (2017). Zinc-modulated Fe–Co Prussian

- blue analogues with well-controlled morphologies for the efficient sorption of cesium. *Journal of Materials Chemistry A*, 5(7), pp.3284-3292.
- [22] Ge, Z., Chen, X., Huang, X. and Ren, Z. (2018). Capacitive deionization for nutrient recovery from wastewater with disinfection capability. *Environmental Science: Water Research & Technology*, 4(1), pp.33-39.
- [23] A.F. Wells, "Structural Inorganic Chemistry," 5th ed., Clarendon Press, Oxford, 1984,  
p. 1288 (metallic radii for 12-coordination); Huheey, pp. 292 (covalent radii for nonmetals); R.D. Shannon, *Acta Crystallogr., Sect. A: Found. Crystallogr.*, 32, 751 (1976) (ionic radii for 6-coordination).
- [24] Ksenzhek, O. and Volkov, A. (1998). *Plant Energetics*. San Diego, California: Academic Press, p.231.
- [25] Courtney, B., Edwards, H. and Robson, P. (1990). The preparation and characterisation of rubidium dodecamolybdophosphate,  $\text{Rb}_3(\text{MoO}_3)_{12}\text{PO}_4 \cdot 4\text{H}_2\text{O}$ . *Journal of Molecular Structure*, 239, pp.139-148.
- [26] Persson I, Hydrated metal ions in aqueous solution: How regular are their structures? *Pure Appl. Chem.* Vol 82, No 10, 1901-1917, 2010.
- [27] Tuazon, L. (1959). THE NATURE OF CERIUM(IV) IN AQUEOUS NITRIC ACID SOLUTION. Ph.D. Iowa State College.
- [28] Blaustein, B. and Gryder, J. (1957). An Investigation of the Species Existing in Nitric Acid Solutions Containing Cerium(III) and Cerium(IV)1. *Journal of the American Chemical Society*, 79(3), pp.540-547.
- [29] G. R. Choppin, M. K. Khankhasayev, H. S. Plendl, *Chemical Separations in Nuclear Waste Management*, DOE/EM-0591, Battelle Press, Columbus OH, 2002.

- [30] N. Paul, R. B. Hammond, T. N. Hunter, M. Edmondson, L. Maxwell and S. Biggs, *Polyhedron*, 2015, 89. 129-141.
- [31] J. van R. Smit, W. Robb and J. J. Jacobs, *J. Inorg. Nucl. Chem.*, 1959, 12, 104-112.
- [32] R. W. C. Broadbank, S. Dhabanandana and R. D. harding, *Analyst*, 1960, 85
- [33] Lue, A. and Zhang, L. (2008). Investigation of the Scaling Law on Cellulose Solution Prepared at Low Temperature. *The Journal of Physical Chemistry B*, 112(15), pp.44884495.
- [34] Tan, L., Pan, D. and Pan, N. (2008). Gelation behavior of polyacrylonitrile solution in relation to aging process and gel concentration. *Polymer*, 49(26), pp.5676-5682.
- [35] Holdsworth, A. F, Rowbotham. D, Eccles. H, Bond. G, Kavi. P, Ruth Edge. R, The Effect of Gamma Irradiation on the Ion Exchange Properties of Caesium-Selective Ammonium Phosphomolybdate-Polyacrylonitrile (AMP-PAN) Composites. (In preparation)
- [36] Zhang, L., Bai, J., Liang, H., Guo, L., Li, C. and Huang, Y. (2013). Preparation and Characterization of Polyacrylonitrile and Polyacrylonitrile/ $\beta$ -cyclodextrins Microspheres. *Journal of Macromolecular Science, Part B*, 53(1), pp.142-148.
- [37] Tanzifi, M. and Eisazadeh, H. (2011). Effects of various surfactants and solutions on the morphology of polyaniline composite and nanocomposite. *Journal of Vinyl and Additive Technology*, 17(4), pp.274-280.
- [38] Moon, JK., Kim, KW., Jung, CH. et al. *Journal of Radioanalytical and Nuclear Chemistry* (2000) 246: 299. doi:10.1023/A:1006714322455
- [39] Tranter, T., Herbst, R., Todd, T., Olson, A. and Eldredge, H. (2002). Evaluation of ammonium molybdophosphate-polyacrylonitrile (AMP-PAN) as a cesium

selective sorbent for the removal of  $^{137}\text{Cs}$  from acidic nuclear waste solutions. *Advances in Environmental Research*, 6(2), pp.107-121.

- [40] F. Sebesta, J. John, A. Motl and K. Stamberg, SAND95-2729 Report, Sandia National Laboratories, USA, Nov 1995.
- [41] K. L. N. Rao, C. Mathew, R. S. Deshpande, A. V. Jadhav, B. M. Pande and J. P. Shulka, *Radiat. Phys. Chem.*
- [42] K. L. Narasimharao, K. S. Sarma, C. Mathew, A. V. Jadhav, J. P. Shulka, V. Natarajan, T. K. Seshagiri, S. K. Sali, V. I. Dhiwar, B. Pande and B. Ventakataramani, *J. Chem. Soc., Faraday Trans.*, 1998, 94, 11, 1641-1647.
- [43] R. J. Taylor, C. R. Gregson, M. J. Carrott, C. Mason and M. J. Sarsfield, *Solv. Extract. Ion Exch.*, 2013, 31, 442-462.
- [44] H. Eccles, J. D. Emmott and G. Bond, *J. Chromatog. Sep. Tech.*, 2017, 8, 348.
- [45] K. L. Narasimharao, K. S. Sarma, C. Mathew, A. V. Jadhav, J. P. Shulka, V. Natarajan, T. K. Seshagiri, S. K. Sali, V. I. Dhiwar, B. Pande and B. Ventakataramani, *J. Chem. Soc., Faraday Trans.*, 1998, 94, 11, 1641-1647.
- [46] A. A. Farghali, M. Bahgat, A. E. Allah and M. H. Khedr, *Beni-Suef Uni. J. Basic Appl. Sci.*, 2013, 2, 61-71.
- [47] C. Mahendra, P. M. Sathya Sai, C. A. Babu, K. Revathy and K. K. Rajan, *J. Enviro. Chem. Eng.*, 2015, 3, 1546-1554.
- [48] S. Rengaraj, J.-W. Yeon, Y. Kim, Y. Jung, Y.-K. Ha and W.-H. Kim, *J. Haz. Mater.*, 2007, 143, 469-477.
- [49] A. A. Farghali, M. Bahgat, A. E. Allah and M. H. Khedr, *Beni-Suef Uni. J. Basic Appl. Sci.*, 2013, 2, 61-71.
- [50] D. Ding, PhD Thesis, University of Tsukuba, Japan, 2014.



- [51] K. J. Parikh, P. N. Pathak, S. K. Misra, S. C. Tripathi, A. Dakshinamoorthy and V. K. Manchanda, *Solv. Extract. Ion Exch.*, 2009, 27, 2, 244-257.

## Chapter 4 Strontium removal from spent fuel dissolver liquors

### 4.1 Review of selective strontium adsorbents

The scope of materials available for strontium adsorption is extensive; therefore, the most promising are reported. Many of the adsorbents are highly selective for strontium and extract with high yield and efficiency, recovering most of the strontium from solution. Most of the materials available, however suffer from a substantial decrease in ion exchange performance when exposed to strong acidic media ( $\text{pH} < 3$ ). Consequently, for UCLan's ART concept development and synthesis of selective strontium adsorbents with fast kinetics that are stable in low pH values is required.

#### 4.1.1 Mixed oxides – Zirconium and Manganese

Zirconium - Manganese oxide/PAN composites can be synthesised in a similar way to AMP/PAN composites and show good stability in pH 2-4 with very small amount of weight loss. At pH 3 Strontium removal has been reported at about 41% which is notably underperforming for an ion exchange resin <sup>[1]</sup>. One suggestion for increasing the efficiency of Sr removal at low pH values is to switch Zr and Mn for other oxides with different ionic radii. A distinct advantage of this synthetic procedure is it is easy one pot preparation and expandable.

The knowledge gained from the synthesis is readily transferable.

The protonation of the adsorbent at a lower pH results in low uptake of strontium as the  $\text{Sr}^{2+}$  ions are cationic. As the surface of the adsorbent becomes positively charged, exchange is less prominent than at lower pH values and more favoured at a higher pH. [1]

#### 4.1.2 Crown ethers

Crown ethers have also been reported to be effective strontium adsorbents such as the crown ether/TBP complex reported by Zhang et al. The adsorbent is a macroporous silica based composite with formula  $\text{DtBuCH}_{18}\text{C}_6+\text{TBP}/\text{SiO}_2\text{P}$  that has shown to have high adsorption and selectivity of strontium in 2M  $\text{HNO}_3$  and even with competing  $\text{Ba}^{2+}$  ions present [2]. The difference in this work to others using these crown ethers is the presence of TBP which has a high affinity for  $\text{HNO}_3$ . A major advantage of crown ethers is that they can be tailored to achieve selectivity for different ions; this can be achieved by changing the functional groups and the structure. For example, a crown ether mentioned before in chapter 3 reviews its affinity for cesium. In this case, the crown ether has no affinity for cesium but is very selective for strontium. The solubility of  $\text{DtBuCH}_{18}\text{C}_6+\text{TBP}/\text{SiO}_2\text{P}$  is however, high in acidic media due to its affinity for hydrogen. [2]

Although this type of composite is a selective strontium adsorbent, there are inherent challenges to be addressed; for example crown ethers are not as simple to synthesise as other simple composites such as metal oxide/polymer materials and AMP/PAN, i.e. a one pot synthesis. They are also expensive, their radiation/acid stability is not sufficiently proven, and therefore any realistic application of new materials based on crown ethers in nuclear reprocessing will require investigation that is far more extensive. The impact of adsorbed radioactive Sr will also require additional studies. [3]

#### 4.1.3 Layered Metal Sulfides

The ion exchange abilities of layered metal sulfides have not been studied less so than metal oxide materials.

Layered crystalline metal sulfide ion exchange materials allow easy access to the internal surfaces of each layer with the metal ions bonding strongly with  $\text{Sr}^{2+}$  ligands. They are fairly simple to synthesise as a common route is to partially reduce a metal disulfide with a reducing agent such as n-BuLi <sup>[4]</sup>. Any metal cations that are positioned within the anionic layers can be swapped out easily for other species. These materials have many sub-groups, one common group being KMS materials with the general formula  $\text{K}_2\text{X}\text{M}_x\text{Sn}_{3-x}\text{S}_6$ . There are many derivatives with KTS materials ( $\text{K}_2\text{Sn}_4\text{S}_9$ ) showing excellent ion exchange capabilities for both  $\text{Sr}^{2+}$  and

$\text{Cs}^+$ .<sup>[4][5]</sup>

One paper reports the success of a layered metal sulfide material in removing  $\text{Sr}^{2+}$  ions from aqueous solution. Maximum capacity of the material was achieved in at pH value of 7 (~50mg/g) but was tested using a pH range of 1-10 <sup>[4]</sup>. In lower pH values than 7, the  $\text{H}^+$  were shown to compete with the  $\text{Sr}^{2+}$  ions to great effect which reduced the adsorption of  $\text{Sr}^{2+}$  resulting in a capacity of around 18mg/g in a pH value lower than 2. The material synthesised -  $[\text{ZnGe}_3\text{S}_9(\text{H}_2\text{O})]^{4-}$  - showed fast kinetics and equilibrium was reached within 2 hours <sup>[4]</sup>. Like most ion exchange materials, the struggle for efficient adsorption is to overcome competing  $\text{H}^+$  ions in order for materials to be able to perform with high effectiveness in low pH values.

#### 4.1.4 Ion-imprinted polymers

Imprinting polymers with template ions produces “tailor-made” binding sites on the polymers being formed, which, produces a highly selective support for the target ions. There are some complications with previously synthesised ion-imprinted polymers, which includes the low mass transfer and inaccessibility for the ions to reach the binding sites. [6] Imprinting techniques have been developed in order to improve mass transfer kinetics. More recent techniques have included surface-imprinting using silica and alumina as support materials. Palygorskite has been identified as a support in surface imprinting due to its high chemical and thermal stability accompanied by its low cost. [6]

A sacrificial support used in the surface-imprinting process can help to produce uniformly sized adsorbents, improve adsorption and desorption kinetics by increasing specific area and pore volume. The desired form of the imprinted polymer is hollow spherical particles. [6]

In one report, chitosan and  $\text{Sr}^{2+}$  ( $\text{SrCl}_2 \cdot 6\text{H}_2\text{O}$ ) are dissolved in acetic acid and silane KH-560 is added to initiate a cross linking polymeric reaction. [6] Activated palygorskite is added producing wet beads which are subsequently dried at RT. This composite exhibited a high degree of crosslinking and hollow microspheres were formed with high surface area;  $28.56\text{m}^2/\text{g}$  [6]. The capacity of these materials is  $0.1\text{mg}/50\text{ml}$ , which has the potential to be improved substantially. A great advantage that these ion imprinted polymers have is their stability in acidic media and the ability to retain uptake capabilities. An ion-imprinted polymer with palygorskite support exhibited 96% adsorption at pH 0 with fast kinetics. [6] The adsorbent materials may function better at different temperatures, which could produce better accessibility of active binding sites. Their possible application in chromatography is strengthened by the easy elution of strontium using dilute ammonia. The disadvantage however is their performance after

several experiments declines, less strontium is adsorbed <sup>[6]</sup>; their non-uniform structure and particle size would not be suitable for application in column processes. Work by Sarabadani et al reported the successful extraction of radioyttrium ( $T_{1/2} = 14.7\text{h}$ ) using an ion imprinted polymer based on an anthraquinone in high yield (~99%)..<sup>[7]</sup> A stable strontium impurity is formed thus suggesting some degree of radiolytic stability of these compounds and reinforcing their potential use in a nuclear reprocessing technique

#### 4.1.5 Lead Hexacyanoferrates

Hexacyanoferrates (HCF) have a high affinity for strontium but low stability at low pH values and therefore are not suitable alone for nuclear reprocessing. Binding them to a support could increase their stability whilst not compromising the high selectivity and adsorption capacity for strontium. In a report by Vashnia et al. lead HCF is bound to MCM-41 (MCM-41 has uniform pore size, large surface area and ordered nano-channels). The volume of the pores is also large and makes it an ideal support for metal HCF's <sup>[8]</sup>.

The results backed up the large surface area of MCM-41 ( $771\text{m}^2/\text{g}$ ) and when lead HCF is impregnated onto the surface the surface area of the composite decreases to  $365.5\text{m}^2/\text{g}$ . The decrease is justified by probable blocking of MCM-41 pores by lead HCF. Despite the decrease in surface area, it is still appropriate for selective strontium removal applications <sup>[8]</sup>.

The maximum adsorption capacity of  $\text{Sr}^{2+}$  onto PbHCF-MCM-41 was  $97\text{ mg/g}$ , but the capacity is reduced almost ten fold when the pH is lowered to around 2. This trend is common for most popular strontium adsorbents. The kinetics are slightly slower than other strontium adsorbents, reaching equilibrium after 5 hours, but with over 80% uptake achieved within the first hour <sup>[8]</sup>. This composite provides selective removal of strontium

with good capacities in aqueous solution but modifications/additions would be needed to increase the stability in pH values lower than 2.

#### 4.1.6 Antimony oxides

Antimony oxides have been used before in the selective removal of strontium in LLRW. Most applications have been with waste water, and their effectiveness in low pH environments is unknown. These compounds do however, have a high selectivity and capacity (5 meq/g) for strontium in acidic media <sup>[9]</sup>.

Ion exchange can occur rapidly in the hydroxyapatite structure of certain antimony oxides ( $\text{Sb}_2\text{O}_6$ ) due to the formation of tunnels (pyrochlore structure<sup>[10]</sup>). The protons present in the tunnels can be exchanged by cations such as  $\text{Sr}^{2+}$  relatively easy and quickly. The selectivity can be further enhanced by exchanging the Sb(V) ions for others such as Sn(IV) and Zr(IV). These lower valences and ionic radii will regulate the tunnel sizes in the structure. The quantity of exchangeable protons is also increased due to defects in the lattice which increases the capacity of ions exchanged. Favourable ionic radii sizes are 0.04 – 0.078nm <sup>[9]</sup>.

The performance of antimony oxides below pH 2 is similar to other strontium adsorbents i.e. pH dependent with low pH values reducing uptake. Although, at pH values slightly above 2, 100% adsorption is achieved <sup>[9]</sup>

This is a very attractive feature of these oxides, and with further development focussed around increasing pH stability, these could be very useful in nuclear reprocessing. Reducing the synthesis time, as it currently takes around 10 hours<sup>[9]</sup>, would also be beneficial.

The adsorption is near spontaneous and therefore kinetics is hard to study, although it has been proven that they favour temperatures higher than ambient temperatures.

#### 4.1.7 Molybdophosphates

The molybdophosphates are interesting compounds, AMP has shown incredibly cesium selective adsorption with high capacities but only a small affinity for strontium, there are however other known phosphate materials for selective strontium removal. Again the major issue with selective strontium adsorption for the nuclear industry is the acidic conditions of the spent fuel dissolver liquor. Many materials produced for the adsorption of strontium exhibit low stability in acidic media and perform as efficient ion exchangers in pH levels above 2. There is a paucity of information for this application. One report studied the adsorption of strontium onto a stannic molybdophosphate ion exchanger that increased uptake with decreasing pH values  $<3$ . This material would be suitable for nuclear reprocessing as the pH of 3M-7M nitric acid ranges from 0-3. It was reported that increased concentration of sodium caused a decrease of adsorption of strontium which suggests that this particular molybdophosphate may not be employed into multi-element liquors where competing ions are present, without modification to the material itself to overcome this.<sup>[11]</sup>

#### 4.1.8 Commercial ion exchangers

A library of commercially produced ion exchangers exist for the separation of strontium from solution. Purolite® resins have been tested to evaluate their capabilities in various media when employed in a chromatographic method. In a thesis by J. Emmott, he reported single column for several Purolite® resins when exposed to solutions with different ionic species. The acid concentration of the solutions was 1 to 5M, with acidity being an influential factor on their cationic uptake capabilities.<sup>[12]</sup> In the thesis by Emmott, he



reported that a series of amidoxime and sulfonic acid resins exhibited varying degrees of separation as a function of zirconium in multi-element solutions.<sup>[12]</sup> These resins have warranted further investigation into their uptake capabilities and possible employment in an SMBC technique.

## 4.2 Results and Discussion

The use of phosphate materials for separation of radionuclides in the nuclear industry is well documented. In the case of cesium separation, AMP exhibits fast uptake with high selectivity and capacity for cesium, discussed in the previous chapter. Development of mixed-metal phosphates (MMP) for the selective separation of strontium was therefore an interesting area of research to explore. Despite a wide library of materials existing for strontium separation from different media, no material exists that would exhibit fast kinetics with high capacity in highly acidic conditions as such that could be employed in spent nuclear fuel liquor treatment. The results of a selection of potential strontium adsorbent materials and their composites are discussed and compared in various conditions to observe pH stability, solubility and effective strontium uptake. As most ion exchangers rely on porosity to increase diffusion in a solution, a high accumulative pore size and volume should increase the  $K_d$  values and subsequently, the kinetics.

The chemical composition of the mixed metal phosphates was known, partially from the preparative route employed and previous work <sup>[13]</sup> identified prior to obtaining the adsorbent powders being passed on for ion exchange performance studies. This prior knowledge is underpinned by the FT-IR spectra in figures 4.1 and 4.2

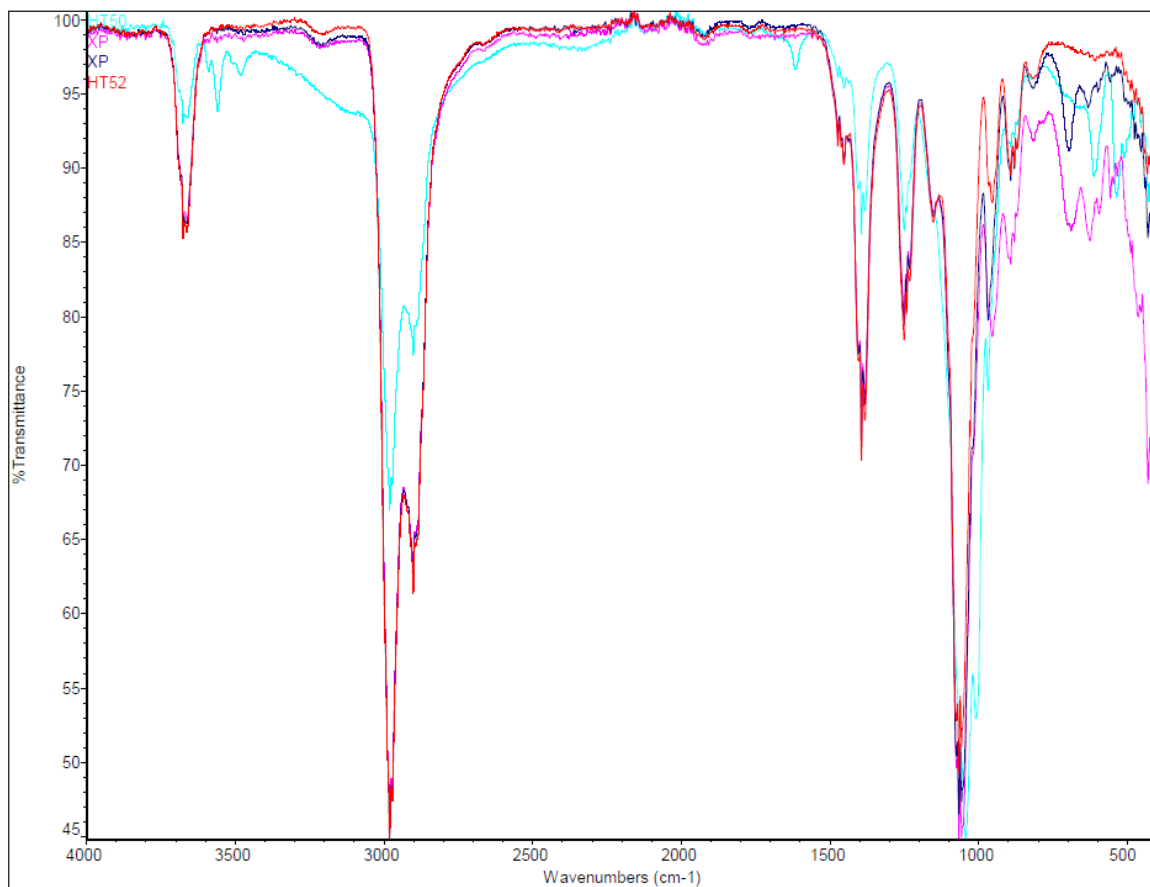


Figure 0.1 FT-IR of Sr adsorbent powders

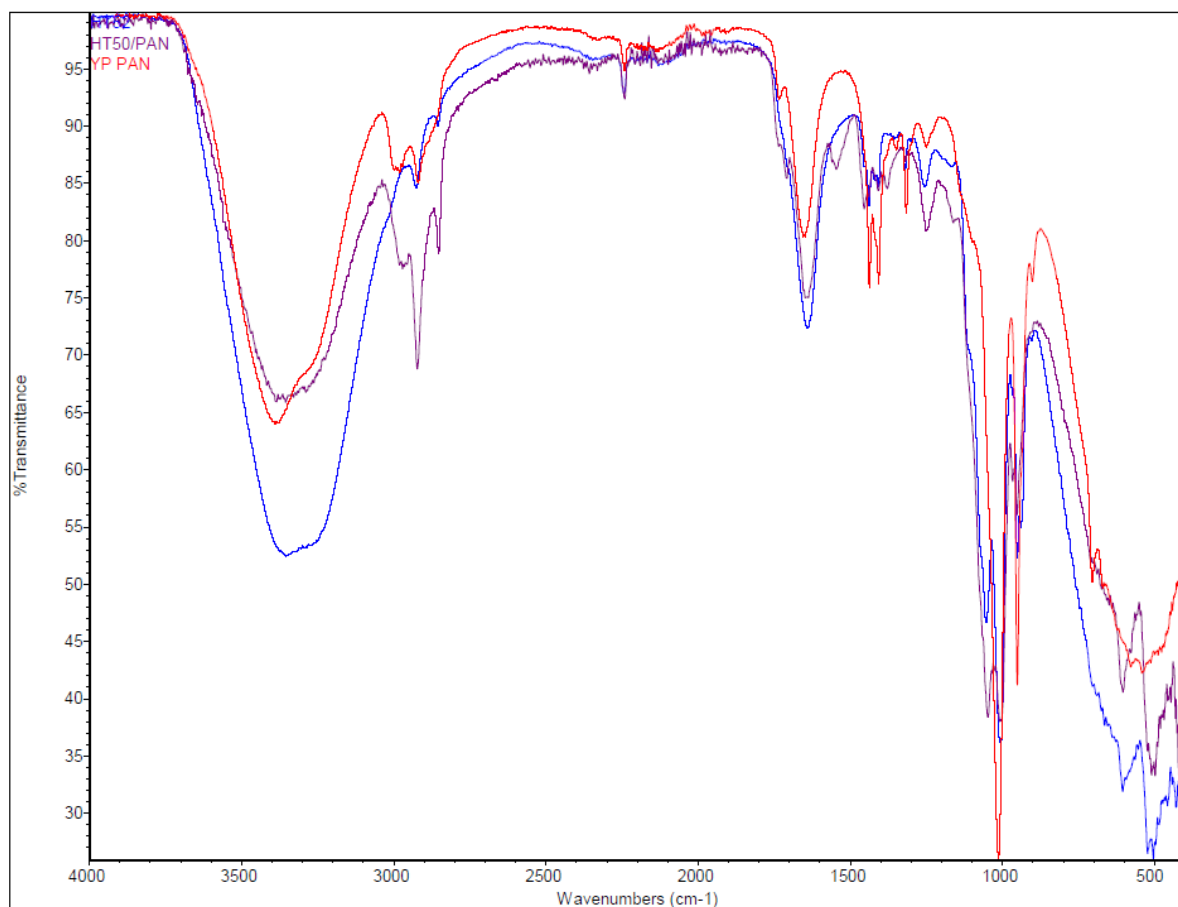


Figure 0.2 FT-IR of Sr adsorbent PAN composites

The IR spectra is typical for the composition of these MMP's as is shown by the peaks of interest in table 4.1.

Table 0.1 IR peaks present in the MMP and MMP/PAN materials

Functional group	Peak (wavenumbers cm <sup>-1</sup> ) <sup>1)</sup>	Bond vibration type	Intensity
C≡N	1670-1820	Stretch	Strong
-C-H	1350-1480	Bend	varied
P-O	1100-1200	Stretch	varied
P=O	1600 -2725	Stretch	Broad

The IR spectra of the adsorbent powders displays stronger intensities than the PAN composites possible due to less absorbance of uv radiation by the bonds in the encapsulated powder, as there is less MMP in contact with the sample stage. The shape of the peaks are similar however, with the phosphate peaks still present in the MMP/PAN spectra confirming successful encapsulation.

#### 4.2.1 Strontium batch uptake measurements

##### 4.2.1.1 Powder adsorbents

The adsorbent materials were studied for their strontium ion exchange performance prior to being encapsulated in PAN as to obtain a baseline of strontium uptake. As AMP/PAN has a high affinity for cesium, it is advantageous if these materials also possess the same characteristics but for strontium. Initial studies at ~pH 5 were performed with the powders. The Sr uptake results are presented in Table 4.2. As mentioned in section 3.3.1,  $K_d$  values are dependant on various factors such as the amount of, and the availability of exchange sites being the dominant factors considered for these preliminary strontium uptake studies.

Table 0.2 Strontium uptake of powder adsorbents in de-ionised water (pH of stock solution was 4.86)

Material	Initial Sr Conc (ppm)	Equilibrated Sr Conc (ppm)	$K_d$ (ml/g)	Capacity (mg/g)	SD ( $\sigma$ )
XP	311	0.93	33341	31	0.043
HT51	311	1.23	25185	31	0.021
HT52	311	0.77	40290	31	0.044
YP	311	0.78	39772	31	0.040
HT50	311	0.62	50061	31	0.019

Capacity measurements were low compared to AMP for cesium however higher concentrations of strontium values increase substantially due to the amount of strontium ions available for exchange being limited at lower concentrations. The nano-scale size of these materials results in their high surface area allowing for better exchange site availability. The high  $K_d$  values confirm this characteristic and suggests that the diffusion is efficient. Almost complete uptake of strontium occurred with all the materials tested with each exhibiting similar capacities. These initial studies provided promising results that these could be candidate strontium adsorbents for the ART process but performance at more realistic acid conditions is required. It is well established that the ammonium ion in AMP acts as the exchanger for cesium, the mechanisms of which are still unclear. As there is no ammonium ion present in these adsorbents, it is therefore assumed that the metal ions act as an exchanger for strontium. The mechanism of this exchange could relate to the cationic radii similarities of the metals with strontium and thus resulting in a desirable change that would produce a stable strontium phosphate. It has also been reported that AMP shows no affinity for radioactive strontium suggesting the difference in atomic radii could be a contributing factor to ion exchange<sup>[14]</sup>.

The mechanism of the ammonium exchange with cesium warrants further investigation which could also shed light on the exchange mechanism in strontium adsorbents.

These adsorbents are in their preliminary testing phase and due to limited resources and the higher performance of the other adsorbents, HT51 was not investigated further in this work.

#### 4.2.1.2 Composite MMP/PAN adsorbents

The kinetics of the MMP powders and MMP/PAN composites are very similar. The seamless transfer of the ion exchange performance of the powder adsorbents into composite beads was a challenge considering the ratio of adsorbent to PAN (1:2) in the reaction mixture. The ratio of AMP to PAN is much higher (5:2) and an excess of adsorbent results in higher cation uptake values and hence capacities are higher. An excess of PAN would result in non-saturated beads and thus reduce the amount of exchangeable sites.

Table 4.3 presents the results of strontium uptake using MMP/PAN.

Table 0.3 Equilibrated Strontium uptake measurements of MMP/PAN

Material	Initial Sr Concentration (ppm)	Equilibrated Sr Concentration (ppm)	$K_d$ (ml/g)	Capacity (mg/g)	SD ( $\sigma$ )
YP/PAN	298.27	166.13	79.54	13.21	0.035
HT50/PAN	298.27	123.75	141.03	17.45	0.014
XP/PAN	298.27	159.76	86.70	13.85	0.024
HT52/PAN	298.27	164.76	81.03	13.35	0.006

As expected, the excess of PAN resulted in a reduced uptake of strontium due to the low amount of adsorbent per gram of composite, which also influenced the  $K_d$  values. The results of strontium uptake however, were not too discouraging, as despite the low saturation of the composite beads with MMP, a respectable capacity was achieved for all materials with the highest performing material being HT50/PAN. Interestingly, the low surface area of this material compared with the high surface area of XP/PAN did not hinder its ion exchange performance (discussed in more detail later). The initial studies of these new MMP/PAN composites provided promising results to which further adsorption studies could be compared.

Capacities of the MMP's and their composites are summarised in figure 4.3.

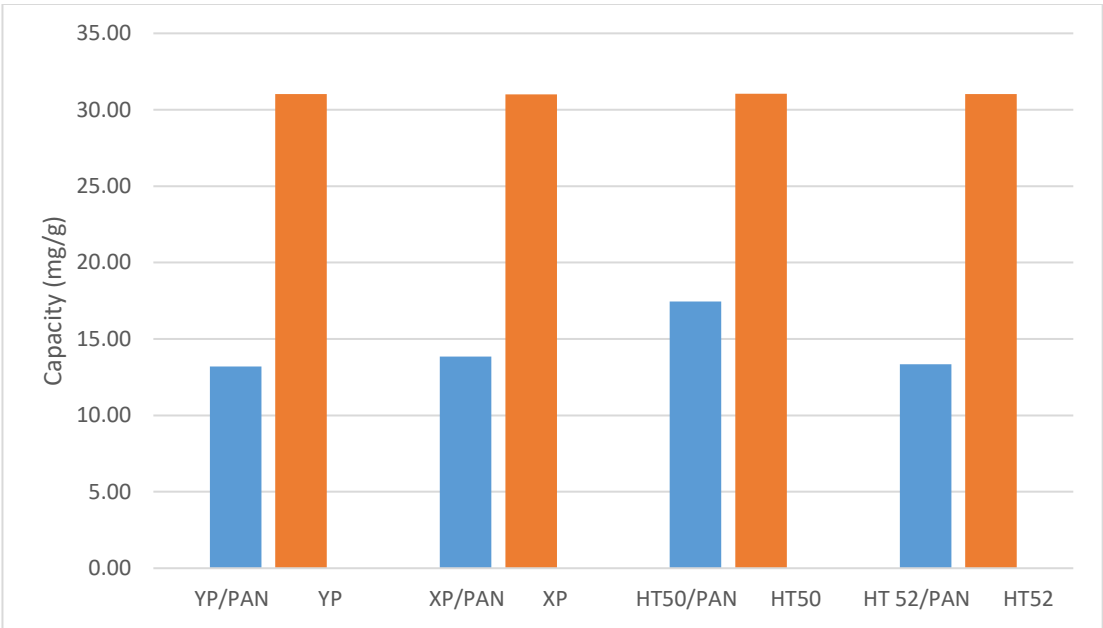


Figure 0.3 Maximum Capacity observed for MMP and MMP/PAN adsorbent materials

## 4.2.2 Kinetics

As mentioned throughout this thesis, a vital characteristic of the ART concept is the rate of uptake of selective species. Optimising porosity of saturated composite beads should result in efficient diffusion of ions in solution, high porosity favouring rapid uptake. The kinetics of the MMP's prior to encapsulation in PAN were evaluated, for these studies, YP was not included due to the interest of the other promising MMP's.

### 4.2.2.1 Powder adsorbent Kinetics

The rate of uptake of strontium was measured as described in the methodology (Chapter 2). The kinetics were measured in the natural pH of the stock solutions (4.86) due to limited stability in acidic media (discussed later). The uptake of strontium is fairly quick with HT52 exhibiting the slowest rate of uptake yet achieving near complete uptake of strontium and almost 77% of adsorption maxima achieved within 1 hour.



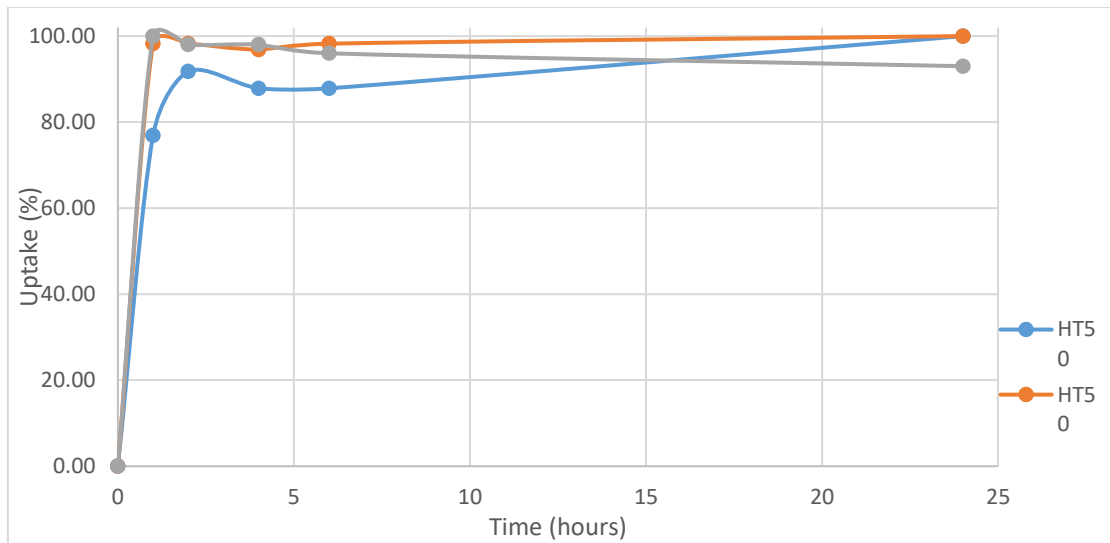


Figure 0.4 Rate of uptake of strontium using powder adsorbents in a 311ppm Sr solution (pH stock solution 4.8)

The results (figure 4.4) show the MMP's exhibited rapid strontium uptake, with HT50 only displaying slightly slower kinetics than HT50 and XP. There was no substantial leaching of strontium from the solid throughout the experiment however a slight decrease in uptake was observed for HT50 at 4 hours. It is also apparent that equilibration could be achieved within 1 hour, but to ensure equilibrium had been achieved the experiments were allowed continued for 24 hours, in part to observe any long-term potential leaching of strontium. The best kinetic performance was observed by HT52 which equilibrated after 1 hour and showed no leaching after 24 hours. HT50 continued to adsorb ~10% of adsorption maxima between 4 and 24 hours and XP desorbed roughly 3% between the same timeframe. The rapid uptake of strontium in all the studied materials suggested the development of all of these materials into PAN composites should be considered. It was envisaged that similar adsorption kinetics would be present when the adsorbents were encapsulated in PAN. The next subsection discusses these results.

#### 4.2.2.2 Composite MMP/PAN adsorbent kinetics

The rates of uptake of strontium using MMP/PAN composites are presented in figure 4.5.

The results show some transfer of the kinetic capabilities of the MMP powders to the MMP/PAN composites.

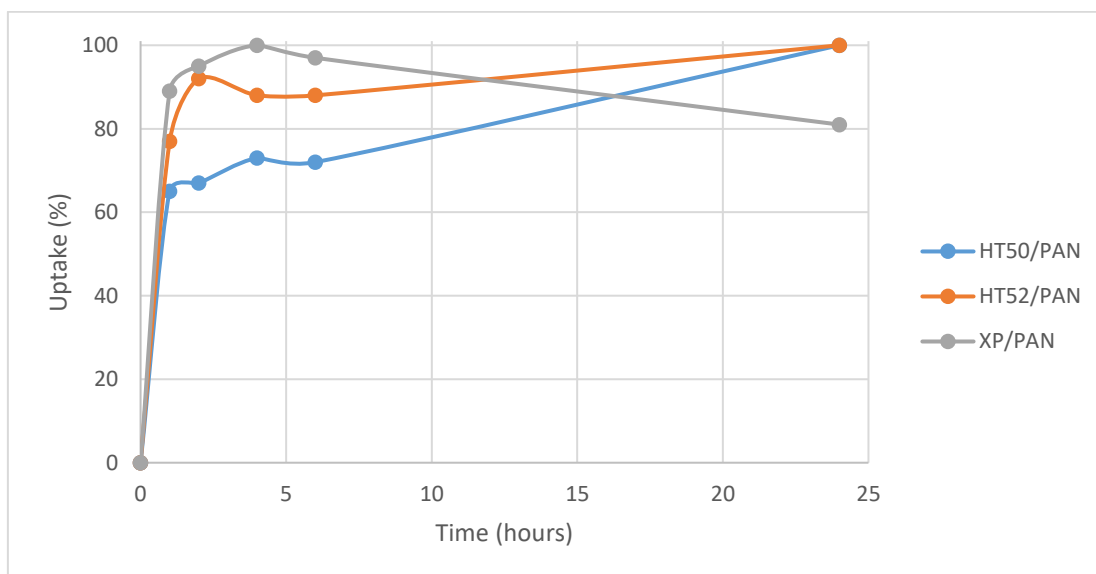


Figure 0.5 Rate of uptake of strontium using MMP/PAN materials in de-ionised water (pH stock solution 4.8)

Although a large percentage of adsorption maxima was achieved after 1 hr using HT50/PAN, this is a substantial decrease in rate of uptake compared to the HT50 alone and can be attributed to a lower  $K_d$  value observed in table 4.3. The diffusion rate was not as efficient in its encapsulated form, as confirmed by the substantial increase in uptake of strontium between 6 and 24 hours. This increase is also observed for HT52/PAN however, the kinetics were much faster for this material, exhibiting an uptake of ~90% in the first hour. The difference in saturation levels of MMP in these composite beads may be attributed to this difference. XP/PAN was consistent with its starting material XP,

leaching almost 20% of strontium between 6 and 24 hours despite exhibiting the fastest rate of uptake in the first 4 hours.

#### 4.2.3 Acid Stability

As mentioned throughout this thesis, acid stability is a key component that must be present in adsorbents for use in the ART concept. It was therefore necessary to test the stability of these potential strontium adsorbents in acidic media. The pH sensitive nature of AMP (soluble in alkali solutions) caused suspicions that the nature of these materials (MMP) may also exhibit similar properties. The solubility of phosphate based materials in low pH values has been studied previously<sup>[15]</sup> and thus some expectations of the low stability of the adsorbents were confirmed. Interestingly, AMP – despite being a phosphate based material – exhibits increased ion exchange performance at higher acidity levels up to around 5-6M HNO<sub>3</sub>. It would be beneficial in future work to understand the mechanics behind this stability for development of adsorbents for ART.

##### 4.2.3.1 1M HNO<sub>3</sub> Experiments

An almost non-existent strontium capacity in acidic media by these adsorbents was recorded, table 4.4 present the Sr uptake results for 1M HNO<sub>3</sub> experiments.

Table 0.4 Strontium uptake of MMP's in 1M HNO<sub>3</sub> (pH 2.8)

Material	Initial Sr Conc (ppm)	Equil Sr Conc (ppm)	K <sub>d</sub> (ml/g)	Capacity (mg/g)	SD ( $\sigma$ )
YP	295.8	283.7	4.27	1.21	0.020
HT52	295.8	290.4	1.86	0.54	0.046
XP	295.8	278.3	6.29	1.75	0.017
HT50	295.8	267.1	10.75	2.87	0.041

After the first hour of equilibration, the pH increased from ~2.8 to 7.6 and thereafter remained constant for the remainder of the experiments with some adsorbent visibly dissolving. This solubility in acidic media would be undesirable for the ART concept. It was envisaged that encapsulation by PAN may provide some protection of the ion exchange adsorbents from acid sensitivity. The results of 1M HNO<sub>3</sub> experiments using MMP/PAN materials are presented in table 4.5.

Table 0.5 Strontium uptake of MMP/PAN composites in 1M HNO<sub>3</sub>

Material	Initial Sr Conc (ppm)	Equil Sr Conc (ppm)	K <sub>d</sub> (ml/g)	Capacity (mg/g)	SD ( $\sigma$ )
YP/PAN	295.8	275.5	7.37	2.03	0.028
HT52/PAN	295.8	281.7	5.01	1.41	0.022
XP/PAN	295.8	279.4	5.87	1.64	0.002
HT50/PAN	295.8	280.7	5.38	1.51	0.007

As was observed previously, the pH of the liquor increased (7.1) upon contact of the adsorbents with solution. The encapsulation of PAN did therefore not provide any protection from acidity. The beads, however, appeared not to dissolve being encapsulated into an acid resistance polymeric matrix (PAN). As the porosity of the beads must allow solution to diffuse through, this exposes the adsorbent to the low pH and would thus dissolve the MMP. Although these materials are stable at pH values of ~5, they are not stable in more acidic media and thus in their current form are not suitable for applications in spent fuel dissolver liquors. Future development could investigate the use of potential additives in order to change the pH within the bead and produce a stable matrix for the exchange to take place.

#### 4.2.4 Selectivity

The concept of ART relies on the selectivity of adsorbents unlike PUREX, the uranium and plutonium must not be extracted. The MMP's studied must therefore exhibit similar selectivity to AMP/PAN. Cerium was used as the non-radioactive surrogate for uranium and plutonium in high excess in order to replicate simulated levels in spent fuel dissolver liquors. The selectivities of the MMP/PAN composites were studied and the results are presented in table 4.6

Table 0.6 Selectivity of MMP/PAN composites in natural pH of stock solution (4.4)

XP/PAN Sr  $\sigma$  0.045, Ce (iv)  $\sigma$ 0.033, YP/PAN Sr  $\sigma$  0.031, Ce(iv)  $\sigma$ 0.012, HT50/PAN Sr  $\sigma$ 0.029, Ce (iv)  $\sigma$ 0.039, HT52/PAN Sr  $\sigma$  0.018, Ce (iv)  $\sigma$ 0.004

	Sr (ppm)		Ce(iv) (ppm)		Uptake (%)		K <sub>d</sub> (ml/g)		Capacity (mg/g)	
	Initial	24hrs	Initial	24hrs	Sr	Ce	Sr	Ce	Sr	Ce
XP/PAN	5.81	2.14	455.24	358.50	63.17	21.25	172	27	0.37	9.67
YP/PAN	5.81	2.41	455.24	406.63	58.52	10.68	141	12	0.34	4.86
HT50/PAN	5.81	2.15	455.24	412.77	62.99	9.33	170	10	0.37	4.25
HT52/PAN	5.81	0.98	455.24	433.84	83.13	4.70	492	5	0.48	2.14

The results show that the materials exhibited a small affinity for cerium, with both HT50/PAN composites adsorbing the least. The high affinity of the MMP/PAN composites for strontium was again demonstrated in these studies. The selectivities of these materials for Sr to Ce ranged from 6 to near 100 but with XP/PAN and YP/PAN registering a small yet significant uptake of cerium. Although the higher selectivity may be practical for the ART process, it has to be reemphasised the acid conditions of these solutions bear no resemblance to spent nuclear fuel dissolver liquor. Higher concentrations of strontium, comparable to those found in spent fuel dissolver liquor, may improve the selectivity values by saturating the exchange sites thus inhibiting cerium ion uptake. HT52/PAN showed the lowest affinity for cerium whilst adsorbing over 80% of the available strontium. Despite some visible affinity for cerium, all MMP/PAN composites with the exception of XP/PAN displayed promising selectivity for strontium in the presence of cerium.

#### 4.2.5 Morphology

The internal and external morphologies of the composite beads were similar to the structure of AMP/PAN. Non-uniform pores and large voids towards the centre of the bead were observed which could allow for a high saturation of composite beads with cation under investigation. The beads were of a spongy consistency and consequently more malleable than AMP/PAN beads which made a clear dissection considerably more difficult. Figures 4.6 – 4.10 present SEM images of typical composite beads. Less voids were present in comparison with AMP/PAN composite possibly due to viscosity differences of the reaction mixtures resulting in different consistencies of droplets. The lack of a porous channel network is not a hindrance as is explained in chapter 3. The apparent lack of porosity near the surface of the beads, may be affecting the diffusion of ions and thus a higher porosity at the surface may produce higher  $K_d$  values, but at the expense of capacity.

Similar to AMP/PAN particulate is observed to sit within the bead and additionally on the surface, presenting exchangeable sites for strontium exchange to occur rapidly.

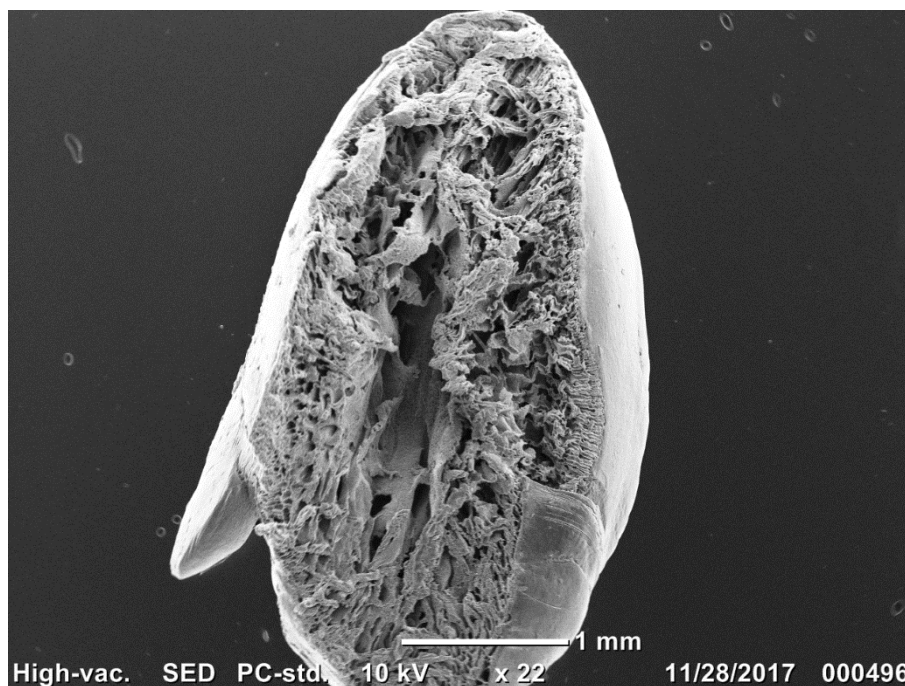


Figure 0.6 Cross section of HT50/PAN bead

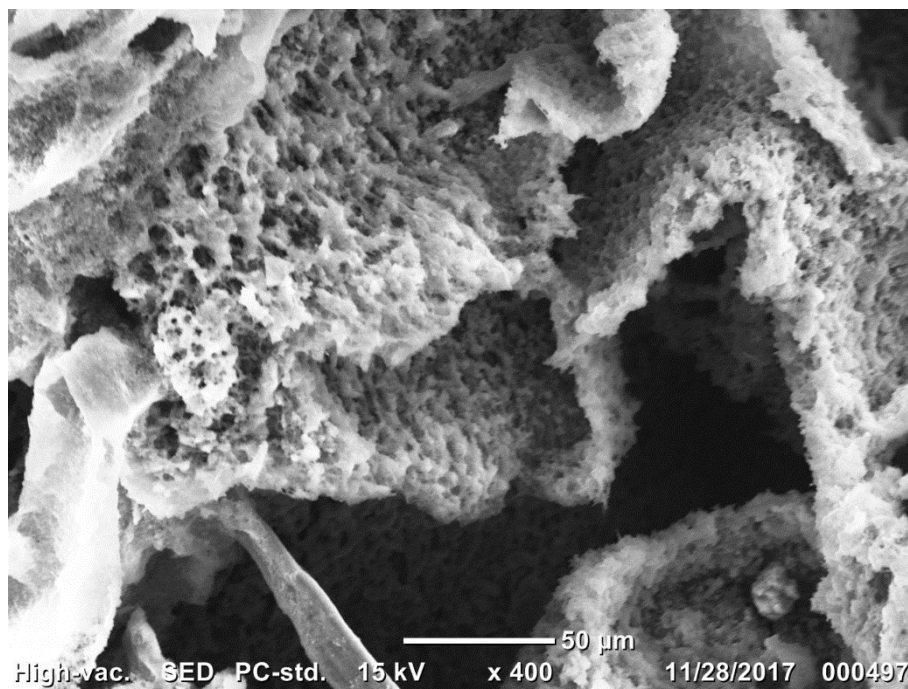


Figure 0.7 Internal section of HT50/PAN bead

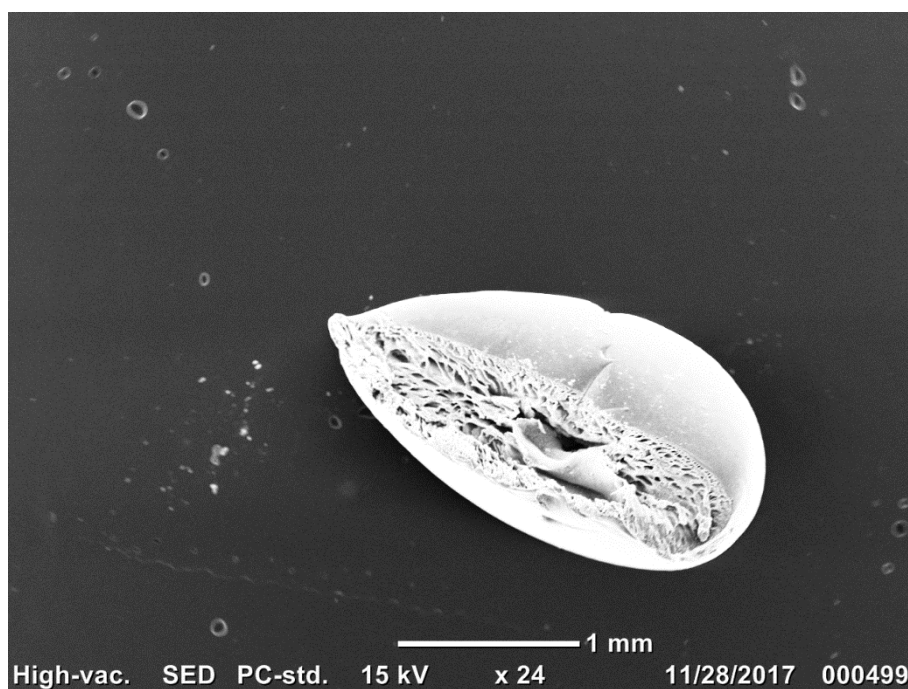


Figure 0.8 Cross section of HT52/PAN bead



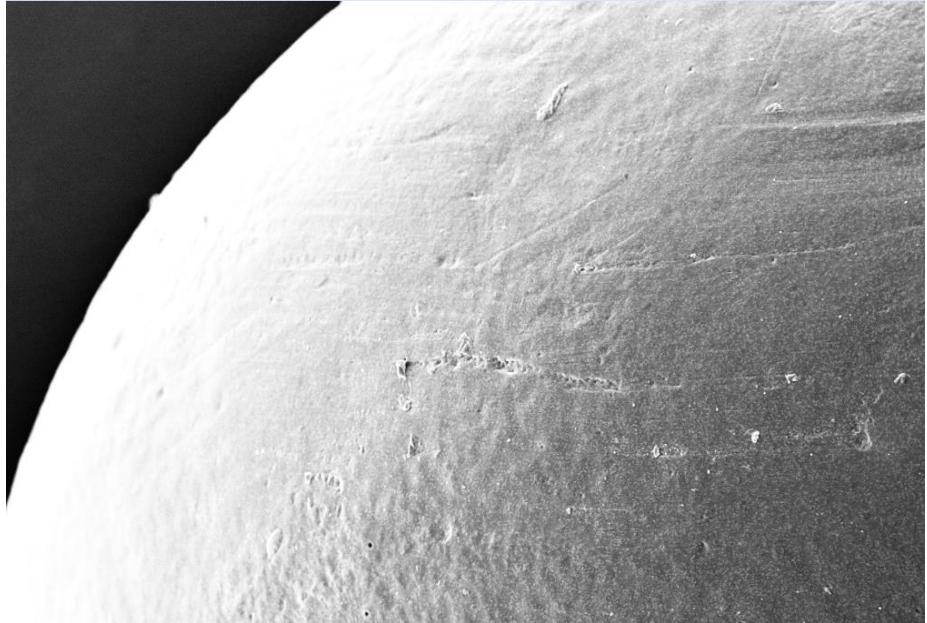


Figure 0.9 Figure 4.9 External image of HT52/PAN bead Magx100

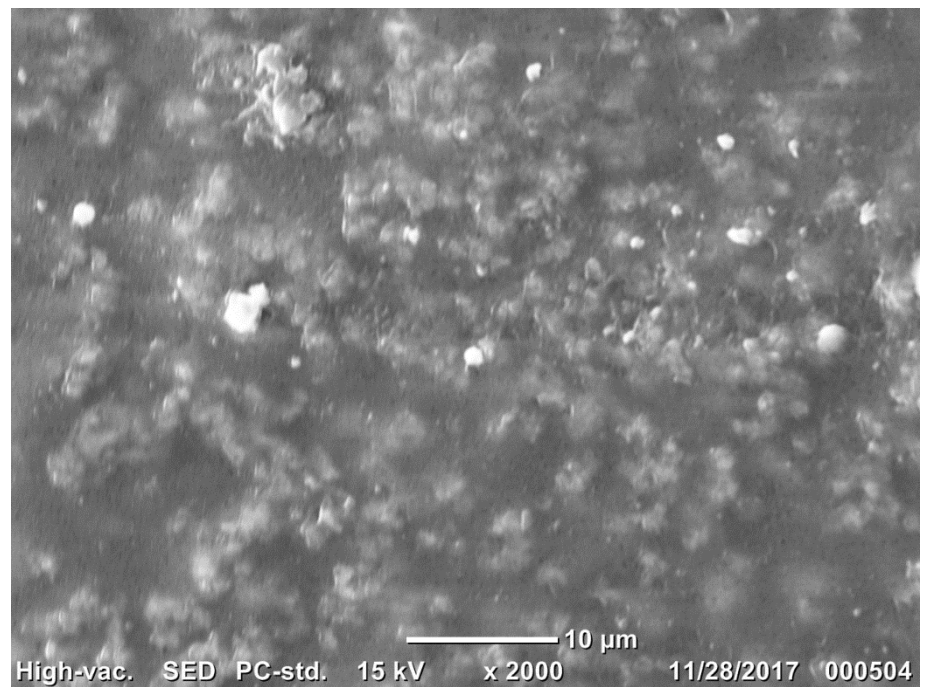


Figure 0.10 External section of HT52/PAN bead

#### 4.2.6 Thermal Stability

The analysis of the composites by TGA (figure 4.11) showed their low thermal stability when compared to AMP/PAN. The initial drop in mass occurs at around 100°C, which can be attributed to the evaporation of water. Denature does not occur until after 150°C and is much lower than expected due to the high thermal stability of PAN. Despite the excess of PAN within the reaction mixture and subsequent low saturation of the composite beads with adsorbent material, decomposition should not occur until higher temperatures. XP/PAN displayed an expected TGA plot that is typical of materials of this nature and exhibits an increased stability with no further change in mass after 750°C. Spent fuel dissolver liquors would not reach temperatures higher enough to fully denature these materials.

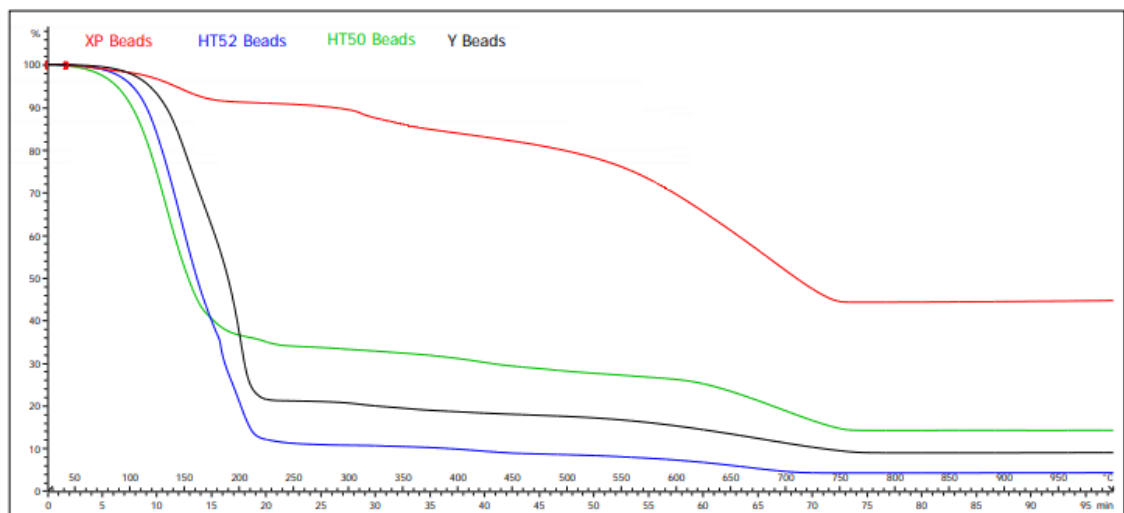


Figure 0.11 TGA spectrum of MMP/PAN

#### 4.2.7 Porosity and Surface area

The porosity and surface area measurements focussed on the MMP/PAN composites in order to better understand the ion exchange performance of these materials. Table 4.7 presents the surface area measurements.

Table 0.7 Surface area of MMP/PAN composite beads

Material	BET surface area (m <sup>2</sup> /g)
HT50/PAN	14.45
HT52/PAN	14.37
XP/PAN	95.37

Similar surface areas were observed for HT50/PAN and HT52/PAN beads ranging from 0.51mm in diameter. The large surface area of XP/PAN was uncharacteristic of beads of this size, but could be attributed to a lack of uniformity in size. The fast kinetics of XP/PAN material could be attributed to this high surface area. Of course, surface area of large beads will be much lower than micro-crystalline powders as is discussed in chapter 3, but similar surface areas to AMP/PAN were achieved by HT52/PAN and HT52/PAN composites thus presenting respectable surface areas for these materials. The high surface area of XP/PAN suggests the possibility of this material being employed into column techniques where maximum surface area of a packed out column would result in efficient ion exchange.

Table 0.8 Average pore diameter of MMP/PAN composite beads

Material	Average pore diameter (nm)
HT50/PAN	6.5
HT52/PAN	4.4
XP/PAN	8.11

The visible decrease in pores compared to AMP/PAN composites did not impact on the size of the pores as is shown by the results in table 4.8. As expected the pore size of XP/PAN was much larger than its cousin materials despite the same volume of surfactant being used in the synthesis of each material. These larger pores offer the potential to increase the amount of adsorbent particulate present in the composite and thus offer potentially higher uptake performance.

Table 0.9 Accumulative pore volume of MMP/PAN composite beads

Material	Accumulative pore volume ( $\mu\text{m}^3/\text{g}$ )
HT50/PAN	419.5
HT52/PAN	260.8
XP/PAN	1933.65

The large surface area and pore diameter of XP/PAN resulted in an expected substantially large pore volume (table 4.9) reinforcing the ability of this compound to encapsulate a large amount of MMP. The large porosity is not complimented by high  $K_d$  values and as such cannot be attributed to the fast kinetics associated with XP/PAN. HT52/PAN and HT50/PAN exhibited a lower pore volume than AMP/PAN 70 beads despite possessing slightly larger pores. If these materials contained more adsorbent material per composite bead, then the high surface area porosity could increase the  $K_d$  values significantly via an increased availability of exchange sites.

### 4.3 Conclusions

Several novel mixed metal phosphate/polyacrylonitrile composites were successfully synthesised and characterised for their strontium uptake capabilities.

The initial studies of the micro-crystalline adsorbents in their powder form exhibited fast kinetics and high uptake capacity for strontium in relatively high pH values (~4.8). This was undesirable as spent fuel dissolver liquors are ~3M HNO<sub>3</sub> and neutralising the acidity to achieve more stable, higher uptakes, would not be acceptable. The regulatory authorities would be concerned with low acidic liquors containing plutonium radionuclides

When the adsorbents were encapsulated in PAN, the resulting composite beads exhibited a reduced uptake capacity however the beads were not saturated with adsorbent material. The results were promising then, as despite a very low amount of adsorbent powder per gram of composite, the materials exhibited some uptake of strontium.

The thermal stability was not as high as desired, however the decomposition of the adsorbents began at around 150°C, which is adequate enough for these to be employed in

spent fuel liquors. Acidic stability was limited in pH values below 3 but further development could potentially solve this issue.

Surface area was significantly high for beads of this size (~0.5-1mm) and due to the low density of the composites there was a high number of individual beads per gram. The high pore volume of the majority of the composites suggests that if the beads were saturated with adsorbent powder, there would be a substantially large amount of adsorbent per bead and thus strontium uptake would increase significantly.

The most promising materials from this study were concluded to be HT50, HT52 and XP as these exhibited fast kinetics and high uptake in their powder form and additionally performed well in their composite bead form.

It should be noted that these materials are in their preliminary development phase and modifications to their synthesis present further work.

#### 4.4 References

- [1] İnan, S. and Altaş, Y. (2011). Preparation of zirconium–manganese oxide/polyacrylonitrile (Zr–Mn oxide/PAN) composite spheres and the investigation of Sr(II) sorption by experimental design. *Chemical Engineering Journal*, 168(3), pp.1263-1271.
- [2] Zhang, A., Wang, W., Chai, Z. and Kumagai, M. (2008). Separation of strontium ions from a simulated highly active liquid waste using a composite of silica-crown ether in a polymer. *Journal of Separation Science*, 31(18), pp.3148-3155.
- [3] Zakurdaeva, O., Nesterov, S., Sokolova, N., Dorovatovskii, P., Zubavichus, Y., Khrustalev, V., Asachenko, A., Chesnokov, G., Nechaev, M. and Feldman, V. (2018). Evidence for Indirect Action of Ionizing Radiation in 18-Crown-6 Complexes with Halogenous Salts of Strontium: Simulation of Radiation-Induced Transformations in Ionic Liquid/Crown Ether Compositions. *The Journal of Physical Chemistry B*, 122(6), pp.1992-2000.
- [4] [19] Li, X., Liu, B., Jian, Y., Zhong, W., Mu, W., He, J., Ma, Z., Liu, G. and Luo, S. (2012). Ion-Exchange Characteristics of a Layered Metal Sulfide for Removal of Sr<sup>2+</sup> from Aqueous Solutions. *Separation Science and Technology*, 47(6), pp.896-902.
- [5] Manos, M. and Kanatzidis, M. (2016). Metal sulfide ion exchangers: superior sorbents for the capture of toxic and nuclear waste-related metal ions. *Chemical Science*, 7(8), pp.4804-4824.
- [6] Pan, J., Zou, X., Yan, Y., Wang, X., Guan, W., Han, J. and Wu, X. (2010). An ionimprinted polymer based on palygorskite as a sacrificial support for selective removal of strontium(II). *Applied Clay Science*, 50(2), pp.260-265.

- [7] Arabadani, P., Payehghadr, M., Sadeghi, M., Es'haghi, Z., Soltani, N. and Rajabifar, S. (2014). Solid phase extraction of radioyttrium from irradiated strontium target using nanostructure ion imprinted polymer formed with 1-hydroxy-4-(prop-2-enyloxy)-9,10anthraquinone. *Applied Radiation and Isotopes*, 90, pp.8-14.
- [8] Vashnia, S., Tavakoli, H., Cheraghali, R. and Sepehrian, H. (2014). Supporting of Lead Hexacyanoferrate on Mesoporous MCM-41 and its use as Effective
- [9] Zhang, L., Wei, J., Zhao, X., Li, F., Jiang, F. and Zhang, M. (2015). Strontium(II) adsorption on Sb(III)/Sb<sub>2</sub>O<sub>5</sub>. *Chemical Engineering Journal*, 267, pp.245-252.
- [10] Garbout, A. and Férid, M. (2018). Pyrochlore structure and spectroscopic studies of titanate ceramics. A comparative investigation on SmDyTi<sub>2</sub>O<sub>7</sub> and YDyTi<sub>2</sub>O<sub>7</sub> solid solutions. *Spectrochimica Acta Part A: Molecular and Biomolecular Spectroscopy*, 198, pp.188-197.
- [11] Marageh, M., Husain, S. and Khanchi, A. (1999). Selective sorption of radioactive cesium and strontium on stannic molybdophosphate ion exchanger. *Applied Radiation and Isotopes*, 50(3), pp.459-465.
- [12] Emmott J, " Chromatographic Separation of Metals" PhD. University of Central Lancashire, 2016.
- [13] Burnell, V. The Synthesis, Characterisation and Ion Exchange of Mixed Metal Phosphates. PhD. 2011.
- [14] DiPrete, C., DiPrete, D., Edwards, T., Fink, S., Hobbs, D. and Peters, T. (2013). Effects of ammonium molybdophosphate (AMP) on strontium, actinides, and RCRA metals in SRS simulated waste. *Journal of Radioanalytical and Nuclear Chemistry*, 298(1), pp.265-275.



- [15] Solubility of Phosphates, Rates of Solution of Calcium Phosphates in Phosphoric Acid Solutions E. O. Huffman, W. E. Cate, M. E. Deming, and K. L. Elmore  
*Journal of Agricultural and Food Chemistry* **1957** 5 (4), 266-275 DOI:  
10.1021/jf60074a001

## **Chapter 5 Separation of Fission products via Simulated Moving**

### **Bed Chromatography**

These studies were performed to gain a better understanding of the SMBC technique for use in ART and also to expand previous work with specific resins that have showed promise in batch column studies and warranted application in a continuous chromatographic mode. Although AMP/PAN was produced in a composite bead form suitable for chromatographic techniques, SMB was evaluated for its applicability to the downstream processes in the ART concept. This technique would be employed after the cesium and strontium have been removed from spent fuel dissolver liquors, hence the claim that HLW can potentially be eliminated due to the initial removal of these species. The SMB technique was in its preliminary testing phase for the ART concept, as this is the first time it has been applied to separating ions in simulated spent fuel dissolver liquors. The information of principles and parameters of SMBC were received from the manufacturer – Semba Biosciences.

#### **5.1 Principles of SMB**

Simulated Moving Bed Chromatography relies on different parameters for different modes to achieve an efficient separation with high yield and selectivity. A schematic of a typical SMBC setup can be seen in figure 5.1.

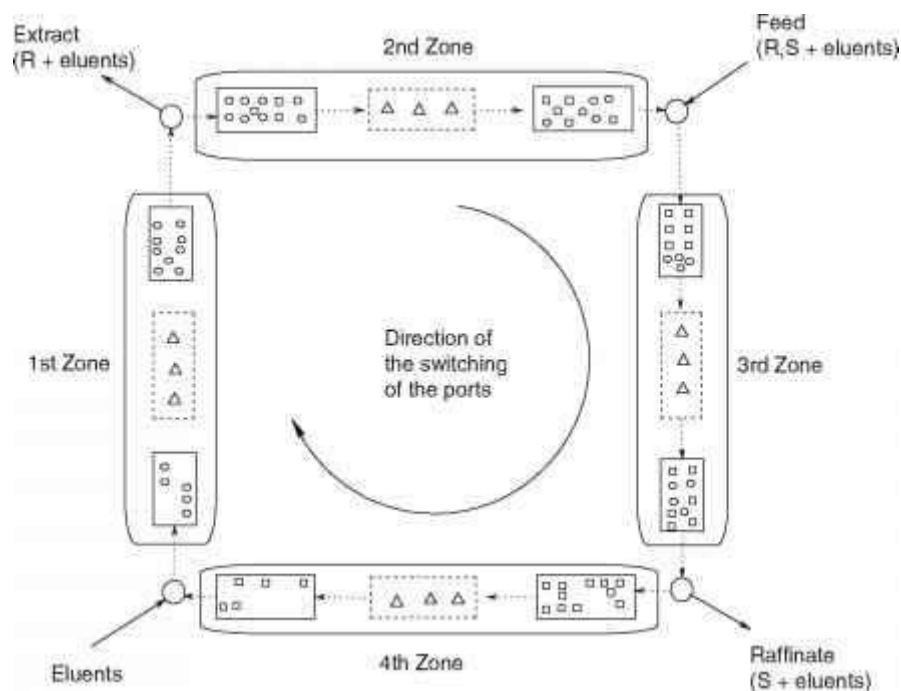


Figure 0.1 Schematic of four zone SMBC <sup>[1]</sup>

The SMBC system can be operated in 2 modes; isocratic and step method. Each method offers different conditions of separation depending on the requirements of the user. <sup>[2]</sup> The initial SMB configuration was derived from single column studies undertaken by Emmott <sup>[3]</sup> and therefore the following experiments should be regarded as scoping studies, which will require refinement.

### 5.1.1 Step mode

The fundamentals of step mode involve 4 or more zones whereby the concentration of the desorbent varies throughout each of these zones. A typical step sequence in a continuous step mode follows as such; bind-wash-elute-clean-equilibrium. The ions adsorbed in each

column will be subject to a wash and elution to enable the column to be re-used again, hence why SMBC is a continuous process.

This mode is useful when certain ions elute at different concentrations and separation cannot be achieved otherwise, the same is true of feed concentration where the concentration of specific ions may drastically change throughout the process. For the ART concept, this method may not be employed due to the controlled concentration of nitric acid needed in spent fuel dissolver liquors to ensure the Pu isotopes, in particular, stay in solution. This mode was not studied in this work but warrants investigation in future work.

### 5.1.2 Isocratic mode

This mode uses a mathematical model called Triangle Theory to achieve efficient separations of a binary mixture. Triangle Theory explains the relation of the Henry coefficients ( $H$ ) of the components of the mixture and the ratio of the net fluid flow rate to the phase flow rate in each of the zones ( $m_j$ ). Different zones use different columns for varying parts of the chromatographic process. For example in an isocratic 3-zone mode, Zone 1 is the delivery of the feed solution to the columns and zone 2 and 3 are where separation occurs. Each zone employs a number of columns (varies on the mode) for the designated process that takes place.

The Henry coefficient is an adsorption isotherm that describes the amount of adsorbate on a surface is proportional to the concentration of the solution. Henry coefficients ( $H$ ) can be calculated using equation..

$$H_i = [(t_i^R - t_0)/t_0] [\varepsilon/(1 - \varepsilon)]$$

Where:  $t_i^R$  = retention time of component i

$\varepsilon$  = overall void fraction

$t_0$  = retention time of inert tracer (acetone)

Equation 5.1 Calculation of Henry coefficient

The flow rate ratio can be calculated as such:

$$m_j = (Q_j t_{\text{switch}} - V_\varepsilon - V_j^D)/V(1 - \varepsilon)$$

Where:  $m_j$  = ratio of net fluid flow rate to phase flow rate

$Q_j$  = fluid flow rate in zone j

$V_j^D$  = extra column volume in zone j

Equation 5.2 Calculation of flow rate ratio

Using Triangle Theory then, for an isocratic mode to achieve efficient separation, the following conditions must be obeyed:

$$m_1 > 1.1H_2 > m_3 > m_2 > H_1 > m_4$$

Equation 5.3 Mass balancing equation

Following the manufacturer's guidelines it is possible to identify and solve possible problems that may be encountered with separations studies. The separation of a binary mixture should result in component 1 and 2 in the raffinate and extract respectively. If this

does not occur then it can be identified in the manufacturers manual which zones are not working effectively.

Possible solutions relate to the flow rates of the feed, desorbent, raffinate and extract.

As described by Semba Biosciences, isocratic is the 'classical' mode of SMBC that uses true counter-current flow to achieve separation. The concentration of the desorbent is constant which proves useful for pH sensitive species that may precipitate out of solution should the concentration of the solvent change. Separation zones are defined by the feed and adsorbent inlets which separates into two outlets; raffinate and extract. Two zone configurations can be used; also 3-zone and 4-zone. These studies employed 3-zone due to the application of more columns to the separation zones (2 and 3) and assumed that this method would offer the most efficient separation. In addition, a fourth zone is not needed in most applications as the volume of desorbent used is low enough to eliminate the need for recycling; this method is usually used for binary solutions.

The presence of the cerium in our studies is for an indication of selectivity to observe potential binding affinities the resins may have for uranium and plutonium in spent fuel dissolver liquors and to observe the effect a competing ion in high excess may have on the performance of SMBC. Therefore cerium retention times were observed but not included in the SMBC parameter calculator as components 1 and 2 were attributed only to zirconium and molybdenum. Component 1 was the species with fastest retention time and component 2 was the slowest.

The parameters of both modes can be controlled to achieve separation, the SembaPro software provides calculators that allow the user to enter precise flow rates into the scripts. Although the concentration of the feed solution remained constant throughout the

experiments as stock solutions simulated spent fuel dissolver liquors concentrations, different feed concentrations may require different flow rates. Previous work employing single column studies have proven that some ions may have delayed elution<sup>[3]</sup>.

For each experiment, both the raffinate and extract compositions were analysed by ICP-MS to understand how to optimise the parameters to achieve the desired separation in high yield and purity. Isocratic mode does not account for various adsorption effects that result in non-linear behaviour. The final concentration of ions in both the raffinate and the extract can provide information on the behaviour of each separation; these are discussed later.

### 5.1.3 Parameters

To gather the required information for the SembaPro calculator, single column experiments were performed according to chapter 2 for each resin with chosen feed and desorbent. The data needed is:

- $V$  = Volume of a single column
- $t_0$  = retention time of inert tracer at flow rate  $Q$
- $t_t^R$  = Fastest retention time of a component
- $t_b^R$  = Slowest retention time of a component
- $V_{SMB}$  = Volume of a single column used for SMB
- $V_t^D$  = extra column volume for one column position in SMB.

Entering the obtained data into the calculator, the following information is obtained:

- Void fraction;

- Henry constants;
- Target selectivity; - Zone flow rate.

The information obtained above is then used by the software to calculate switch times and feed flow rates that obey the mass balancing equation (equation 5.3).

Column measurements are detailed in chapter 2. The retention times obtained for the calculator are presented below in table 5.1. The values represent the time taken for the ions initially to breakthrough, whereas the work by Emmott measured the bed volume<sup>[3]</sup>.

Table 0.1 Retention times for Zr,Ce,Mo in 1M HNO<sub>3</sub> at flow rate 5ml/min

	Retention time t <sup>R</sup> (minutes)		
	Zr	Mo	Ce
S910	1.39	1.82	1.71
C100x10MBH	1.42	1.03	1.51

Table 0.2 Retention times for Zr,Ce,Mo in 3M HNO<sub>3</sub> at flow rate 5ml/min

	Retention time t <sup>R</sup> (minutes)		
	Zr	Mo	Ce
S910	1.42	1.35	1.62
C100H	1.26	1.14	1.29
C100x10MBH	1.31	1.40	1.19

These retention times are a guide for operating the SMB for separating a binary mixture. As is explained in chapter 1, SMBC provides a more efficient ion exchange process than conventional batch processes due to a more efficient application of the adsorbent via the counter current flow. The elution studies in this work may not underpin the development



of the ART concept but may shed light on the fundamental operating conditions required for its capabilities to be employed in a nuclear reprocessing technique.

## 5.2 Results and Discussion

Each experiment was performed as detailed in chapter 2 using the resins of interest (Purolite S910, C100H and C100x10MBH) in isocratic 3-zone mode. As AMP PAN has a high affinity for cesium it was excluded from these studies, also with the ART concept the adsorbed cesium would remain on the composite and ultimately be vitrified. A chromatographic technique could be employed thereafter as the radioactivity present is now comparatively low and hence a wider array of materials could be used without being damaged by radiolysis. The resins in these studies were selected on promising batch column work performed by Emmott. As is mentioned in his work, zirconium presents various problems in spent fuel dissolver liquors and therefore included this work in addition to molybdenum which also has some interesting chemistry/complexes.

### 5.2.1 SMBC experiment 1: 1M HNO<sub>3</sub> C100x10MBH

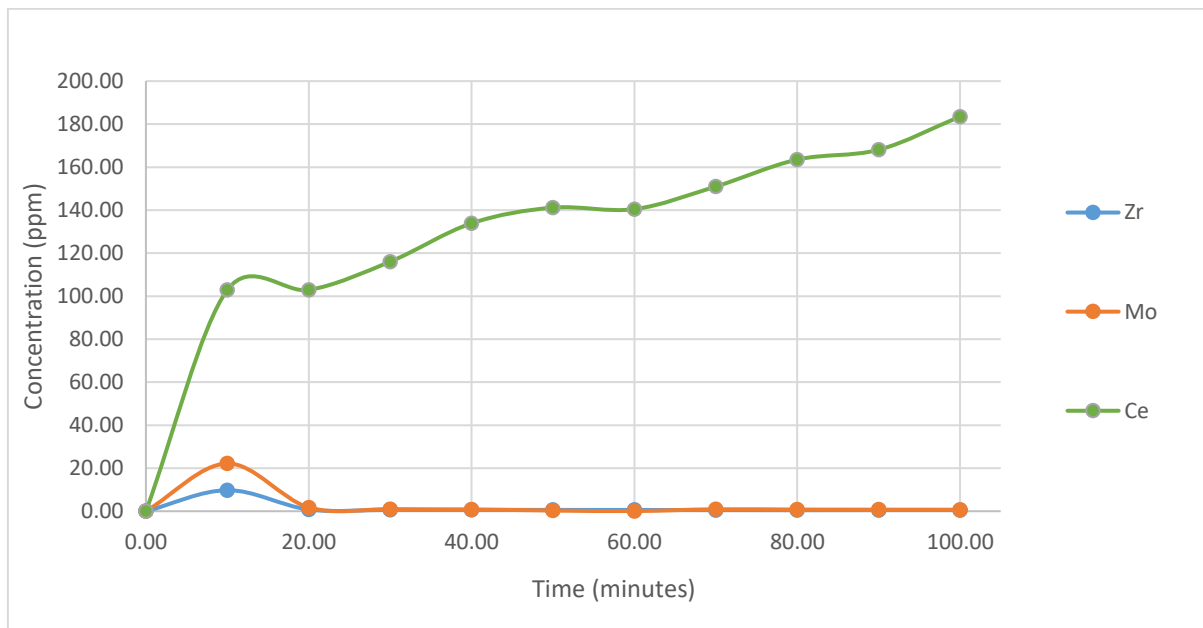


Figure 0.2 Raffinate from SMBC elution using C100x10MBH, 1M HNO<sub>3</sub>

As spent fuel dissolver liquors are highly acidic (~3M), 1M HNO<sub>3</sub> was used as the benchmark desorbent for each experiment in addition to separate 3M experiments for each resin of interest. The chromatogram of the raffinate for experiment 1 provided promising results (figure 5.2). The affinity of zirconium and molybdenum are in direct contrast to the affinity for cerium based on the elution curves. This difference could be due to their affinities in 1M HNO<sub>3</sub> but also the concentration of cerium in solution was 10 fold larger than the concentrations of zirconium and molybdenum. The high affinity of the resins for zirconium in 1M HNO<sub>3</sub> is characteristic of batch studies performed previously<sup>[3]</sup>. Interestingly, at the same concentration, this resin exhibited high uptake in batch studies for cerium in an excess of zirconium. The high excess of cerium in these solutions presents

a small, but promising proof of concept that employing a continuous technique in ART could separate problematic fission products from spent fuel dissolver liquors.

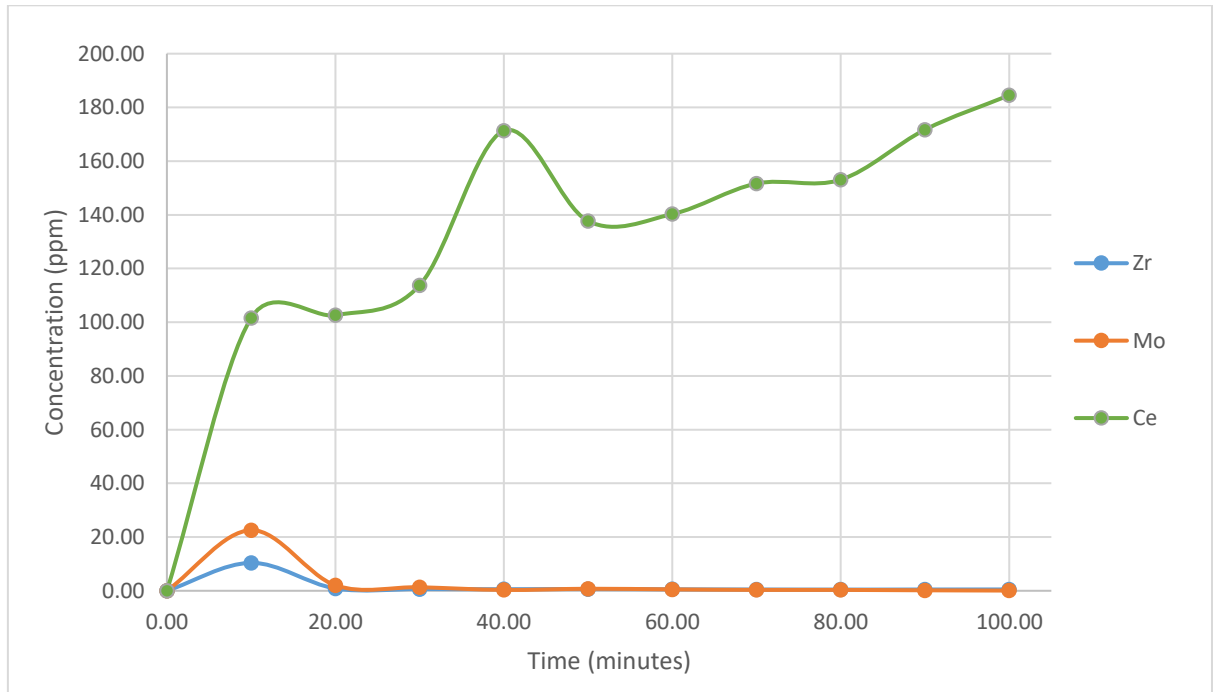


Figure 0.3 Extract from SMBC elution using C100x10MBH, 1M HNO<sub>3</sub>

The extract displayed similar results to the raffinate chromatogram. This may be undesirable depending on where the outlets of both were routed. The use of SMBC is to promote a more efficient separation than batch techniques – as is outlined in chapter 1 – and the presence of cerium in both exit streams does not discourage the potential application of this technique. A possible explanation for this phenomenon is that zone 1 was not purged enough and flow rates of the feed solution did not optimise zone 2 (where separation occurs). The lack of a Gaussian peak for cerium does however reinforce a low

affinity of the resin for this species and a comparatively high affinity for zirconium and molybdenum.

### 5.2.2 SMBC experiment 2: 3M HNO<sub>3</sub> C100x10MBH

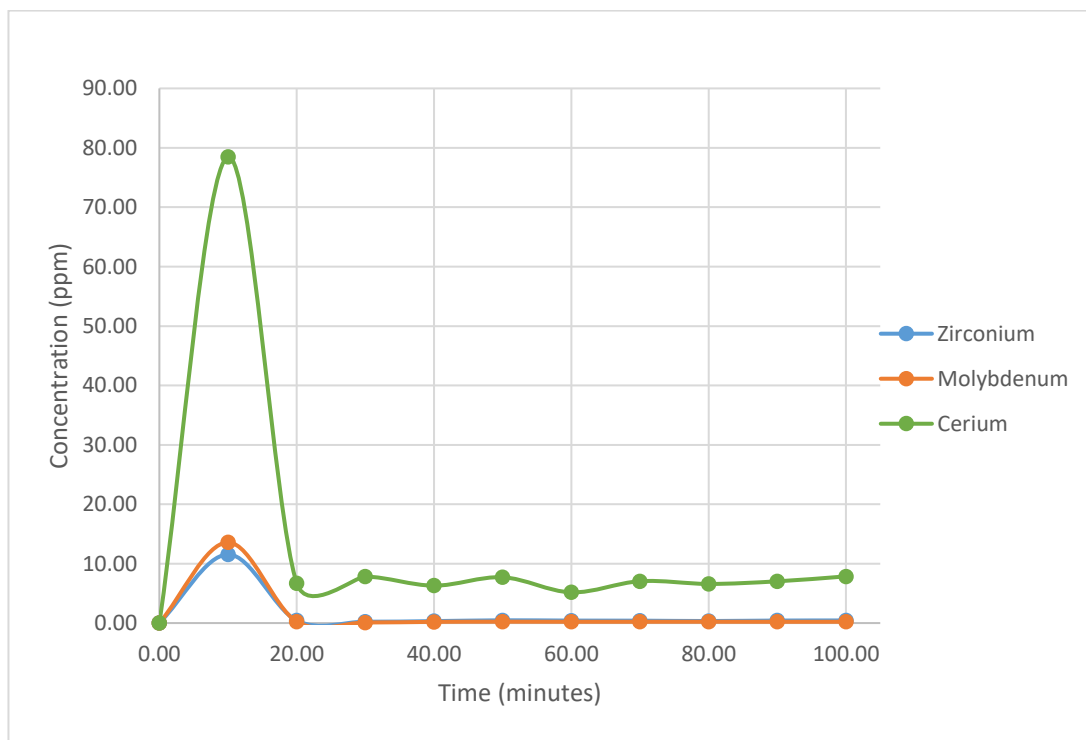


Figure 0.4 Raffinate from SMBC elution using C100x10MBH, 3M HNO<sub>3</sub>

Figure 5.4 presents the results of sulphonic acid resin C100x10MBH eluted using 3M HNO<sub>3</sub>.

The Gaussian shape of all 3 ions in the first 10 minutes suggests a low binding affinity for each with possible long-term adsorption of cerium thereafter represented by the low concentration eluted into the raffinate.

Previous work by Emmott reported high uptakes of Zr and Ce (>85%) in 1M HNO<sub>3</sub> batch studies and would be suggested to be uncharacteristic for this resin. Of course, the fundamentals of batch studies are much different to SMBC processes as eluted bed volumes are not considered; rather, SMBC uses flow rates to achieve separation.

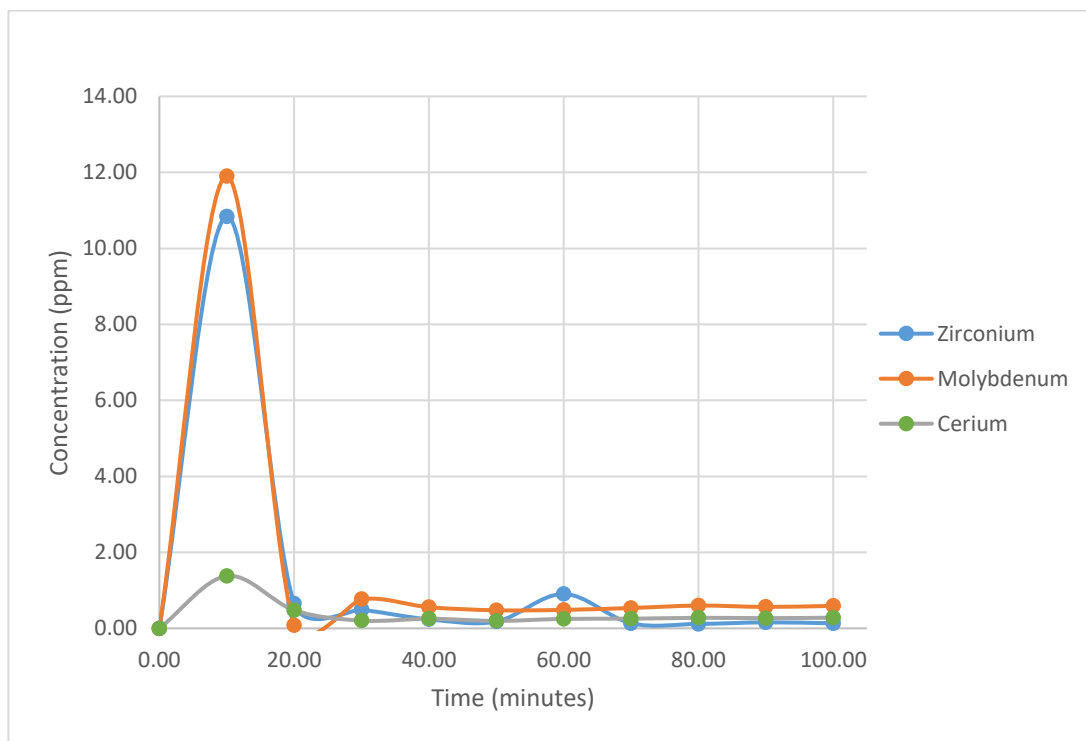


Figure 0.5 Extract from SMBC elution using C100x10MBH, 3M HNO<sub>3</sub>

The extract chromatogram demonstrated that separation was viable despite displaying some affinity for cerium, this could be counter-productive for the ART concept, (in our studies cerium is substituted for U and Pu as explained in chapter 3). In addition, sulphonic acid resin stability in nitric acid liquors (3M) is uncertain/limited. The zirconium and molybdenum exhibited a Gaussian shape peak suggesting no binding affinity for these materials at higher concentrations of nitric acid, complementing the observations of the raffinate chromatograms. This is contrary to batch studies, which have previously

confirmed a lower affinity for cerium at higher concentrations of nitric acid. The presence of zirconium and molybdenum in both the raffinate and the extract and the cerium in the raffinate suggests that zones 2 and 3 were not working at optimal conditions despite the adherence to calculated parameters. For future development, decreasing the feed and extract flow rates may improve the separation and slow down the elution of zirconium and molybdenum, allowing the resins to time to adsorb the ions. Increasing flow rates after the first switch may allow ions to be adsorbed slowly and then eluted quicker after the first step. In addition, if the Triangle Theory is obeyed, the calculated parameters are independent of the amount of columns used, then the optimisation of four columns could be applied to a system incorporating an increased number of columns.

### 5.2.3 SMBC experiment 3: 3M HNO<sub>3</sub> C100H

C100H has been extensively applied to single column studies and providing some promising results that warranted application of this resin into a continuous system. The performance of this resin at various concentrations of nitric displayed an affinity for zirconium and cerium. Based on previous single column work this resin was only studied using a 3M HNO<sub>3</sub> desorbent stage.

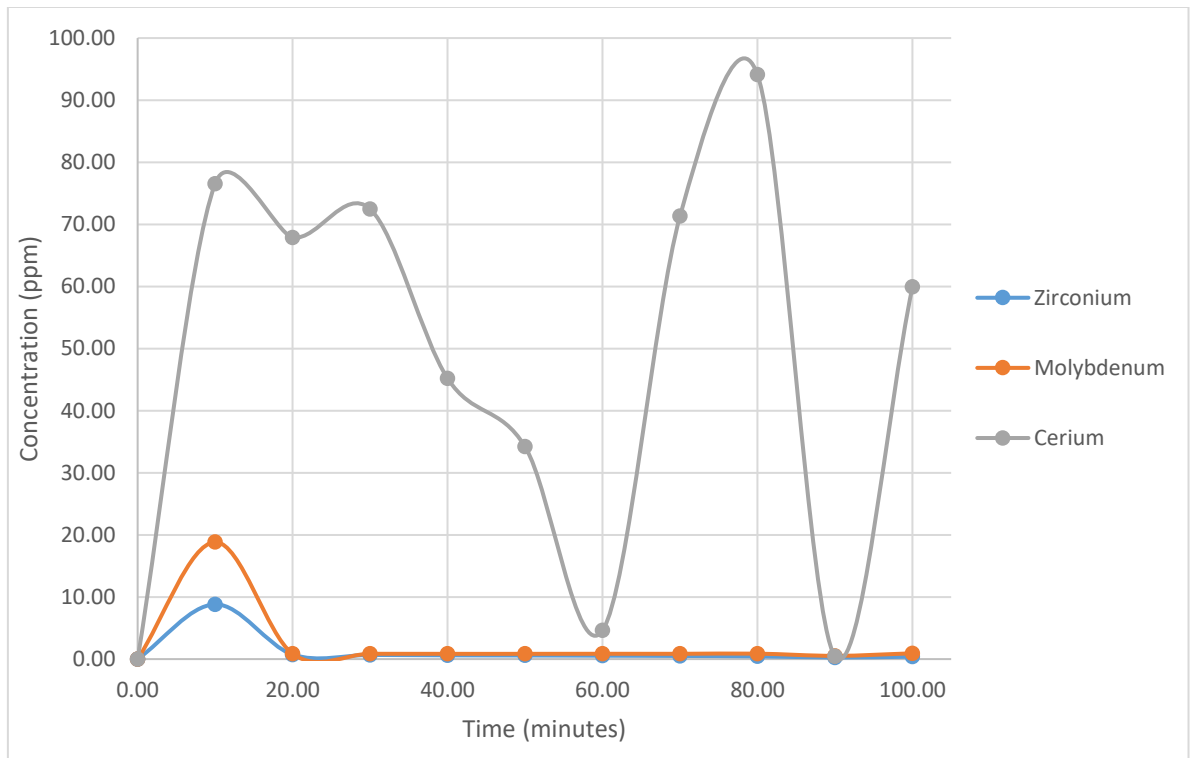


Figure 0.6 Raffinate from SMBC elution using C100H, 3M HNO<sub>3</sub>

The chromatogram (figure 5.6) shows that the affinity for zirconium was not consistent with previous work [Emmott] however as only a low concentration was eluted in the first 10 minutes, this suggested some adsorption of zirconium and molybdenum may have occurred. The separation of the majority of these two ions from cerium had been achieved, although not optimally as some zirconium and molybdenum was not retained. Cerium exhibited interesting elution characteristics, with a large amount eluting over the first 40 minutes and adsorbing onto the resin for 20 minutes before peak maxima was observed at 80 minutes. The flow rate of the desorbent and the switch time between the protocol steps could have contributed to this. It would be beneficial to increase flow rate of the feed solution and raffinate in order completely elute the cerium with faster kinetics.

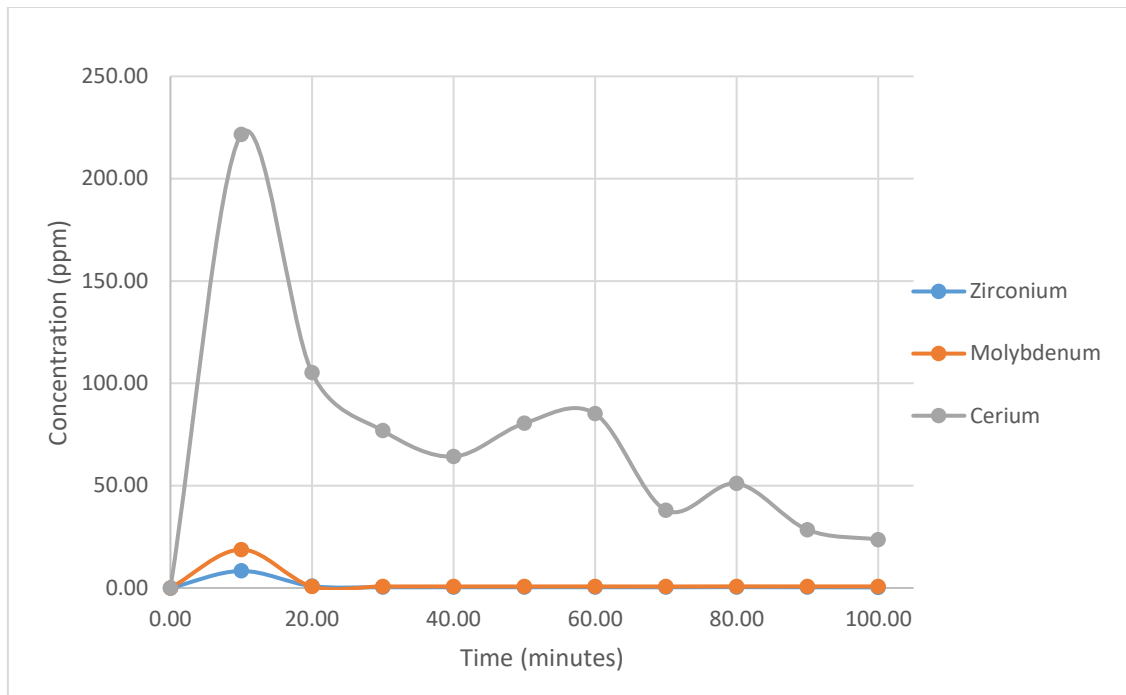


Figure 0.7 Extract from SMBC elution using C100H, 3M HNO<sub>3</sub>

The raffinate, figure 5.6, shows an increased amount of cerium eluted into this outlet compared to the extract. The chromatogram suggests a lower affinity for cerium contrary to raffinate analysis. Cerium does however continue to be eluted over time whereas zirconium and molybdenum near complete elution after 10 minutes.. Increasing the flow rate of desorbent could potentially result in a quicker elution of cerium and overcome the binding affinity.



#### 5.2.4 SMBC experiment 4: 1M HNO<sub>3</sub> S910

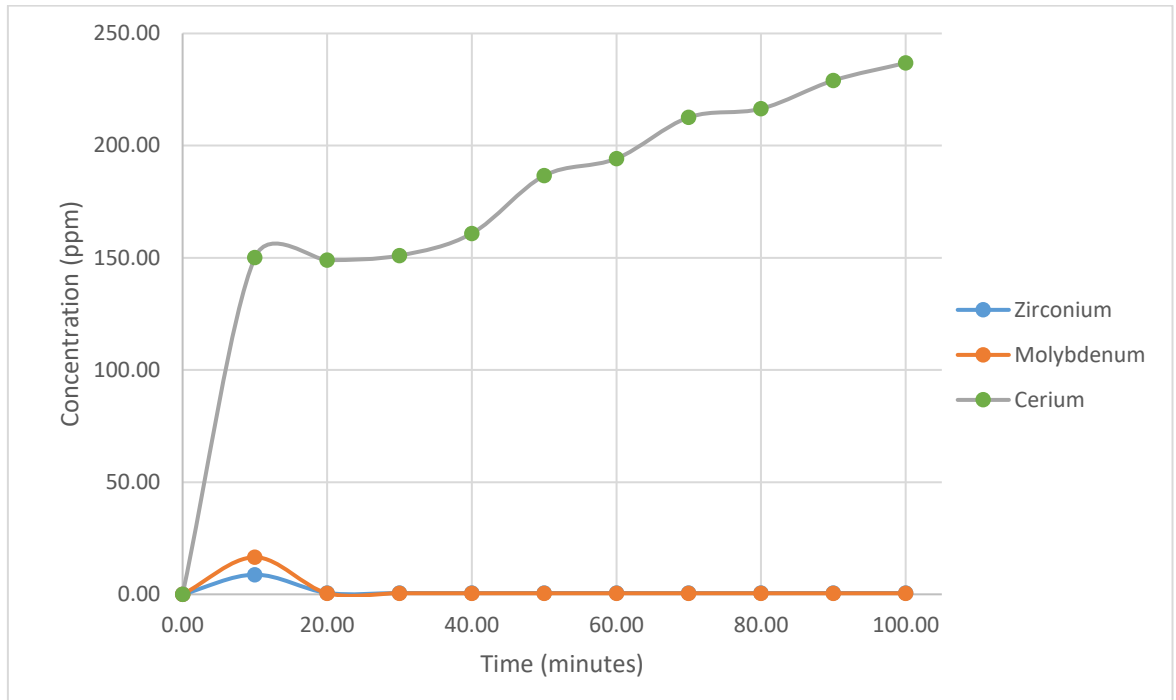


Figure 0.8 Raffinate from SMBC elution using S910, 1M HNO<sub>3</sub>

The results of the 1M HNO<sub>3</sub> experiments displayed in figure 5.8 and Figure 5.9 shows similar elution trend for cerium. The resin showed a substantial affinity for cerium and elution concentration increased with time. Despite the low concentrations of zirconium and molybdenum these eluted into the raffinate far quicker and some degree of separation was achieved. The feed and desorption flow rate to the separation zones (2 and 3) however, may not have been optimised.

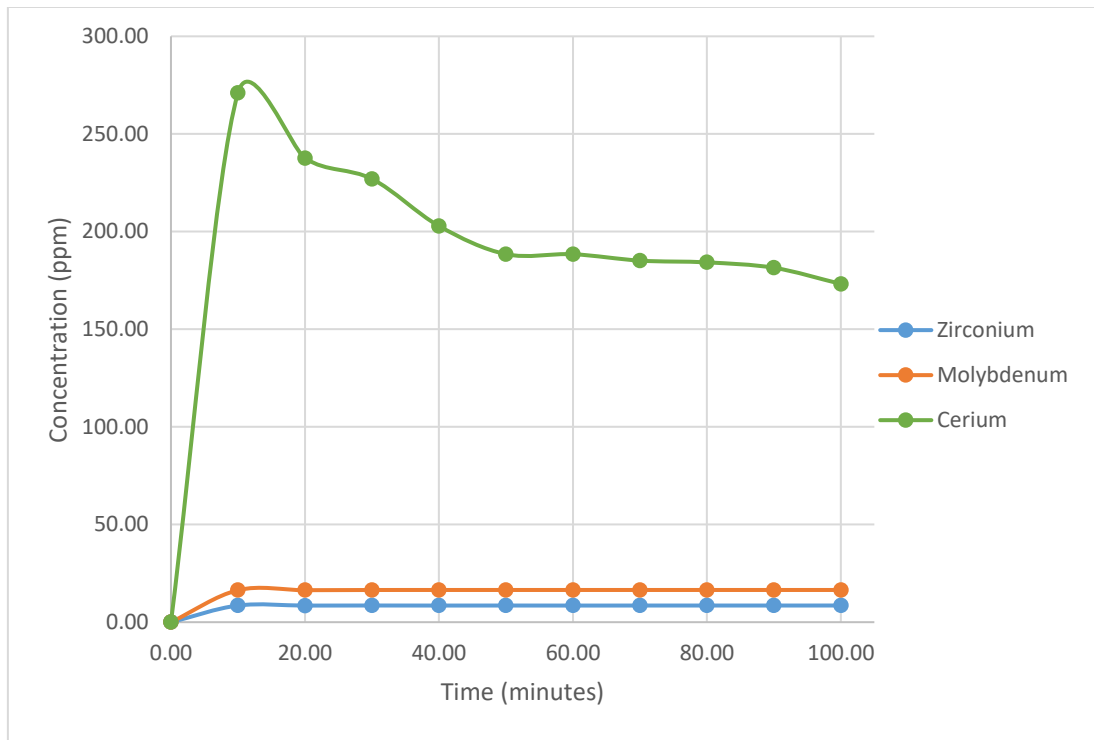


Figure 0.9 Extract from SMBC elution using S910, 1M HNO<sub>3</sub>

The decrease in elution over time for cerium displayed in figure 5.9 suggests a peak maxima was achieved at.. The affinity of the amidoxime S910 resin for cerium is limited yet displays some adsorption due to the continuous elution over time and may be unfavourable characteristic for ART. The complete elution of cerium was slow and would continue for a prolong time period. The presence of zirconium and molybdenum in the raffinate, but low concentrations in the extract, suggest that zones 2 and 3 performed some separation of these ions and thus optimisation could possibly separate the zirconium and molybdenum into separate streams from the cerium if flow rates were optimised.

### 5.2.5 SMBC experiment 5: 3M HNO<sub>3</sub> S910

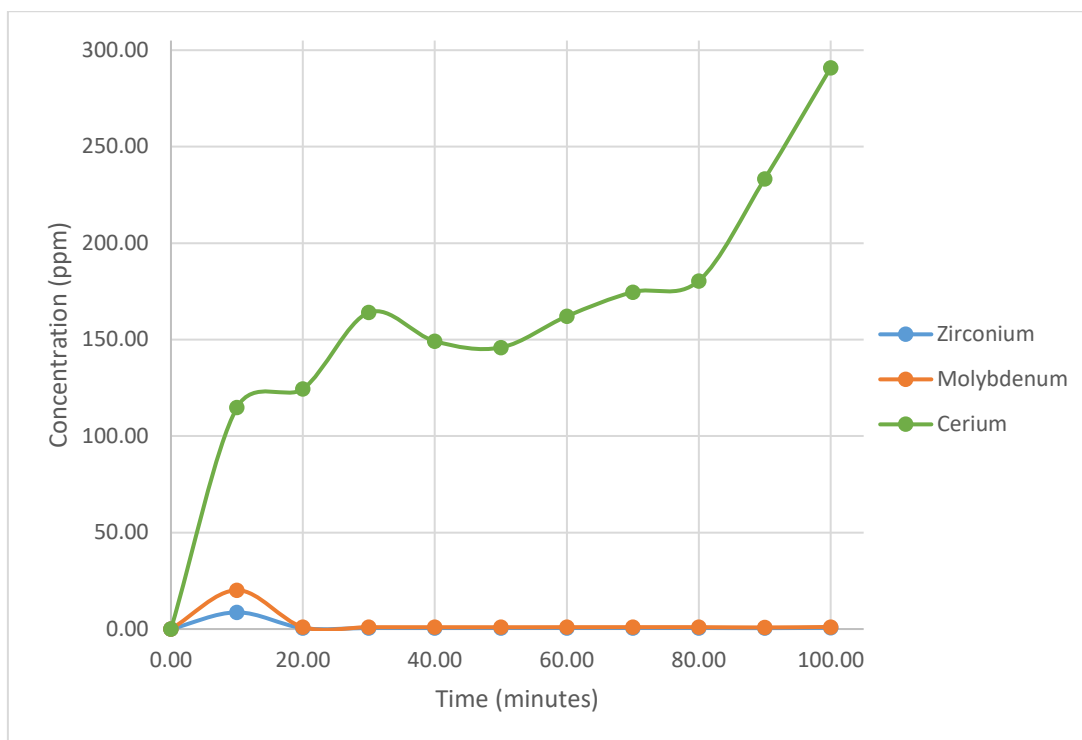


Figure 0.10 Extract from SMBC elution using S910, 3M HNO<sub>3</sub>.

Increasing the concentration of desorbent did not produce any significantly different results to 1M HNO<sub>3</sub> experiments with this resin as displayed in Figure 5.10. There was no apparent binding of S910 to zirconium or molybdenum and in contrast, there was a higher affinity for cerium represented by the increase in concentration over time. The affinity of this material for cerium makes it unsuitable for the ART concept.

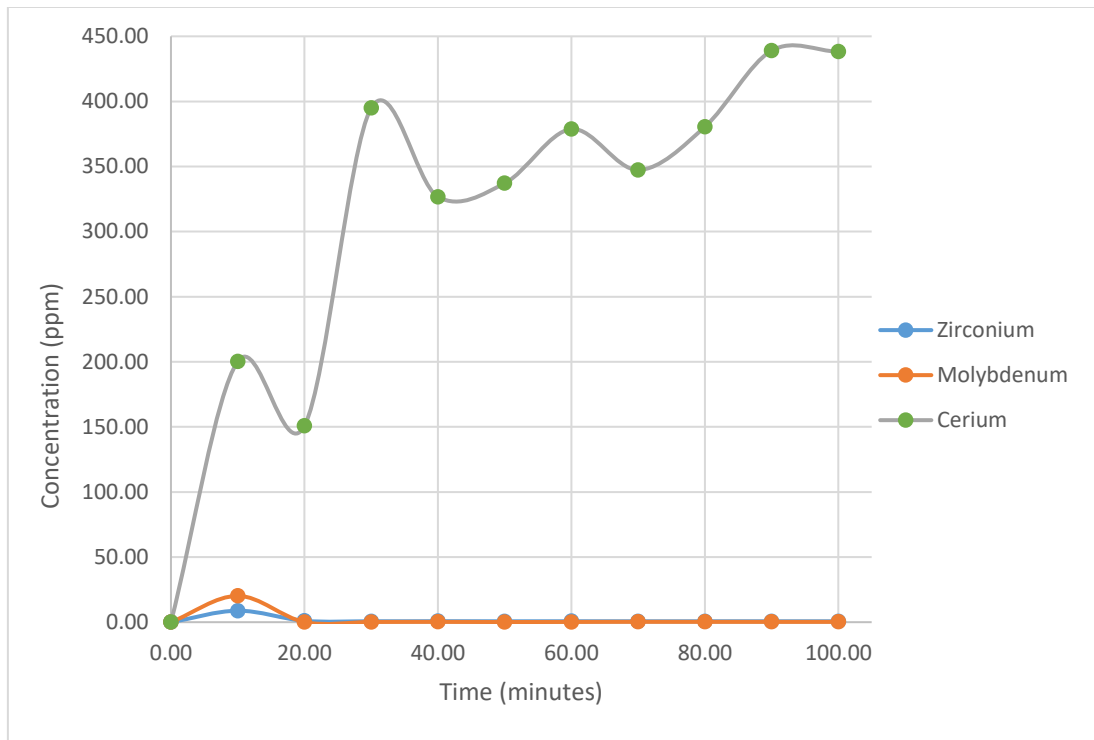


Figure 0.11 Extract from SMBC elution using S910, 3M HNO<sub>3</sub>

The raffinate chromatogram displayed similar results to the extract of this resin as is seen in Figure 5.11. The extract of 1M HNO<sub>3</sub> studies for S910 showed a decrease in cerium concentration over time however for 3M HNO<sub>3</sub> studies the concentration continued to increase suggesting as an increased volume of desorbent was processed, this caused the elution of cerium over time. The separation zone was not optimised possibly due to the presence of cerium in both extract and raffinate. Although the affinity for cerium is not desired, the result of the increasing cerium concentration is indicative of a separation of ions, albeit the undesirable species. The high excess of cerium presents the challenge of competing ions in spent fuel dissolver liquors, and thus why SMBC must be optimised in order to overcome these large concentrations. This could be achieved by changing flow rates of the feed and step times to allow selective ions to flow into the separation zone and thus ensuring they are adsorbed onto the resin before competing ions.

### 5.3. Conclusions

The aim of these studies was to undertake preliminary scoping studies using SMBC to evaluate its potential for in use the ART concept. The results do not allow for definitive conclusions to be made as the underlying fundamentals of the SMB instrument have not been fully explored/appreciated. The commercial resins employed are unlikely to be used for the ART concept, as they have previously shown to exhibit an affinity for Ce (U and Pu simulant). They were used to obtain a baseline of isocratic separation using SMBC, as AMP/PAN has such a high affinity for cerium even in 3M nitric acid, negating the need for a chromatographic technique in the ART concept.

The solutions employed in these studies had comparatively high concentrations of Zr and Mo with Ce acting as a competing ion for selectivity purposes. The relatively quick elution of cerium in 1M HNO<sub>3</sub> studies could suggest the separation zones have the potential to be optimised, due to the high affinity of C100x10MBH for cerium in batch studies. The countercurrent flow and optimisation of flow rates obeying Triangle Theory could initially explain the reason for the presence of high concentrations of cerium in the raffinate and extract, i.e.

separation was successful due to an optimised flow of desorbent. It can be proposed that despite the elution of most of the zirconium, affinities studied previously for these species could be the same, but the high concentration of the competing Ce is reducing the amount of exchangeable sites available to Zr and Mo.

As there is little literature for comparison, single column studies of these resins have acted as baseline separations. Now however, the results obtained from these studies can be used as the baseline for isocratic separation of a binary mixture with a competing ion simulating

spent fuel dissolver liquor concentrations. The SMB technique did however present several advantages over static processes:

- The SMBC process was fully automated once the protocol was started;
- Less manual parameters are needed to achieve separations as the SMB uses retention; times to calculate possible flow rates.
- The flow rate can be adjusted mechanically; - The process was much faster.

The fundamentals of SMBC could take several years to fully develop and understand hence why these preliminary tests could not fully explain the separation behaviours.

## 5.5 References

- [1] Mudd, E. (2020) Simulated Moving Bed in the Commercial Production of Sertraline - Chiral Drugs. Available at: <https://www.pharmacologicalsciences.us/chiral-drugs/simulated-moving-bed-in-the-commercial-production-of-sertraline.html> (Accessed: Jul 30, 2020).
- [2] Chemicals, Kathleen Mihlbachler, Eli Lilly and Company, and Olivier Dapremont, Aerojet Fine Simulated Moving Bed Chromatography Offers Real Attractions. Available at: <https://www.chemicalprocessing.com/articles/2005/538/> (Accessed: Jul 30, 2020).
- [3] Emmott J, " Chromatographic Separation of Metals" PhD. University of Central Lancashire, 2016.

## Chapter 6 Summary and Future work

The challenges of the current reprocessing technique – PUREX – were addressed in this work. The limited selectivity and degradation of TBP limits the efficient extraction of uranium and plutonium from spent fuel dissolver liquors. In addition, the production of HLW arising from PUREX is subject to strict control procedures due to its high radioactivity and heat decay. This is problematic as storage space for HLW is finite, hence the development of an Alternative Reprocessing Technique (ART) in this work.

The ART concept describes the design of a novel reprocessing technique employing Simulated Moving Bed Chromatography and was conceptualised circa 2012. This work presented the initial research that has begun a lengthy development process of an SMB technique for its potential application in nuclear reprocessing. It is of paramount importance to understand the workings of the instrument which provide completely different results to static chromatographic techniques and thus conventional elution studies may not be the experiment of choice. This is due to the principles that underpin SMB and allow for a more efficient application of adsorbent materials and subsequently result in a more efficient ion exchange process. It should be emphasised that this concept is novel and no published work in the UK exists that suggests other researchers are using SMB for the potential extraction and/or separation of radionuclides from spent fuel dissolver liquors.

Considering the aims and objectives of this research project, the initial objective of modifying the synthesis of AMP/PAN to prove that ion exchange performance can be optimised through this method was achieved. The following modifications to AMP/PAN composite bead production achieved positive results regarding the uptake of cesium;



- Using a reduced Mw of polyacrylonitrile reduced the synthesis cost by almost half whilst maintaining high thermal and radiolytic stability in addition to high uptake capacities, rapid kinetics and high  $K_d$  values;
- Employing different types of nozzle saw a gradual increase in the quality and uniformity of composite bead production, with a dual stainless steel nozzle being the latest and most successful of the other nozzles used;
- Reducing the amount of DMSO in the reaction mixture resulted in the production of composite beads with a higher saturation of AMP per bead of AMP/PAN. This increased ion exchange performance when compared with previous work;
- Altering the ratios of AMP: PAN showed that AMP/PAN 70% was expectedly more superior to lower ratios due to the increased amount of adsorbent material available to the cesium ions in solution. Combined with efficient diffusion, this resulted in high  $K_d$  values and kinetics.

Selectivity of AMP/PAN 70 for cesium in the presence of uranium (cerium used as a simulant) had not been previously studied at the ratios employed in this work. Even in the presence of a large amount of cerium ions (~1:450 Cs:Ce) AMP/PAN 70 exhibited high selectivity for cesium and an almost non-existent affinity for cerium. Confirming that AMP/PAN 70 could be employed in a reprocessing technique where uranium is in high excess compared to cesium, ensuring the uranium is not taken out of solution by AMP/PAN. It was however, concluded that the oxidation state of cerium would have some effect on the selectivity of AMP/PAN for cesium. Ce(III) seemed to have a negative impact on the selectivity factor and was attributed to the similarity in ionic radii of Ce(III) to that of cesium – relation between ionic radii could underpin the fundamentals of ion exchange, as was suggested in this work between cesium and ammonium.

Irradiation of AMP/PAN was employed at low doses compared to the potential radiolytic stability reported in the literature. Visible colour changes attributed to the change in oxidation state of molybdenum (+4 to +5) were observed after irradiation however had no significant impact upon ion exchange performance for cesium. The radiolytic stability of

AMP/PAN thus being confirmed by the studies. This reinforced the potential use of this material in spent fuel dissolver liquors.

The thermal stability was also shown to be above the temperatures of spent fuel dissolver liquors, thus confirming temperature (if AMP/PAN is employed in reprocessing) would not be a contributing factor to any potential degradation of AMP/PAN. Additionally, AMP/PAN performed much better as an ion exchanger in 3M HNO<sub>3</sub>, thus exhibiting high stability in acidic media.

As strontium is another highly radioactive species contributing to the classification of HLW, new adsorbents would ideally be synthesised that exhibit similar ion exchange performances as AMP/PAN, but for strontium. The diversity of polyacrylonitrile led to the focus of encapsulating potential strontium adsorbents within this polymeric support to produce uniform composite beads. The mixed metal phosphates studied in this work exhibited fast kinetics and near complete strontium uptake in relatively high pH values (~5) compared to AMP/PAN's employment in pH levels below 3. The MMP/PAN composites showed relatively good uptake of strontium despite the low saturation of a composite bead with adsorbent MMP. Selectivity was limited however with XP/PAN showing a significant affinity for cerium (>20%). Interestingly, HT50/PAN and HT52/PAN exhibited a good selectivity for low concentrations of strontium and low affinities for cerium. Low acidic stability of these MMP's must be overcome if they are to be potential applicants for a nuclear reprocessing.

The results from SMBC studies were far from conclusive as the technique was in its preliminary stage of testing. The commercial resins employed in this technique were not indicative of potential adsorbents for the ART concept, and were only applied to SMBC to further studies from previous work that suggested they warranted study using this technique. They were subject to a feed solution containing Zr and Mo – two species in high

concentration in spent fuel dissolver liquors and subsequent PUREX raffinate. Ce was used as a simulant for uranium and plutonium to observe competitive ion exchange. Possible elution of the zirconium and molybdenum (despite previous work reporting high affinities of the employed resins for these species in 1M and 3M HNO<sub>3</sub>) was attributed to the high excess of Ce (~10x higher than Zr and Mo). As the commercial resins have displayed affinities for cerium previously, the high concentration could be limiting the amount of exchangeable sites for Zr and Mo. The difference in behaviours and conditions of the SMB to conventional static techniques were considered to be contributing factors to unexpected adsorption behaviour. However, if a better understanding of the technique is acquired, these unexpected behaviours could be explained in more detail.

Future work may include but not be limited to:

- Understanding how AMP is located within the PAN structure, this will require more investigation of the morphology of bead structure;
- Understanding the cesium extraction mechanics, i.e. the exchange of ammonium ions and their diffusivity through the bead, could this be the rate controlling step. This may require producing large beads possibly 10mm diameter and/or other structures.
- Modification of MMP/PAN synthesis to include potential additives to aid in acid stability and thus uptake capabilities in low pH values
- Possible synthesis and development of Sr Ion imprinted polymers incorporating PAN as the support.
- Development of the SMB technique as to produce a set of parameters that can be related to certain separations/ion exchange process. This development needs to be extensive as the results in this work were preliminary.
- Producing a single material that can adsorb both cesium and strontium in high capacities in the presence of uranium and plutonium.

These might be achieved by:

- Closer inspection of morphology using SEM with EDAX software to identify that the presence of particulate material and the nature of its locality. X-Ray diffraction to analyse crystal structures will be performed. Analysis of the reaction gel mixture, possibly by centrifugation and/or freeze drying coupled with Infrared Spectroscopy for identification of the solid once the supernatant is removed.
- Producing beads of differing porosity and surface area, possibly remove the surfactant from the reaction mixture to remove porosity. Electro-spin fibres of AMP/PAN with differing thickness. Perform cesium uptake experiments in a variety of temperatures to ascertain order of kinetics.
- Understanding the mechanisms of Sr exchange and the subsequent modification to the synthesis to prevent exposure of the encapsulated adsorbent to acidity.
- Perform isocratic and step mode SMBC using a wide variety of ion exchange resins with multi-element feed solutions and subsequently, modifying flow rates and switch times to achieve desired separation.
- Developing a method to encapsulate AMP and a suitable strontium adsorbent into PAN or other suitable support in one medium. The internal morphology will need to be manipulated to accommodate ion exchange.

## **Publications from this project**

1. Eccles H., Bond G., Kavi P., Holdsworth A., and Rowbotham D: Removal of Caesium from simulated spent nuclear fuel dissolver liquor, J Chromatogr Sep Tech, vol 10, 417, 2019
2. Alistair F. Holdsworth, Harry Eccles, Daniel Rowbotham, Gary Bond, Parthiv C. Kavi, and Ruth Edge: The Effect of Gamma Irradiation on the Ion Exchange Properties of Caesium-Selective Ammonium Phosphomolybdate-Polyacrylonitrile (AMP-PAN) Composites under Spent Fuel Recycling Conditions , accepted for : Novel Polymeric Materials for Application in Liquid Phase Separations
3. Alistair F. Holdsworth, Harry Eccles, Daniel Rowbotham, Gary Bond, Parthiv C. Kavi, and Ruth Edge: The Effect of Gamma Irradiation on the Physiochemical Properties of Caesium-Selective Ammonium Phosphomolybdate-Polyacrylonitrile (AMP-PAN) Composites, in preparation.